DP-1125

DP-1125

AEC RESEARCH AND DEVELOPMENT REPORT

ZERO POWER EXPERIMENTS WITH ^{235}U-ENRICHED THORIA AND THORIUM METAL LATTICES FOR THE HWOCR

D. J. PELLARIN

N. P. BAUMANN

J. L. CRANDALL

G. F. O'NEILL

R. M. SATTERFIELD

Savannah River Laboratory

Aiken, South Carolina

LEGAL NOTICE

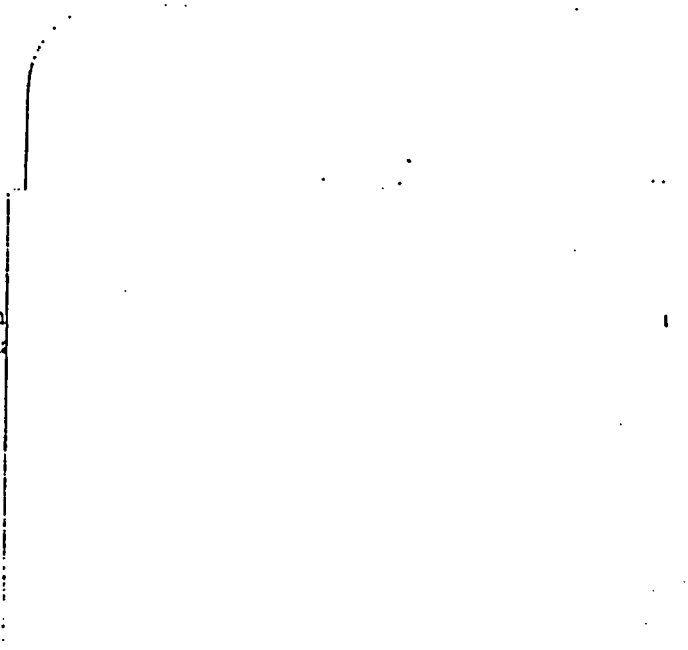

DP-1125

Reactor Technology
(TID-4500)

ZERO POWER EXPERIMENTS WITH ^{235}U-ENRICHED THORIA AND THORIUM METAL LATTICES FOR THE HWOCR

by

D. J. Pellarin
N. P. Baumann
J. L. Crandall
G. F. O'Neill
R. M. Satterfield

Experiments performed by

N. P. Baumann
S. E. Burdette
W. E. Graves
J. L. Jarriel
C. E. Jewell
R. L. Olson
G. F. O'Neill
D. J. Pellarin
W B. Rogers
R. M. Satterfield
V. D. Vandervelde

Approved by
J. L. Crandall, Research Manager
Experimental Physics Division

November 1967

E. I. DU PONT DE NEMOURS & COMPANY
SAVANNAH RIVER LABORATORY
AIKEN, S. C. 29801

CONTRACT AT(07-2)-1 WITH THE
UNITED STATES ATOMIC ENERGY COMMISSION

ABSTRACT

Lattice physics experiments were performed in the Process Development Pile (PDP) and the Subcritical Experiment (SE) to investigate thorium loadings for the Heavy Water Organic Cooled Reactor (HWOCR). The test fuel assemblies consisted of 85-rod clusters of THUD fuel, aluminum-clad rods of 0.234-inch UO_2-ThO_2 pellets with a $Th/^{235}U$ ratio of 49.03, and of coaxial U-Th metal tubes with approximately the same $Th/^{235}U$ ratio. These fuel assemblies were arranged into regular lattices at pitches of 9.0, 9.5, 10.5, and 12.12 inches in D_2O and tested with D_2O, air, and "Dowtherm" A occupying the fuel coolant channels.

Measurements included critical and exponential substitution buckling determinations and a variety of foil activations aimed at determining the subcadmium neutron distributions, the neutron temperatures, the cadmium ratios for ^{232}Th and ^{235}U, the ^{232}Th captures, and the $^{232}Th/^{235}U$ fission ratios. Most of the measurements were performed at room temperature, but some foil activations were performed with the thoria fuel and with urania fuel in "Dowtherm" A coolant at temperatures up to 195°C. The experimental results were compared with calculations by the HAMMER code, which performs lattice cell calculations in 84 neutron energy groups by integral transport methods. Agreement between the calculated and measured bucklings was within ±25 μB. From the detailed parameter measurements, it was estimated that the HAMMER code could calculate the neutron economy of all the systems studied within 1%.

CONTENTS

	Page
List of Tables	4
List of Figures	6
Introduction	8
Summary	9
Discussion	10
Experimental Fuel Assemblies	10
THUD Fuel	11
Thorium Metal Tubes (TMT)	14
UO_2 Tubes	18
Reference Lattices (NUOR, EUMT, NUMT)	19
Experimental Facilities	22
Subcritical Experiment (SE)	22
Process Development Pile (PDP)	22
SE Buckling Measurements	25
The Successive Substitution Technique	25
THUD Lattices	28
TMT	29
PDP Buckling Measurements	30
TMT	30
UO_2 Fuel Assembly	32
Activation Measurements in the SE	35
THUD I	36
THUD II	41
TMT	49
Hot Organic Loop	56
THUD A and THUD B	57
"Dowtherm" A	57
UO_2 Tubular Assembly	60
Calculations	63
The HAMMER Code	63
Models of the Experimental Fuel Assemblies	64
HAMMER Cross Sections	69
Calculations and Experiments	70
Comparison of Bucklings	70
Foil Activation	71
Appendix A - Physical Properties of "Dowtherm" A	72
Appendix B - Details for SE Buckling Measurements	72
Appendix C - Details for PDP Buckling Measurements	81
Appendix D - Details of Activation Measurements	84
Appendix E - Thorium Data Reduction Code (THODAT)	94
Bibliography	98

LIST OF TABLES

Table		Page
I	THUD Fuel Rod Specifications	11
II	^{235}U-Th Alloy Specifications for TMT Fuel	14
III	Specifications for ^{235}U-Th Metal Tube Assemblies	17
IV	THUD I Bucklings from SE Substitution Measurements	28
V	THUD II Bucklings from SE Substitution Measurements	29
VI	TMT Bucklings from SE Substitution Measurements	29
VII	TMT Bucklings from PDP by HERESY Analysis	33
VIII	TMT Bucklings from PDP Measurements	34
IX	Bucklings of Tubular UO_2 Fuel Assemblies from PDP by Persson Analysis	34
X	Foils and Counting Conditions for THUD and TMT Activation Measurements	35
XI	THUD I Activation Measurements	36
XII	THUD I Fast Fission Measurements	39
XIII	THUD II Lattice Parameter Measurements	41
XIV	THUD II Resonance Capture Measurements	45
XV	THUD II Fast Fission Measurements	45
XVI	TMT Lattice Parameter Measurements	49
XVII	Thorium Resonance Capture in TMT Lattices	52
XVIII	^{235}U Cadmium Ratio Measurements in TMT Lattices	52
XIX	Fast Fission Effect in TMT Lattices	53
XX	TMT Regions for HAMMER Calculations	65
XXI	Tubular UO_2 Regions for HAMMER Calculations - Hot Organic Loop	65
XXII	Tubular UO_2 Regions for HAMMER Calculations - PDP Measurements	66
XXIII	THUD I Regions for HAMMER Calculations	66
XXIV	THUD II Regions for HAMMER Calculations	67
XXV	THUD A Regions for Homogeneous Model HAMMER Calculations	67
XXVI	THUD B Regions for Homogeneous Model HAMMER Calculations	68

Table		Page
XXVII	HAMMER Computed Parameters for THUD I Lattices . .	69
XXVIII	Atom Densities for "Dowtherm" A	72
XXIX	SE Fuel Loading Patterns - THUD I Buckling Measurements	73
XXX	SE Fuel Loading Patterns - THUD II Buckling Measurements	75
XXXI	SE Fuel Loading Patterns - TMT Buckling Measurements	76
XXXII	PDD Fuel Loading Patterns - TMT - 12.12-inch Triangular Pitch	81

LIST OF FIGURES

Figure		Page
1	THUD Rod	11
2	THUD I and THUD II Fuel Assemblies	13
3	Three-Tube ^{235}U-Th Metal Fuel Assembly (Type I)	15
4	Two-Tube ^{235}U-Th Metal Fuel Assemblies (Types II and III)	16
5	Tubular Natural UO_2 Fuel Assembly	18
6	Natural UO_2 19-Rod Cluster	19
7	Enriched Uranium Metal Tube Assembly	20
8	Components Used in PDP Mixed Lattice Experiments	21
9	Natural Uranium "C" Fuel Assembly	21
10	Isometric of the SP-SE	23
11	Isometric of the PDP	24
12	Persson Cell Assignment	26
13	PDP Substitution Lattice	30
14	THUD I Irradiation Lattices	37
15	THUD I Irradiation Assembly	38
16	THUD I Removable Foil Loading Rod	39
17	Subcadmium Copper Activation Profiles - THUD I	40
18	THUD II Irradiation Lattices	42
19	THUD II Irradiation Assembly Made up of Preassembled Halves	43
20	THUD II Foil Loading	44
21	Subcadmium Copper Activation Profiles - THUD II	46
22	Subcadmium Copper Activation Profiles in the Fuel Only-THUD II	47
23	Spectral Index Profiles - THUD II	48
24	TMT Irradiation Lattices	50
25	TMT Irradiation Slug	50
26	TMT Window Sections	51
27	Foil Loading for TMT Fuel	51
28	Subcadmium Copper Activation Profiles - TMT Type I	54
29	Subcadmium Copper Activation Profiles - TMT Type II	55
30	Spectral Index Profiles - TMT Type I	55

Figure		Page
31	Spectral Index Profiles - TMT Type II	56
32	Hot Organic Loop	56
33	THUD A Fuel Assembly	58
34	THUD B Fuel Assembly	59
35	Foil Loadings for THUD A and THUD B	59
36	Spectral Index Profiles from Organic Loop Measurements	60
37	UO_2 Fuel Assembly for Neutron Temperature Measurements	62
38	Radial Distributions of the Spectral Index for Tubular UO_2	62
39	SE Loadings	77
40	Persson Substitution Analyses - THUD I - SE	78
41	Persson Substitution Analyses - THUD II - SE	79
42	Persson Substitution Analyses - TMT - SE	80
43	Persson Substitution Analyses - TMT - PDP	83
44	Specialized β-Counting Apparatus for ^{233}Th	84
45	Typical Foil Ladder in the Moderator for THUD Measurements	91
46	Foil Ladder in Moderator for TMT Measurements	92

ZERO POWER EXPERIMENTS WITH ^{235}U-ENRICHED THORIA AND THORIUM METAL LATTICES FOR THE HWOCR

INTRODUCTION

The experiments described in this report were conducted over the period 1965 to 1967 in support of the AEC's development program for a Heavy Water Organic Cooled Power Reactor (HWOCR). Overall responsibility for the HWOCR development was assigned to the Atomics International and Combustion Engineering companies[1]. The problem of developing thorium fuel cycles for the HWOCR was separately assigned to the Babcock and Wilcox Company[2]. The overall objective of the SRL experiments was to provide the experimental data required to ensure that the physics design codes being used by Babcock and Wilcox in their thorium fuel cycle studies were sufficiently accurate for conceptual design. No previous experimental work had been reported for the thorium-D_2O-organic reactor system.

The key points at issue were the effects of the thorium and of the hot organic in the fuel assembly geometries being developed by Babcock and Wilcox. These fuel assemblies consisted of clusters of enriched thoria or thorium carbide rods or of coaxial cylinders of enriched thorium metal. In the interest of economy it was desired to use available fuel material for the experimental program. Thoria rods containing about 2% ^{235}U were available from the Argonne THUD program for the EBWR[3]. These rods were used to mock up both the thoria and thorium carbide rod clusters. No thorium metal tubes were available, but existing thorium metal on hand at Savannah River was used by Nuclear Metals, Inc. to fabricate a few specimen tubes, also containing approximately 2% ^{235}U. The experiments with these fuels were carried out at the Savannah River Laboratory in the critical facility, the PDP[4], and in the exponential facility, the SE[5].

Since the primary purpose of the experiments was to test the design calculations, all of the experimental results were compared with calculations obtained from the HAMMER code[6]. The HAMMER code performs reactor cell calculations in 84 energy groups by integral transport methods. It is one-dimensional, and input to the code consists only of the lattice geometry and of a microscopic cross section library. Effective cross sections in the resonance region are calculated internally from individual resonance parameters by means of the Nordheim ZUT and TUZ codes[7]. The HAMMER code thus provides a "first principles" comparison with the calculations.

SUMMARY

Substitution buckling measurements were performed in both the PDP and the SE using 85-rod clusters of the THUD UO_2-ThO_2 fuel at two internal rod pitches and with D_2O, air, and "Dowtherm" A as the assembly coolants. The measurements were made at lattice pitches ranging from 9.00 to 12.12 inches. Similar measurements were also made on two- and three-tube assemblies of the ^{235}U-Th fuel tubes. The buckling measurements were supplemented by foil irradiations performed in the SE to determine detailed lattice parameters. These measurements included determinations of the thermal neutron distributions in terms of subcadmium foil activations, determinations of the thermal neutron temperatures in terms of Lu/(1/v) activity ratios, determinations of epithermal neutron fractions in terms of ^{232}Th capture and ^{235}U fission cadmium ratios, measurements of ^{233}U production in terms of neutron captures in the ^{232}Th, and measurements of the lattice fissions in terms of the $^{232}Th/^{235}U$ fission ratios. A few of the irradiations were performed in a special hot organic loop in the SE at temperatures up to 195°C.

The experimental measurements were all compared with calculations performed by the HAMMER code. Since this code is one-dimensional, it was necessary to develop one-dimensional calculational models of the fuel clusters. Two models were used: one in which all material within the cluster was homogenized into a single region with cross sections given by volume-weighted averages, and one in which the cluster was divided into concentric cylindrical rings of fuel and coolant. The comparisons of the experimental and calculated bucklings are given in Tables IV-VI and VIII. The comparisons show agreement to within about ±25 μB between experiment and computation. They show no systematic dependence on lattice pitch or coolant type. The buckling differences between exporiment and calculation are equivalent to k_∞ differences of about ±0.0075 .

The HAMMER computations were generally in close agreement with the intracell activation profiles except for one series of measurements on the fuel clusters, where they tended to overestimate the moderator-to-fuel flux ratios by about 4%. Agreement between calculation and experiment was less good in the spectral index measurements, where the computations tended to overestimate the spectral index in all coolants: In the reaction rate measurements, the measured resonance capture in the ^{232}Th was 5 to 20% higher than that calculated. These differences amount to about 0.005 to 0.02 in the value of the resonance escape probability. In the rod cluster lattices, the resonance absorption differences were in the same direction as the buckling differences. However, there did not seem to be a

similar correspondence for the metal tube lattices. The HAMMER calculations of the fast fission effect were in close agreement with the thorium metal tube measurements, but were approximately 20% low (in terms of $\epsilon - 1$) for the rod cluster lattices.

The work described in this report was of a survey nature only and suffered on the experimental side from a limited quality and quantity of the test fuel assemblies and on the theoretical side from the necessity of using one-dimensional models in the HAMMER calculations. However, it appeared that all the systems studied could be calculated within about 1% accuracy in the neutron economy. It was thus adjudged that the calculational methods were sufficiently accurate for survey work and that additional experiments would be required only for detailed assessment of particular lattice designs. With the close-out of the HWOCR program, no such additional experiments are currently planned.

DISCUSSION

EXPERIMENTAL FUEL ASSEMBLIES

The purpose of the experiments described in this report was to supply calibration data for use in the design of thorium-bearing lattices for the Heavy Water Organic Cooled Reactor (HWOCR)[1]. The thorium fuel cycle responsibility for the HWOCR was assigned to the Babcock and Wilcox Company, and they undertook three series of HWOCR lattice designs based respectively on fuel assemblies of enriched UO_2-ThO_2 rod clusters, of enriched UC-ThC or UC-ThC_2 rod clusters, and of coaxial enriched U-Th metal tubes[2]. Mockup studies of the candidate B and W lattices were planned for a later stage of the experiments, but for the initial stage it was merely desired to secure some assurance that the physics design codes were adequately treating the essential features of the lattices, i.e., the fuel assembly and lattice geometries and the specific contributions of the thorium and the hot organic coolant. It was believed that this assurance could be gained at minimum expense by small-scale D_2O lattice studies of $^{235}UO_2$-ThO_2 fuel rod clusters and of ^{235}U-Th fuel tube assemblies, supplemented by some auxiliary studies of the nuclear effects of hot organic coolant in tubular UO_2 fuel assemblies. The $^{235}UO_2$-ThO_2 fuel rods, the UO_2 fuel tubes, and a variety of other fuel assemblies used for calibration and substitution experiments were already on hand as part of the AEC's library of fuels for critical experiments. The ^{235}U-Th metal tubes were specially fabricated by Nuclear Metals, Inc. from thorium on hand at Savannah River Laboratory. These fuel assemblies are described separately in the following sections.

THUD Fuel

The THUD (THUD is an ANL originated acronym for Thoria-Urania Deuterium Lattices) fuel was originally prepared at the Argonne National Laboratory for lattice experiments in connection with the EBWR[3] and was obtained on loan from ANL. The individual fuel rods (Figure 1) consist of 0.234-inch-diameter UO_2-ThO_2 pellets clad in 6061 aluminum tubing with an outside diameter of 0.309 inch. The Th/^{235}U atom ratio for the rods used in the Savannah River experiments was 49.03. Table I gives the specifications.

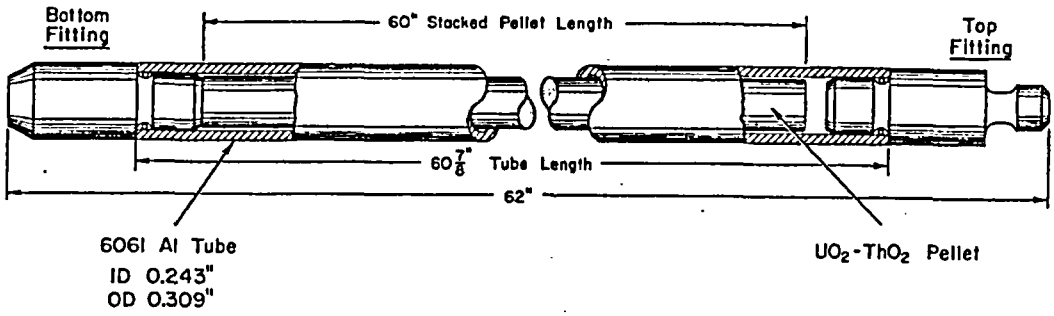

FIG. 1 THUD ROD

TABLE I

THUD Fuel Rod Specifications

Fuel composition, wt %	
Thorium	85.925
^{234}U	0.018
^{235}U	1.775
^{236}U	0.009
^{238}U	0.103
Oxygen	12.15
Fuel density, g/cm^3	8.150

For the SRL experiments, the THUD rods were gathered into fuel clusters. Because the THUD rods were considerably smaller in diameter than the fuel rods proposed for the HWOCR designs, up to 85 rods had to be used in the THUD clusters to get the desired fuel volumes. These large clusters, although providing a somewhat poor mockup of the reference designs, did have the advantage of presenting a relatively homogeneous fuel, cladding, and coolant mix and thus provided a valid comparison for computations using a homogenized cluster model.

Two types of 85-rod THUD clusters were used. The THUD I clusters had the fuel rods on a 0.310-inch triangular lattice pitch within the cluster, and the THUD II clusters had the rods on a 0.351-inch triangular lattice pitch. The rod-to-rod spacing for the THUD II clusters was maintained by small nylon rings girdling individual rods. The THUD I clusters were enclosed in aluminum housing tubes 3.30-inch ID x 3.42-inch OD. The THUD II clusters used 3.90 x 4.00-inch housing tubes. The corner positions in the hexagonal clusters were occupied by dummy aluminum rods, and the spaces between the flats of fuel clusters and the housing tubes were occupied by coolant-displacing aluminum spacers (Figure 2). The aluminum drain plugs at the bottom of the clusters were removed to permit the moderator to enter for experiments simulating D_2O-cooled fuel. For experiments simulating gas- or organic-cooled fuel, these plugs were inserted and the coolant spaces were filled with air or "Dowtherm"* A. Physical properties of "Dowtherm" A are given in Appendix A.

Two special 55-rod THUD assemblies designated THUD A and THUD B were used for experiments in the hot organic loop. These assemblies are illustrated in Figures 33 and 34.

* "Dowtherm" is a trademark of Dow Chemical Company.

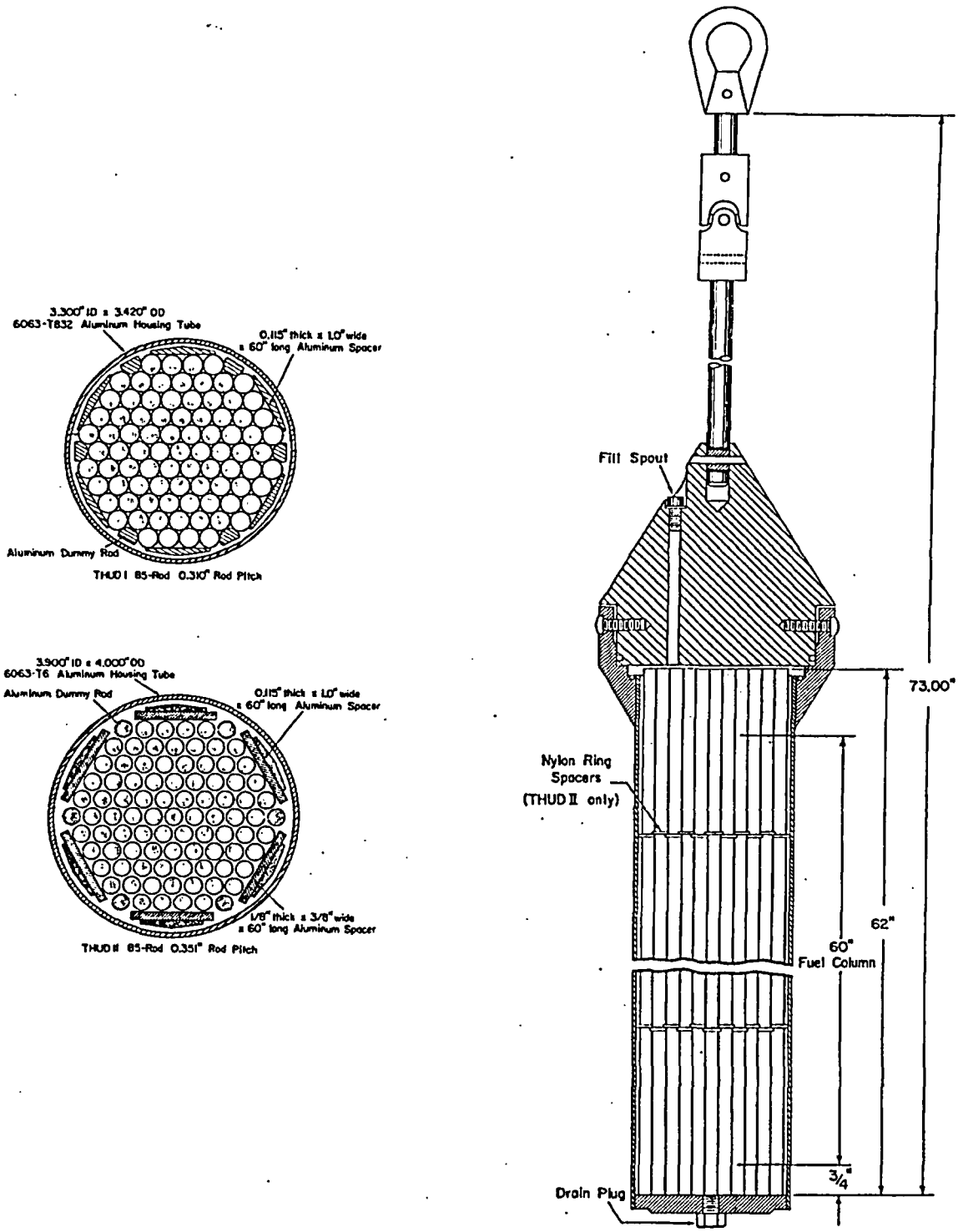

FIG. 2 THUD I AND THUD II FUEL ASSEMBLIES

Thorium Metal Tubes (TMT)

A set of thorium metal tubes (TMT) containing a nominal 2% concentration of ^{235}U was specially fabricated for these experiments by Nuclear Metals, Inc. The metal alloy specifications are given in Table II.

TABLE II

^{235}U-Th Alloy Specifications for TMT Fuel

Composition, wt %	
Thorium	97.838
^{235}U	2.00
^{238}U	0.162
Density, g/cm^3	11.7
Slug length, inches	16.00

The basic TMT test assembly, designated Type I, consisted of three coaxial fuel tubes with aluminum housing and cladding tubes (Figure 3). Two other test assemblies, designated Type II and Type III, respectively, were formed by using only the two outer fuel tubes of the Type I assembly together with a 1.210-inch graphite filler plug at the center and by using only the two inner tubes. These assemblies are illustrated in Figure 4 and their dimensions are listed in Table III. As was the case with the THUD fuel clusters, the drain holes at the bottoms of the TMT assemblies were opened to the D_2O moderator in experiments involving D_2O coolants but were plugged and filled with air or "Dowtherm" A for the simulated gas and organic coolants.

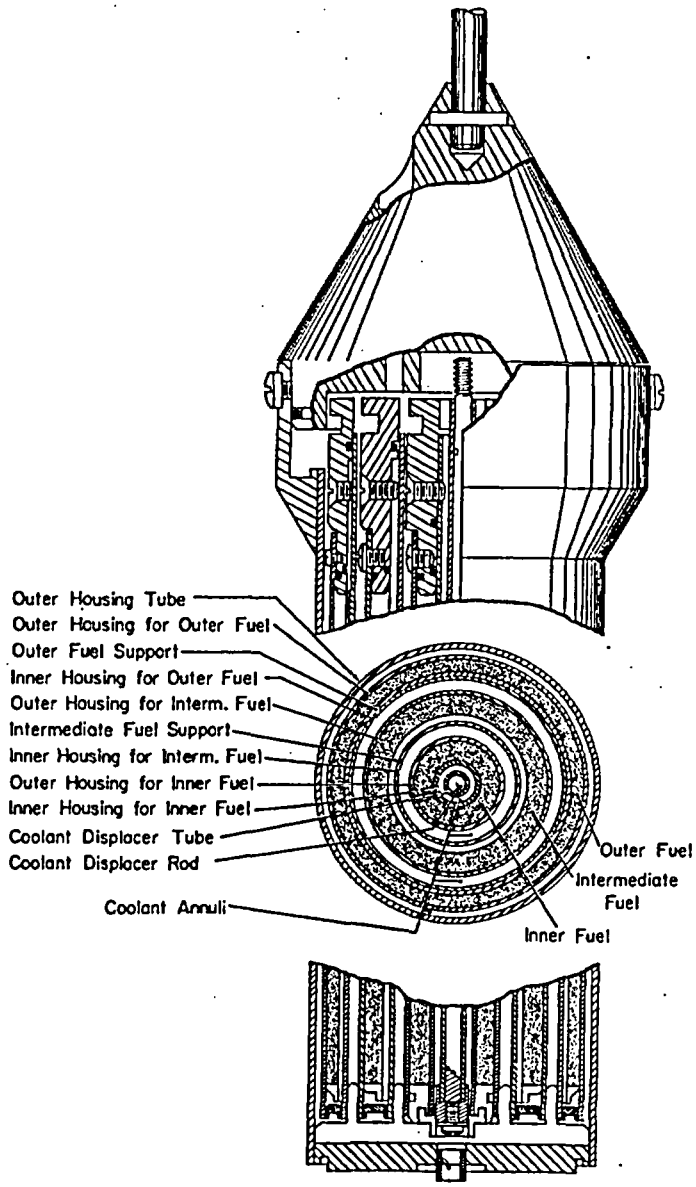

Bare Fuel Dimensions

	ID, in.	OD, in.
Inner Fuel	0.710	1.224
Intermediate Fuel	2.034	2.510
Outer Fuel	3.263	3.640

FIG. 3 THREE-TUBE ^{235}U-Th METAL FUEL ASSEMBLY (Type I)

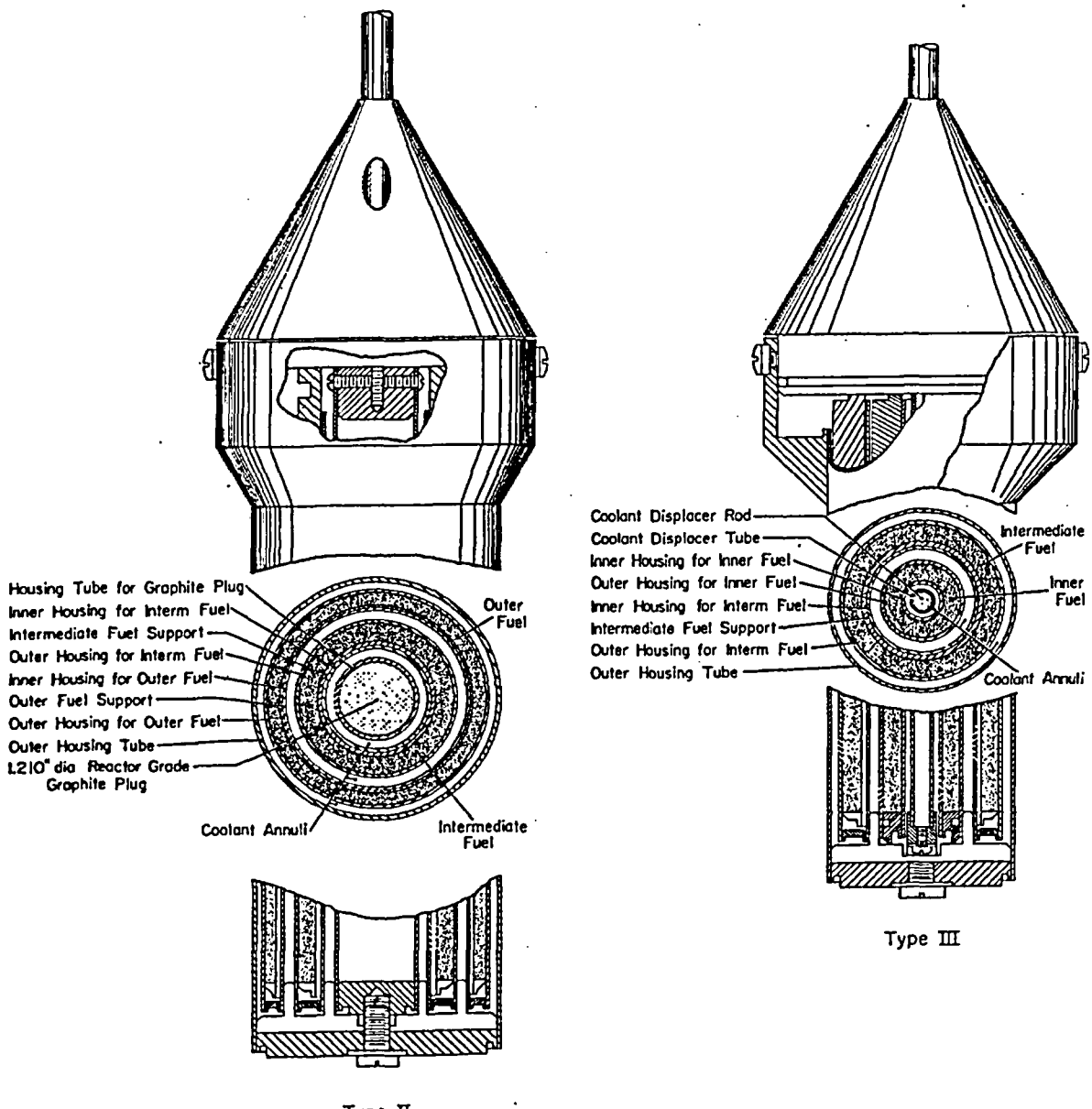

FIG. 4 TWO-TUBE ^{235}U-Th METAL FUEL ASSEMBLIES (Types II and III)

TABLE III

Specifications for ^{235}U-Th-Metal Tube Assemblies

Component	OD, inches	ID, inches
Assembly Type I		
Inner fuel	1.224	0.710
Intermediate fuel	2.510	2.034
Outer fuel	3.640	3.263
Outer housing tube	4.060	3.960
Outer housing for outer fuel	3.760	3.660
Outer fuel support	3.240	3.106
Inner housing for outer fuel	3.085	2.985
Outer housing for intermediate fuel	2.645	2.545
Intermediate fuel support	2.014	1.810
Inner housing for intermediate fuel	1.790	1.690
Outer housing for inner fuel	1.350	1.250
Inner housing for inner fuel	0.660	0.560
Coolant displacer tube	0.360	0.260
Coolant displacer rod	0.250	-
Assembly Type II		
Intermediate fuel	2.510	2.034
Outer fuel	3.640	3.263
Outer housing tube	4.060	3.960
Outer housing for outer fuel	3.760	3.660
Outer fuel support	3.240	3.106
Inner housing for outer fuel	3.085	2.985
Outer housing for intermediate fuel	2.645	2.545
Intermediate fuel support	2.014	1.810
Inner housing for intermediate fuel	1.790	1.690
Housing tube for graphite plug	1.350	1.250
Assembly Type III		
Inner fuel	1.224	0.710
Intermediate fuel	2.510	2.034
Outer housing	3.085	2.985
Outer housing for intermediate fuel	2.645	2.545
Intermediate fuel support	2.014	1.810
Inner housing for intermediate fuel	1.790	1.690
Outer housing for inner fuel	1.350	1.250
Inner housing for inner fuel	0.660	0.560
Coolant displacer tube	0.360	0.260
Coolant displacer rod	0.250	-

UO_2 Tubes

The experiments with the thorium fuels were supplemented by some limited experiments with UO_2 fuel tubes in order to separate the specific effects of the thorium from the effects of the fuel assembly geometry. A two-tube UO_2 assembly used for buckling measurements in the PDP is illustrated in Figure 5. The similar irradiation assembly used in the SE is illustrated in Figure 37.

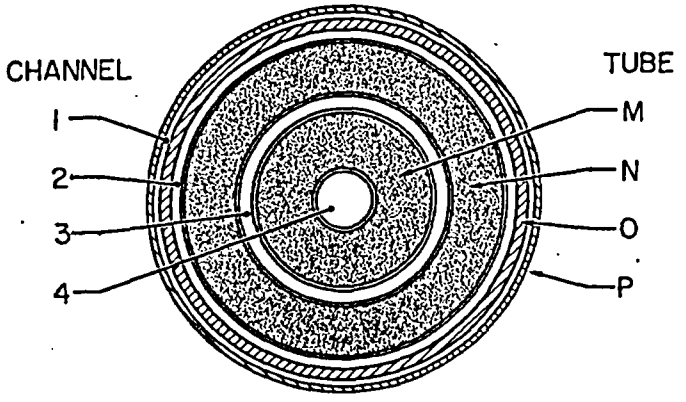

Tube	Description	OD, in.	ID, in.	Aluminum Cladding OD, in.	Aluminum Cladding ID, in.
M	UO_2 Tube	1.560	0.560	1.620	0.500
N	UO_2 Tube	2.870	1.950	2.930	1.890
O	Pressure Tube, Al	3.310	3.110	—	—
P	Calandria Tube, Al	3.550	3.430	—	—

Channel	Channel Width, in.	Remarks
1	0.060	Void
2	0.090	"Dowtherm" A Filled
3	0.135	" "
4	0.500	" "

FIG. 5 TUBULAR NATURAL UO_2 FUEL ASSEMBLY

Reference Lattices (NUOR, EUMT, NUMT)

Since only small numbers of the thorium fuel assemblies were available, almost all of the experiments were performed as substitution measurements in various host or reference lattices.

For most of the SE measurements the reference lattice consisted of 19-rod clusters of natural uranium oxide rods (NUOR lattice). These rods consisted of sintered UO_2 pellets 0.500 inch in diameter and approximately 5/8 inch long, stacked into 6 ft long 6063 aluminum tubes 0.020 inch thick and 0.547-inch OD. The individual pellets were ground to the exact shape of right circular cylinders. The density of the oxide averaged 10.4 g/cm^3. A rod-to-rod spacing of 0.647 inch was maintained by small nylon rings girdling individual rods. These rings were computed to have no measurable effect on the measured bucklings. The clusters were not contained in housing tubes but were held together by polyester tape (also calculated to have a negligible effect on the buckling). A schematic of this rod cluster arrangement is shown in Figure 6.

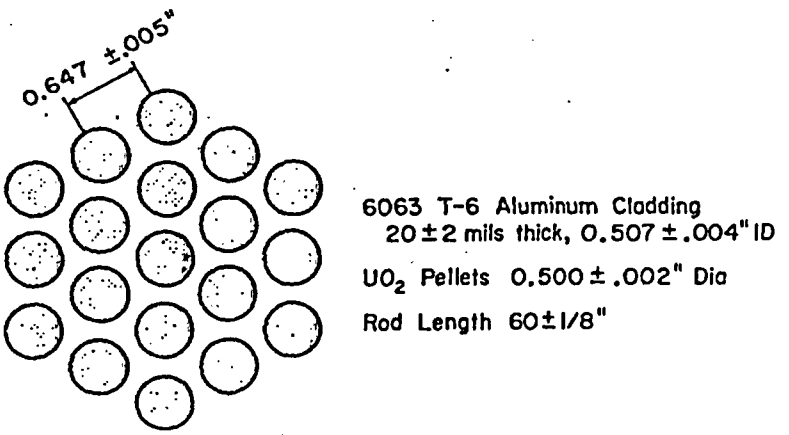

FIG. 6 NATURAL UO_2 19-ROD CLUSTER

A second SE host lattice, used in a few of the early experiments, consisted of enriched uranium metal tubes (EUMT lattice). These fuel assemblies were made up of two coaxial uranium metal tubes enriched to 0.947 wt % ^{235}U and surrounded by inner and outer aluminum housing tubes. Details of these assemblies are given in Figure 7.

The host lattice used for most of the PDP experiments consisted of unclad natural uranium tubes (NUMT)(Figure 8). The PDP experiments with the UO_2 fuel tubes were performed with a host lattice of single natural uranium tubes (Figure 9).

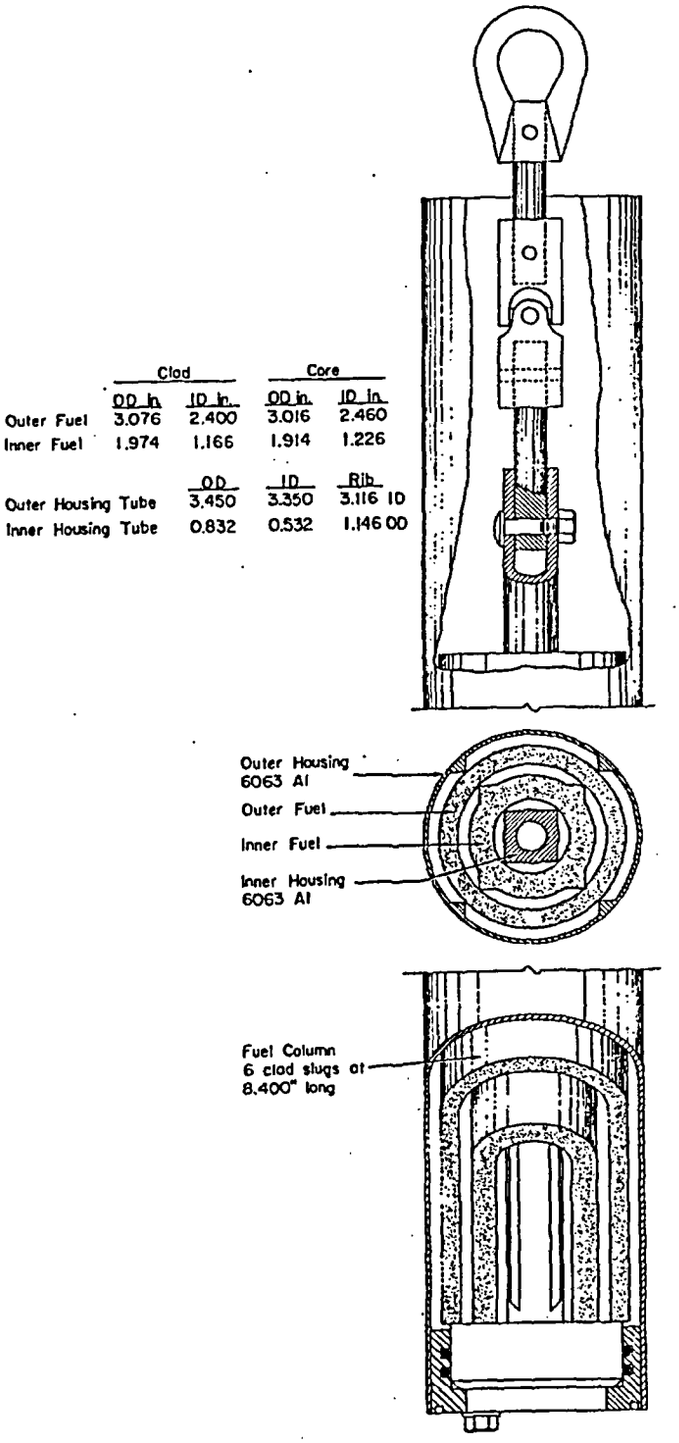

FIG. 7 ENRICHED URANIUM METAL TUBE ASSEMBLY

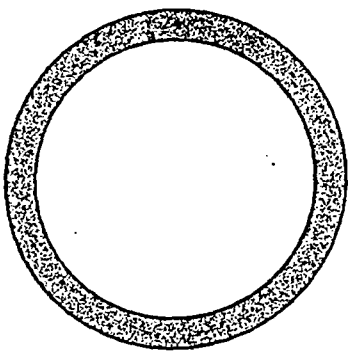

Natural Uranium Metal Tube

Density 18.9 g/cm³
OD 3.500 inches
ID 2.860 inches

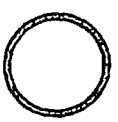

Natural Li-Al Alloy Rod

4.9 wt% Lithium in Aluminum
Density 2.35 g/cm³
OD 0.930 inch
Cladding and Sheath Material 1100 Al
Cladding OD 1.005 inches
Cladding ID 0.930 inch
Sheath OD 1.090 inches
Sheath ID 1.026 inches
Air between Sheath and Clad Rod

FIG. 8 COMPONENTS USED IN PDP MIXED LATTICE EXPERIMENTS

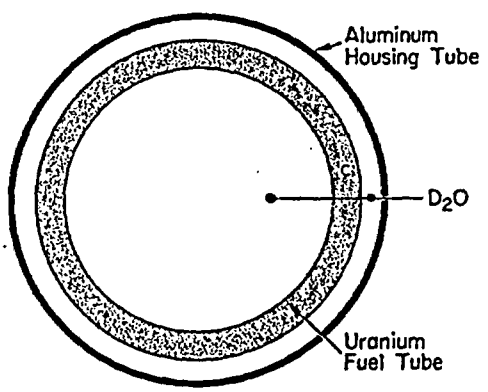

Component	Material	Dimensions OD, in.	Dimensions ID, in.
Fuel Tube	Uranium	3.500	2.860
Housing Tube	6063 Aluminum	4.000	3.900

FIG. 9 NATURAL URANIUM "C" FUEL ASSEMBLY

Experimental Facilities

The fuel assemblies described in the preceding sections were used for exponential buckling measurements and foil activation studies in the Subcritical Experiment (SE) and for substitution buckling measurements in the Process Development Pile (PDP).

Subcritical Experiment (SE)

The Subcritical Experiment[5] is an aluminum tank 5-ft in diameter and 7-ft high wrapped on the sides with 0.060-inch-thick cadmium and a 2-inch-thick layer of fiberglass thermal insulation. It is mounted directly over the Standard Pile[6], a small graphite-moderated reactor which supplies neutrons to the SE through a cylindrical graphite pedestal 16 inches high and 60 inches in diameter. Thermal neutron flux levels as high as 10^8 n/(cm^2)(sec) are available in the SE. A cadmium shutter may be interposed between the SE and the pedestal to interrupt the thermal neutron feed from the SP. Runs with the shutter inserted provide data for unwanted background neutron sources such as fast neutrons and photoneutrons from radiation in the SP. The SP may also be used to irradiate reference foils in thimble positions or in a graphite thermal column during the SE runs.

The SE-SP arrangement is shown in Figure 10. The grid beams at the top of the SE are used to support the test fuel assemblies and other lattice components and may be rearranged into any desired lattice pitch or geometric configuration. Storage tanks and a closed piping system supply D_2O, H_2O, or organic liquids as the SE moderators.

Process Development Pile (PDP)

The Process Development Pile[4] is a critical facility for reactor physics studies at low power levels. Moderated by heavy water, it is designed for maximum experimental flexibility and can accommodate a wide variety of lattice components in almost any desired configuration. The PDP tank is 16 feet 2-3/4 inches in diameter with a height of 15 feet 6 inches. A system of grid beams is used for top support of the lattice components. The control system besides providing systems of safety, shutdown, and control rods also permits the moderator level to be adjusted to within ±0.002 cm. Absolute water heights may be measured to an accuracy of ±0.1 cm and relative water heights to an accuracy of ±0.001 cm in determining critical moderator heights. The maximum allowed flux levels in the PDP are 5×10^8 n/(cm^2)(sec). The facility is illustrated in Figure 11.

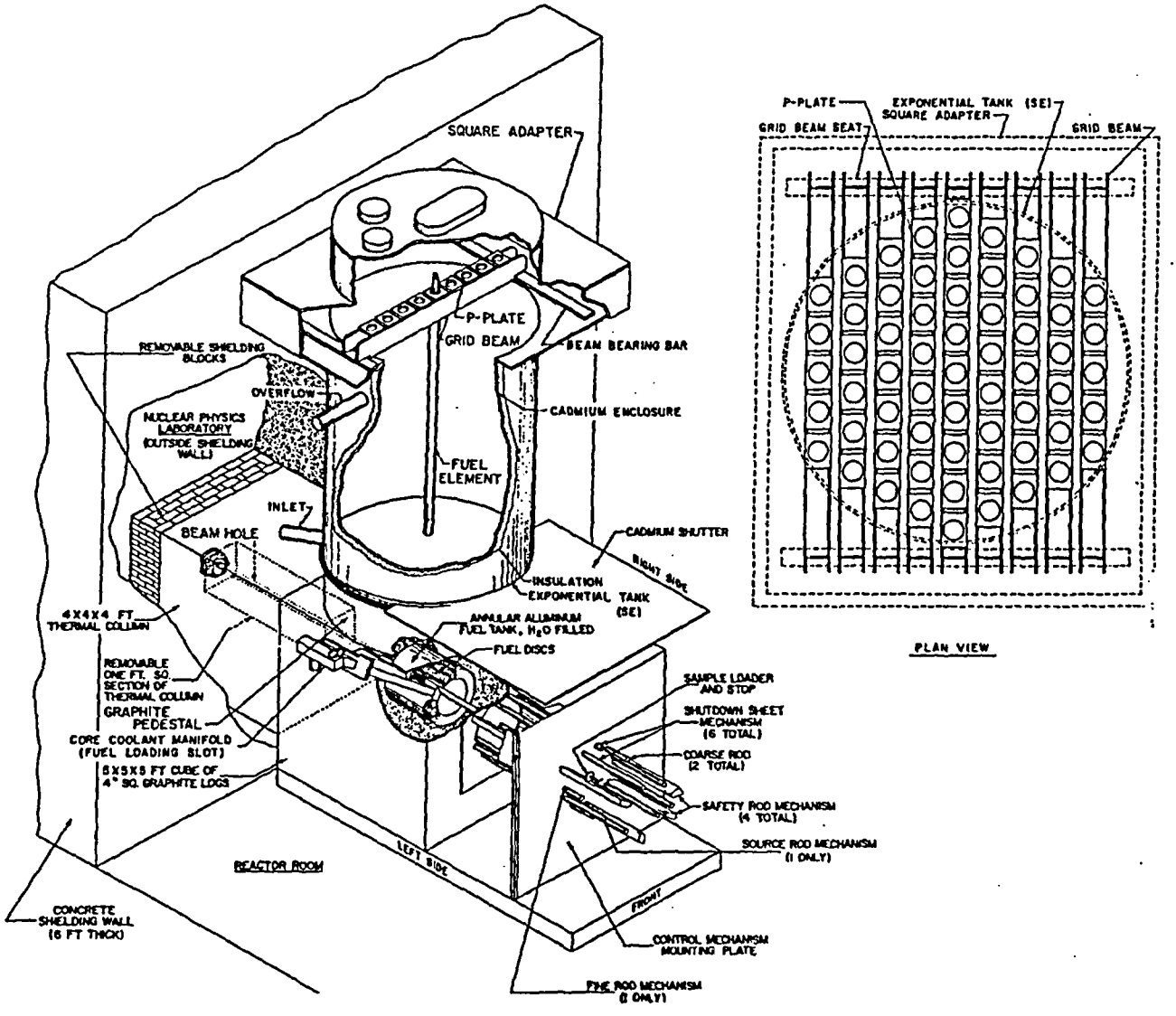

FIG. 10 ISOMETRIC OF THE SP-SE

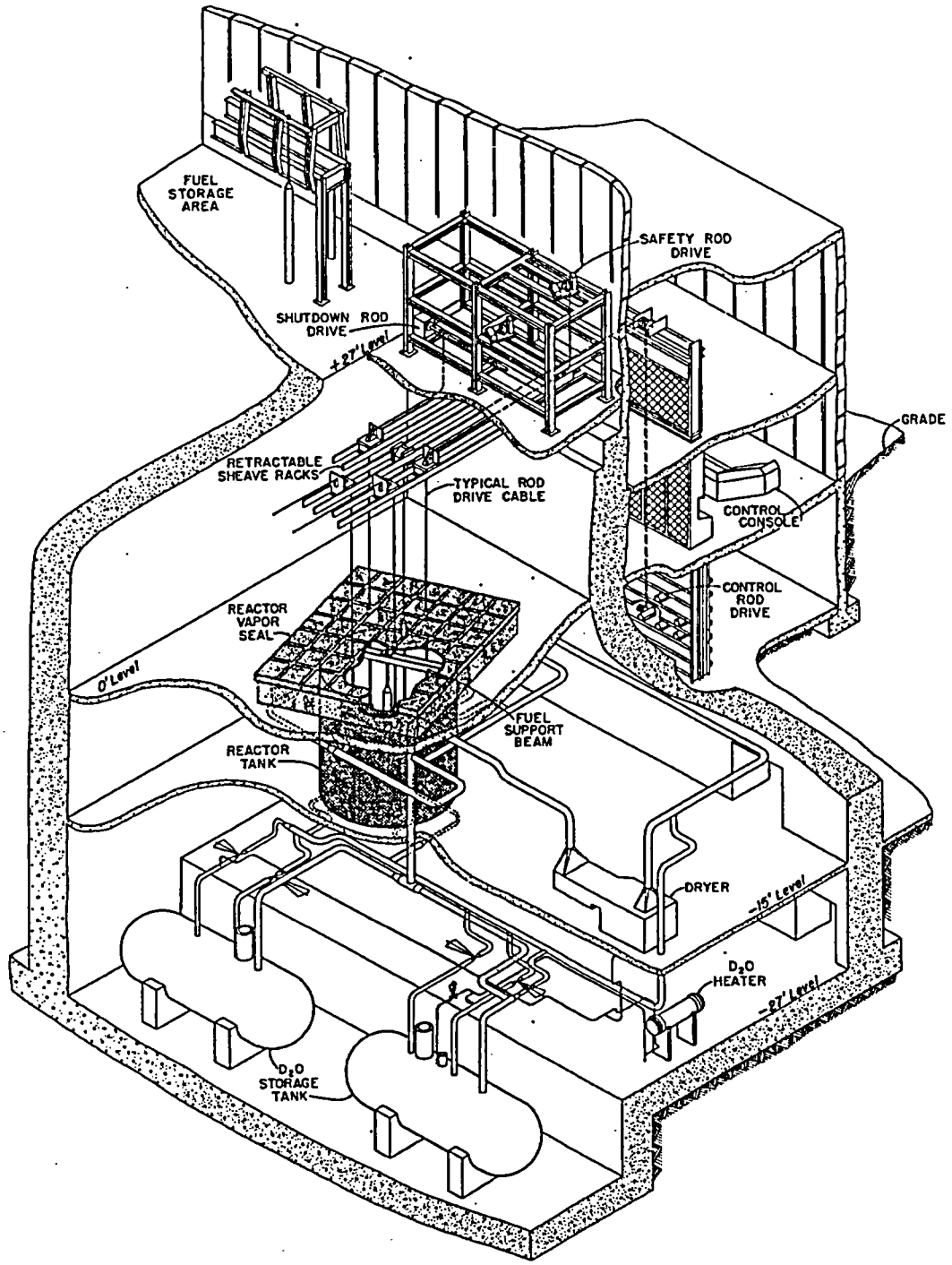

FIG. 11 ISOMETRIC OF THE PDP

SE BUCKLING MEASUREMENTS

The Successive Substitution Technique

Since the numbers of experimental fuel assemblies available for the experiments in general fell just under the number required for full lattice loadings in the SE, a modification of the Persson successive substitution technique[9] was developed for mixed-lattice experiments to make maximum utilization of the existing fuel stocks.

The unique feature of the Persson method is the introduction of the concept of a third mixed lattice at the boundary region in a two-region lattice. A substitution load is thus assumed to consist of three regions: (1) a known reference or driver lattice, (2) a mixed lattice, and (3) the test lattice. The statistical weight equation for a mixed lattice with measured buckling $B^2 = B_R^2 - \kappa_z^2$ is written in terms of statistical weights, W, as

$$W_1 B_1^2 + W_2 B_2^2 + W_3 B_3^2 = B^2 \qquad (1)$$

where B_R^2 is the radial buckling of the mixed lattice, κ_z is the inverse of the axial relaxation length in an exponential loading, and the subscripts refer to the different regions as identified above.

Three different measurements are analytically sufficient to determine the three bucklings, but it is more convenient to cast Equation 1 in the form

$$\frac{B^2 - B_1^2}{W_3 + W_2/2} = \delta B^2 \left(\frac{W_2}{W_3 + W_2/2} \right) + (B_3^2 - B_1^2) \qquad (2)$$

where

$$\delta B^2 \equiv B_2^2 - \frac{B_3^2 - B_1^2}{2}$$

and advantage has been taken of the fact that

$$W_1^2 + W_2^2 + W_3^2 = 1$$

Equation 2 is of the form $y = ax + b$ and thus permits simultaneous evaluation by least squares methods for more than three buckling measurements on a given lattice.

The Persson method, for this application, assumes test and reference fuel assemblies to be on the same lattice pitch, with test assemblies simply replacing one or more reference fuel assemblies. Each Persson cell includes a section (1/4 for square, 1/6 for triangular lattices) of a fuel assembly and a similar section of its nearest fuel neighbor at two opposed corners of an equilateral parallelepiped (Figure 12). If the two fuels are the same, the lattice cell is assigned to that fuel lattice; if they differ the cell is assigned to Region 2, the mixed lattice. For the purpose of calculating statistical weights, each cell is further subdivided into two or more subcells and the flux is evaluated at the centroid of each subcell.

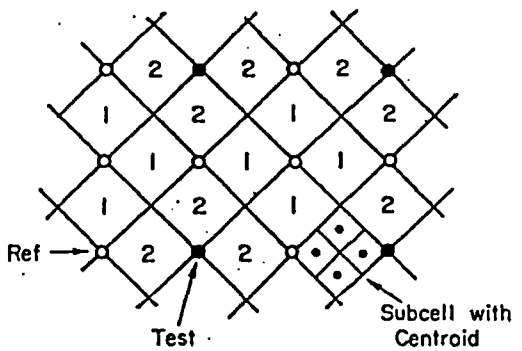

Persson Cells for Square Lattice
(Uniform mixed lattice, 1:3 ratio)

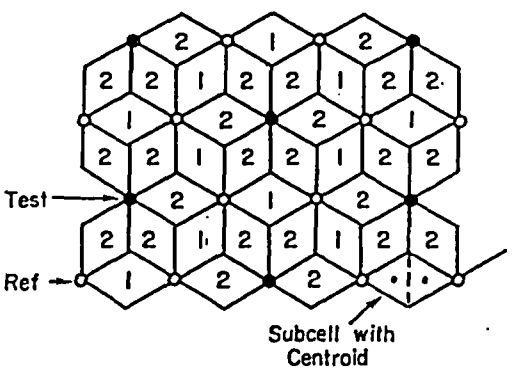

Persson Cells for Triangular Lattice
(Uniform mixed lattice, 1:3 ratio)

FIG. 12 PERSSON CELL ASSIGNMENT

The computation of statistical weights in the one-energy group approximation involves the computation, for each subcell at radius r, of the product of the unperturbed flux [$J_o(B_R r)$, with B_R being the geometrical buckling in the axially uniform, cylindrical SE loads] and the perturbed flux for the mixed load. For loadings with one test and one reference region clearly defined, the perturbed flux is computed by a one-group, two-region diffusion theory from the measured difference in buckling of the mixed lattice from that of the reference lattice. For mixed loads with alternating test and reference fuel, the perturbed flux is taken equal to the unperturbed flux.

The Persson method was designed initially for substitution measurements with a small number of fuel assemblies in a D_2O-moderated critical facility. It relied heavily on the fact that in such a facility, differences in buckling (differences in critical water heights) could be obtained with much higher precision than could overall bucklings (radial and axial activation profiles over the reactor). The lack of precision for measuring differences in an exponential is partially offset by the fact that an amount of test fuel constituting a small load for a critical facility may constitute a major load for an exponential.

The SE buckling determination for each of the test lattices relied primarily on three buckling measurements corresponding to the following load configurations:

1. The full reference lattice.

2. The maximum available number of test assemblies, loaded from the center, with reference fuel used to complete the lattice.

3. A uniform mixed lattice throughout the SE. Test-to-reference fuel ratios of 1:1 or 1:2 were used for the square lattices and 1:2 or 1:3 for triangular lattices.

Additional measurements on other load configurations were also made for corroborative purposes in most of the lattices.

For most of the measurements, the NUOR fuel assemblies (Figure 6) were used as the host lattice, although some corroborative measurements were also made with EUMT host lattice assemblies (Figure 7). Radial bucklings, B_R^2, were measured by fitting a J_o function to foil activation data for both of the one-region calibration lattice loadings. Based on these measurements, a B_R^2 value of 925 μB was used for the lattices. Vertical bucklings, κ_z^2, were measured for each lattice with the SE traveling monitor, a small ^{10}B-lined compensated ion chamber.

The Persson analysis was used for all experiments with D_2O and "Dowtherm" A as the coolant. However in the air-cooled lattices the differences in diffusion coefficients between the host and reference lattices resulted in the Persson analysis giving anomalously high buckling numbers. Although it is possible to take explicit account of the diffusion coefficient effects in the Persson analysis, this was inconvenient for the SE configuration and accordingly a four-group diffusion theory analysis was substituted for those lattices.

THUD Lattices

Substitution buckling measurements were performed according to the technique described above on both the THUD I and THUD II fuel assemblies, the 85-rod UO_2-ThO_2 fuel clusters illustrated in Figures 1 and 2. The measurements were made at a 9-inch triangular and a 10.5-inch square lattice pitch with "Dowtherm" A as the fuel assembly coolant and at 9.5-inch square lattice pitch with "Dowtherm" A, H_2O, D_2O, and air as the coolants. Both NUOR and EUMT reference lattices were used in the THUD I experiments, while only the NUOR reference lattice was used in the THUD II experiments.

Details of the measurements including the SE loading patterns, the measured κ^2's, the moderator purities and temperatures, and the Persson plots are given in Appendix B. The results, including comparison HAMMER calculations to be discussed later, are given in Tables IV and V. As shown by Table IV, the EUMT and NUOR host lattices gave very nearly the same numerical results, but the data show better internal consistency with the NUOR lattice.

TABLE IV

THUD I Bucklings from SE Substitution Measurements

Lattice Pitch		Coolant	Reference Lattice	D_2O Purity, mol %	Material Buckling, μB[a]		
						HAMMER Calculation	
					Experiment	6-Ring Geom	Homog 85 Cell
9"	Δ	"Dowtherm" A	NUOR	99.70	620	578	617
9"	Δ	"Dowtherm" A	EUMT	99.70	625	578	617
9.5"	□	"Dowtherm" A	NUOR	99.70	526	519	549
9.5"	□	"Dowtherm" A	EUMT	99.70	535	519	549
10.5"	□	"Dowtherm" A	NUOR	99.61	438	452	475
9.5"	□	D_2O	NUOR	99.56	592	587	613
9.5"	□	H_2O	NUOR	99.52	478	474	504
9.5"	□	Air	NUOR	99.52	612	582	591

(a) 1 $\mu B = 10^{-6} cm^{-2}$

TABLE V

THUD II Bucklings from SE Substitution Measurements

Lattice Pitch	Coolant	D_2O Purity, mol %	Material Buckling, μB		
			Experiment	HAMMER Calculation 6-Ring Geom	HAMMER Calculation Homog 85 Cell
9" Δ	"Dowtherm" A	99.20	377	396	439
9.5" □	"Dowtherm" A	99.49	347	370	403
10.5" □	"Dowtherm" A	99.46	298	320	342
9.5" □	D_2O	99.17	502	508	525
9.5" □	H_2O	99.14	214	233	270
9.5" □	Air	99.16	560	502	514
			521[a]		
			507[a]		

(a) Values obtained by diffusion theory analysis of 9 and 13 Test Assembly Lattices respectively; all others by modified Persson analysis.

TMT

Substitution buckling measurements were also performed in the SE on the three-tube assemblies of enriched thorium metal (TMT Type I - Figure 3) and on the larger of the two-tube assemblies (TMT Type II - Figure 4). The three-tube assemblies were studied with "Dowtherm" A, D_2O, and air coolants at a 9.5-inch square lattice pitch and with "Dowtherm" A as the coolant at a 10.5-inch square pitch and a 12.12-inch triangular pitch. The two-tube assemblies were investigated with "Dowtherm" A only at a 9.5-inch and a 10.5-inch square lattice pitch. Details of the measurements are given in Appendix B. The results are given in Table VI.

TABLE VI

TMT Bucklings from SE Substitution Measurements

TMT Assembly Type	Lattice Pitch	Coolant	D_2O Purity, mol %	Material Buckling, μB	
				Experiment	HAMMER
I	9.5" □	"Dowtherm" A	99.37	664	662
I	9.5" □	D_2O	99.40	746	712
I	9.5" □	Air	99.39	781	696
				705[a]	
II	9.5" □	"Dowtherm" A	99.36	642	677
II	10.5" □	"Dowtherm" A	99.36	601	603
I	10.5" □	"Dowtherm" A	99.33	607	558
I	12.12" Δ	"Dowtherm" A	99.32	519	527

(a) Value obtained by diffusion theory analysis; all other values by modified Persson analysis.

PDP BUCKLING MEASUREMENTS

TMT

Substitution buckling measurements on the TMT fuel assemblies (Figures 3 and 4) were also performed in the PDP at a 12.12-inch triangular lattice pitch using all three assembly types with "Dowtherm" A, D_2O, and air as the test lattice coolants. The measurements were made in a reference lattice, shown in Figure 13, consisting of 55 unclad assemblies of natural uranium tubes surrounded by a two-ring boundary of lithium-aluminum poison rods. The reference fuel assemblies and poison rods are illustrated in Figure 8. Available test fuel was restricted to six or fewer assemblies of each of the three types. These were arranged in up to five substitution patterns for each test lattice configuration. The critical moderator height in the PDP was the parameter measured for each substitution pattern.

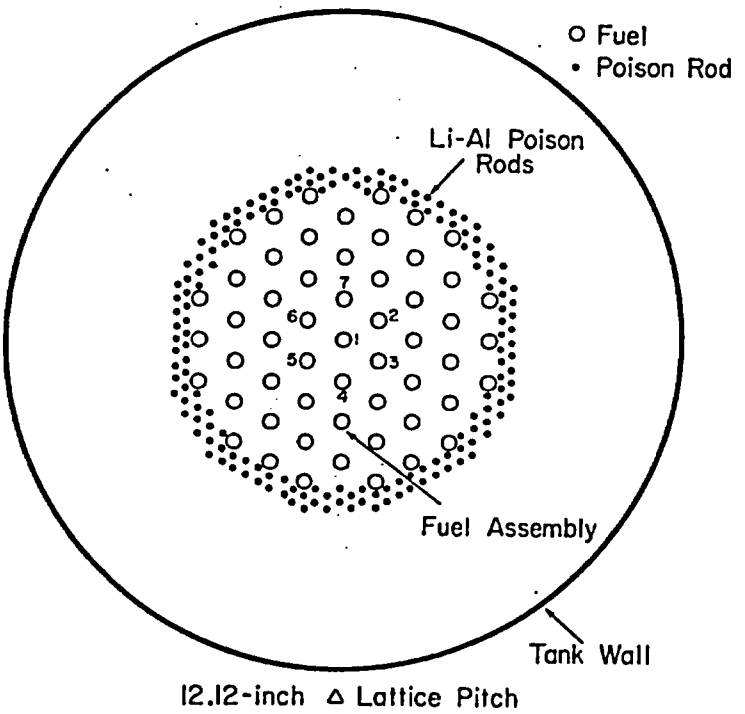

FIG. 13 PDP SUBSTITUTION LATTICE

Chemical analysis of the ^{235}U-Th metal before extrusion by Nuclear Metals, Inc. indicated the possibility of nonuniformity of ^{235}U content in the fuel pieces forwarded to SRL. Because of this, all fuel pieces were assayed in the Test Pile at SRP. For this application the Test Pile indicates reactivity differences between fuel pieces with a uniform ^{232}Th but varying ^{235}U content and a standard fuel piece with similar dimensions. The Test Pile data (period measurements in inhour units) were fed into a fuel matching code which combined fuel pieces into sets of the two or three tubes required for each of the three assembly types. The criteria for matching were uniform bucklings between the matched sets. The first and best assembly was made up of near average tubes of all diameters. The second assembly contained slightly above average and slightly below average individual tubes so as to give the proper overall average. The procedure was continued until six assemblies of each type were obtained. The substitution measurements utilized the "best" assemblies as often as possible, minimizing the effects of ^{235}U segregation.

A detailed listing of the PDP loading patterns for the TMT buckling measurements is given in Appendix C. Also included in Appendix C are the vertical bucklings, B_z^2, (determined from the critical water height) and the moderator purities and temperatures for each measurement. The D_2O and gas coolant studies for each TMT lattice were completed in the same reactor run. This was possible because remote facilities were used to purge the D_2O coolant by helium gas under pressure.

The measured water heights at criticality for each substitution loading were converted to values of vertical buckling, B_z^2, using extrapolation distances measured from foil activations. A correction (0.848 $\mu B/^oC$ for the reference lattice) was applied to reduce the data to a reference temperature of 21.76°C, and an experimentally determined correction for moderator isotopic degradation was applied to correct to a reference purity of 99.50 mol % D_2O. The purity correction was derived from periodic measurements of the one-region natural uranium driver lattice, which gave a closely linear correlation between lattice buckling and time. A radial geometric buckling value of 374.5 μB was determined by fitting a J_o Bessel function to foil activation data for the reference lattice. The same effective pile radius was used for all lattices.

Analysis of the PDP substitution measurements was carried out by two different methods. The first of these was the one-group perturbation method of Persson, discussed under the SE buckling measurements, in which the substitution measurements are used to extrapolate to the vertical buckling of a reactor the size of the reference reactor but containing all test assemblies.[10]

The second method of analysis utilized the SRL HERESY I code, which performs heterogeneous reactor calculations by the source-sink method of Feinberg[11]. The one-region reference lattice was first mocked up with HERESY with all input parameters except η having been calculated with the HAMMER code[6]. The HERESY value of η for the reference lattice was then determined by making the HERESY computation of B_z^2, or equivalently, the critical water height, correspond to that measured experimentally. Next a similar HERESY computation was set up for the substituted lattice, using the previously determined parameters for the reference lattice and HAMMER computed parameters for the test fuel except for η, which again was varied until the computed water height agreed with that measured. A final HERESY problem was then run with a full load of test assemblies to determine the lattice buckling. If all the test assemblies were the same, if no errors existed in the experiments, and if the calculations were exact, then the values of η obtained from all substitutions, using a specific assembly type and coolant, would be the same. Actually one observes some scatter. Values quoted in Tables VII and VIII are a weighted average of the individual substitutions.

The buckling values determined from the HERESY analysis are listed in Table VII and are compared with the Persson results and the HAMMER calculations in Table VIII.

The Persson analysis of the experimental data was hampered somewhat by the lack of a sufficient number of test assemblies. This caused all of the results to be clustered together on the Persson plots (Figure 43), and a large extrapolation was required for the final bucklings. Also, despite the detailed fuel matching, it is apparent from the buckling measurements that differences were still present. The HERESY analysis, in contrast, does not amplify errors from differences in buckling of individual test assemblies; thus HERESY-derived bucklings are believed to be more accurate than those obtained by the Persson analysis.

UO_2 Fuel Assembly

A number of fuel tubes had been fabricated from natural uranium oxide for use in earlier D_2O power reactor studies. Substitution buckling measurements with air and "Dowtherm" A coolants in a two-tube assembly of these fuel tubes were included in the present study because the tubular geometry is compatible with the one-dimensional HAMMER code, and a comparison between experimental and calculated buckling values provides an excellent check on the validity of the organic kernel used in the HAMMER code.

TABLE VII

TMT Bucklings from PDP by HERESY Analysis
12.12-inch triangular lattice pitch at 99.50 mol % D_2O

TMT Assembly Type	Coolant	No. of Fuel Assemblies Substituted	B_M^2, μB	Linear Avg, μB
I	"Dowtherm" A	1	536.8	
		3	537.8	
		4	537.8	
		6	537.8	538
I	D_2O	1	619.8	
		4	625.0	622
I	Air	1	639.1	
		4	642.2	641
II	"Dowtherm" A	1	531.3	
		3	537.4	
		4	533.7	
		6	535.1	534
II	D_2O	1	620.9	
		3	626.4	
		4	623.5	
		6	619.6	623
II	Air	1	628.9	
		3	631.8	
		4	630.8	
		6	626.4	630
III	"Dowtherm" A	1	380.8	
		3	394.4	
		4	393.6	390
III	D_2O	1	502.3	
		3	515.1	
		4	513.1	
		6	511.1	511
III	Air	1	518.3	
		3	529.9	
		4	529.9	
		6	537.0	529

TABLE VIII

TMT Bucklings from PDP Measurements
12.12-inch triangular lattice pitch at 99.50 mol % D_2O

TMT Assembly Type	Coolant	Material Buckling, μB: Experiment: Persson Analysis	Material Buckling, μB: Experiment: HERESY Analysis	Material Buckling, μB: HAMMER Calculation
I	"Dowtherm" A	532	538	546
I[a]	"Dowtherm" A	542	-	546
I	D_2O	619	622	612
I	Air	634	641	616
II	"Dowtherm" A	526	534	557
II	D_2O	612	623	612
II	Air	621	630	603
III	"Dowtherm" A	357	390	379
III	D_2O	509	511	517
III	Air	531	529	526

(a) SE value from Table VI corrected to 99.50 mol % D_2O.

A cross section of the test UO_2 fuel assembly is shown in Figure 5. The fuel tubes were fabricated by vibratorily compacting UO_2 into aluminum tubes to a nominal density of 8.83 g/cm^3.

Substitution measurements were made in reference lattices of natural uranium tubes, shown in Figure 9, at triangular lattice pitches of 9.33 and 12.12 inches. The analysis was performed using the Persson successive substitution technique. The material buckling values derived from the experiments are summarized and compared with HAMMER calculations in Table IX.

TABLE IX

Bucklings of Tubular UO_2 Fuel Assemblies[a] from PDP by Persson Analysis

Lattice Pitch	Coolant	D_2O Purity, mol %	Material Buckling, μB: Experiment	Material Buckling, μB: HAMMER
9.33" Δ	Air	99.58	467	432
9.33" Δ	"Dowtherm" A	99.58	340	297
12.12" Δ	Air	99.58	375	361
12.12" Δ	"Dowtherm" A	99.58	247	240

(a) See Figure 5.

ACTIVATION MEASUREMENTS IN THE SE

Foil activation measurements in the substitution lattices in the SE were used to determine intracell neutron flux distributions, spectral indices, and reaction rates for the various test lattices. Table X lists the foil types and the counting conditions for each type. Except for the ^{232}Th activities all foils were counted for gamma activity with NaI(Tl) counters. The ^{233}Th was counted for beta activity with an NE-102 plastic phosphor 1/16 inch thick. The foils were placed at representative positions throughout the fuel and coolant as detailed under the individual lattice discussions. Reference irradiations were also made in the thermal column of the SP simultaneously with the lattice irradiations.

TABLE X

Foils and Counting Conditions for THUD and TMT Activation Measurements

Detector	Activity	Half-Life	wt %	Other Metals in Alloy	Thickness, Inch	Threshold or Window, kev
^{63}Cu	^{64}Cu	12.9 hr	-	-	.010, .005	400
^{176}Lu	^{177}Lu	6.8 day	15	Al	.020	35
^{235}U	FP	-	5	Al	.005	850
^{232}Th	FP (δ)	-	-	-	.002	850 (FP)
						60-110 (^{233}Th)
^{232}Th	^{233}Th (ρ)	22.1 min	-	-	.002, .008	1300[a] (FP)
						100-400[a] (^{233}Th)

(a) β count

Cadmium ratio measurements with the copper foils were used to determine the thermal neutron flux distributions in terms of the reaction rates of a 1/v detector. When combined with the subcadmium ^{177}Lu activations, the subcadmium ^{64}Cu activations also served to determine the spectral indices for the thermal neutrons in terms of the ratios of ratios between subcadmium ^{64}Cu and ^{177}Lu activations in the thermal column and lattice positions, i.e., as

$$\frac{g_L}{g_R} = \frac{\left[{}^{177}Lu/{}^{64}Cu\right]_{Lattice}}{\left[{}^{177}Lu/{}^{64}Cu\right]_{Reference}}$$

where the g_L/g_R terminology is adopted in analogy to the Westcott[12] g factors. The fission product measurements on ^{235}U and ^{232}Th determined the relative fission rates for these nuclides in the test fuel assemblies, while the ^{235}U cadmium ratio measurements provided indices of the epithermal-to-thermal neutron flux ratios. The $^{232}Th/^{235}U$ fission ratio, δ, was also used to obtain a fast fission factor, ϵ^T, for these lattices from the expression

$$\epsilon^T = 1 + \left[\frac{\nu(^{232}Th) - 1}{\nu(^{235}U)}\right] \delta$$

where $\nu(^{232}Th) = 2.72$ and $\nu(^{235}U) = 2.43$

The ^{232}Th measurements served to determine the spatial distribution reaction rates of the ^{232}Th captures. The ratio, ρ^T, of epithermal-to-thermal neutron captures in ^{232}Th was also determined from a normalization of the thermal ^{232}Th neutron captures to the subcadmium ^{63}Cu captures.

The counting techniques and the methods used for establishing the lattice parameters from the counts are discussed in detail in Appendix D.

THUD I

A summary of the activation measurements made in the THUD I lattices is given in Table XI.

TABLE XI

THUD I Activation Measurements

Lattice Pitch	Coolant	Fast Fission δ Measurement	Thermal Neutron Distribution Measurement
9.0" Δ	"Dowtherm" A	x	x
9.5" □	"Dowtherm" A	x	x
9.5" □	D_2O	-	x
10.5" □	"Dowtherm" A	-	x

The SE lattices used for these measurements are shown in Figure 14. The twelve fuel assemblies immediately surrounding the irradiation assembly at the center were identical to it and provided a uniform environment for the measurement. The remaining fuel positions in the outer region of the SE contained NUOR fuel assemblies (Figure 6).

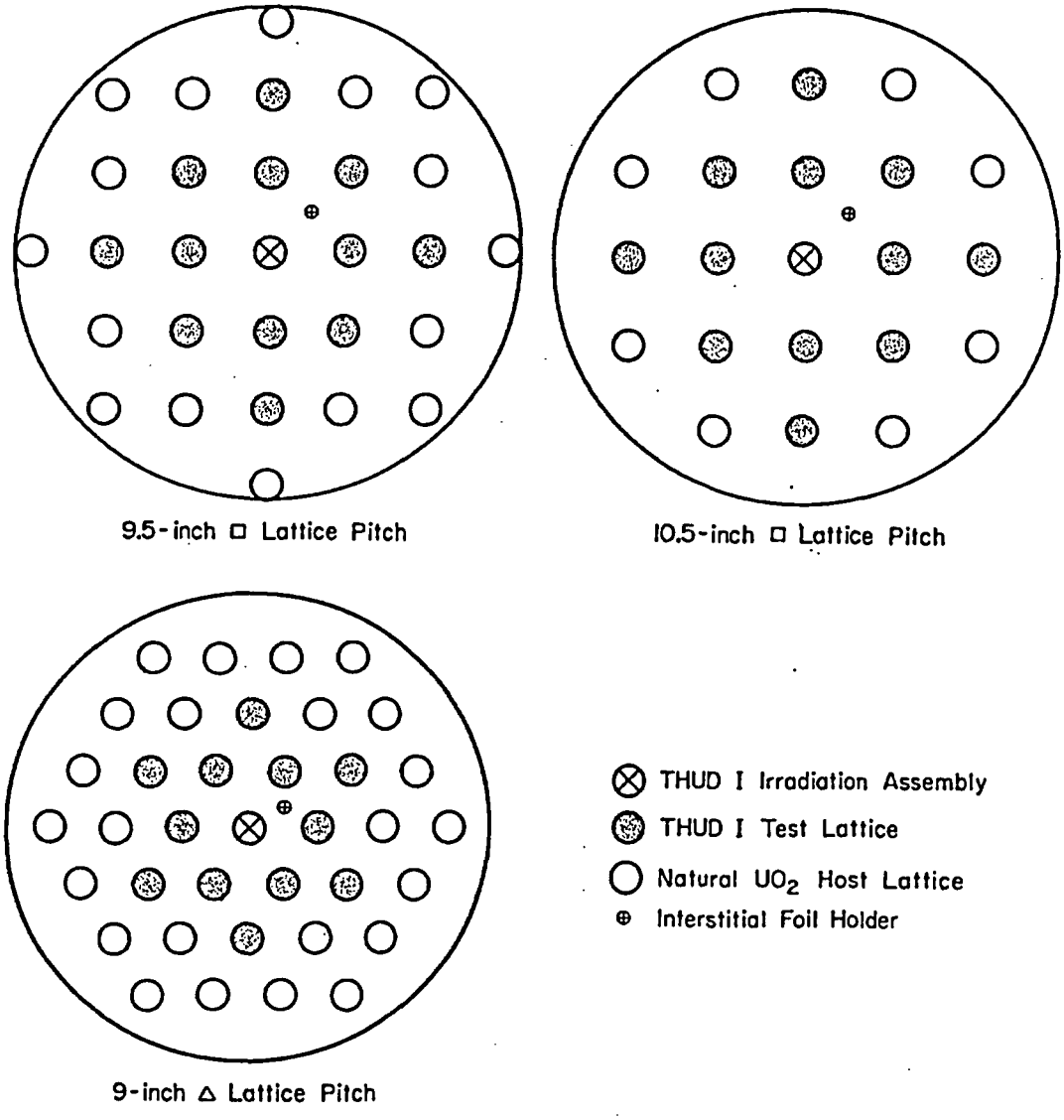

FIG. 14 THUD I IRRADIATION LATTICES

The THUD I irradiation assembly was identical to the THUD I assemblies used in the buckling measurements (Figures 1 and 2) except that a fuel rod representative of each radius, as designated by the numerals in Figure 15, contained a 5-1/4-inch long removable section, in which the foils were loaded. The removable rod sections were centered at 21-5/8 inches from the bottom of the assembly. The details of the removable rod segment and of the foil loadings are given in Figure 16.

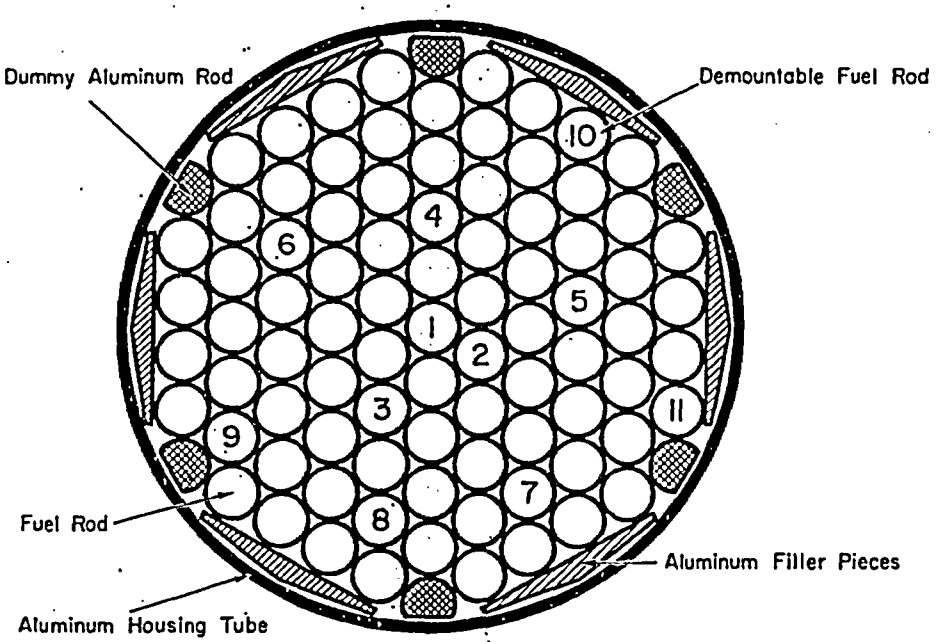

FIG. 15 THUD I IRRADIATION ASSEMBLY

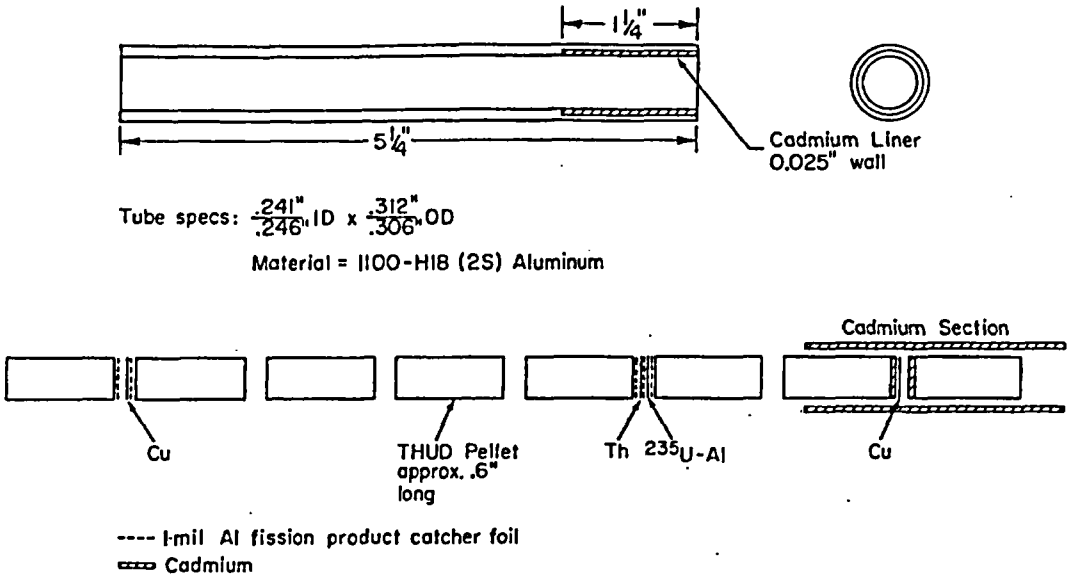

FIG. 16 THUD I REMOVABLE FOIL LOADING ROD

The results of the δ measurements are summarized and compared to HAMMER (6-ring model) calculations in Table XII. The subcadmium copper activation profiles in the fuel and moderator are plotted and compared with HAMMER (homogeneous model) calculations in Figure 17. The experimental data have been normalized to agree with the HAMMER normalization (unity at r = 0) by requiring the volume weighted experimental fuel average value to equal that computed by HAMMER.

TABLE XII

THUD I Fast Fission Measurements[a]

Lattice Pitch	Coolant	D_2O Purity, mol %	$\left[\frac{Th_1}{U_1}\right]^{sso}_{FP}$	$\left[\frac{Th_2}{U_2}\right]^{sso}_{FP}$	$\bar{\gamma}$ (t = 60 min)	ε - 1	P(t)	ε Expt	ε HAMMER
9.5" □	"Dowtherm" A	99.65	.188 x 10^{-3}	.217 x 10^{-3}	.198 x 10^{-3}	.0070	.96	1.0073	1.0055
9.0" △	"Dowtherm" A	99.62	.166 x 10^{-3}	.210 x 10^{-3}	.181 x 10^{-3}	.0064	.96	1.0067	1.0056

(a) See Appendix D for identification of symbols.

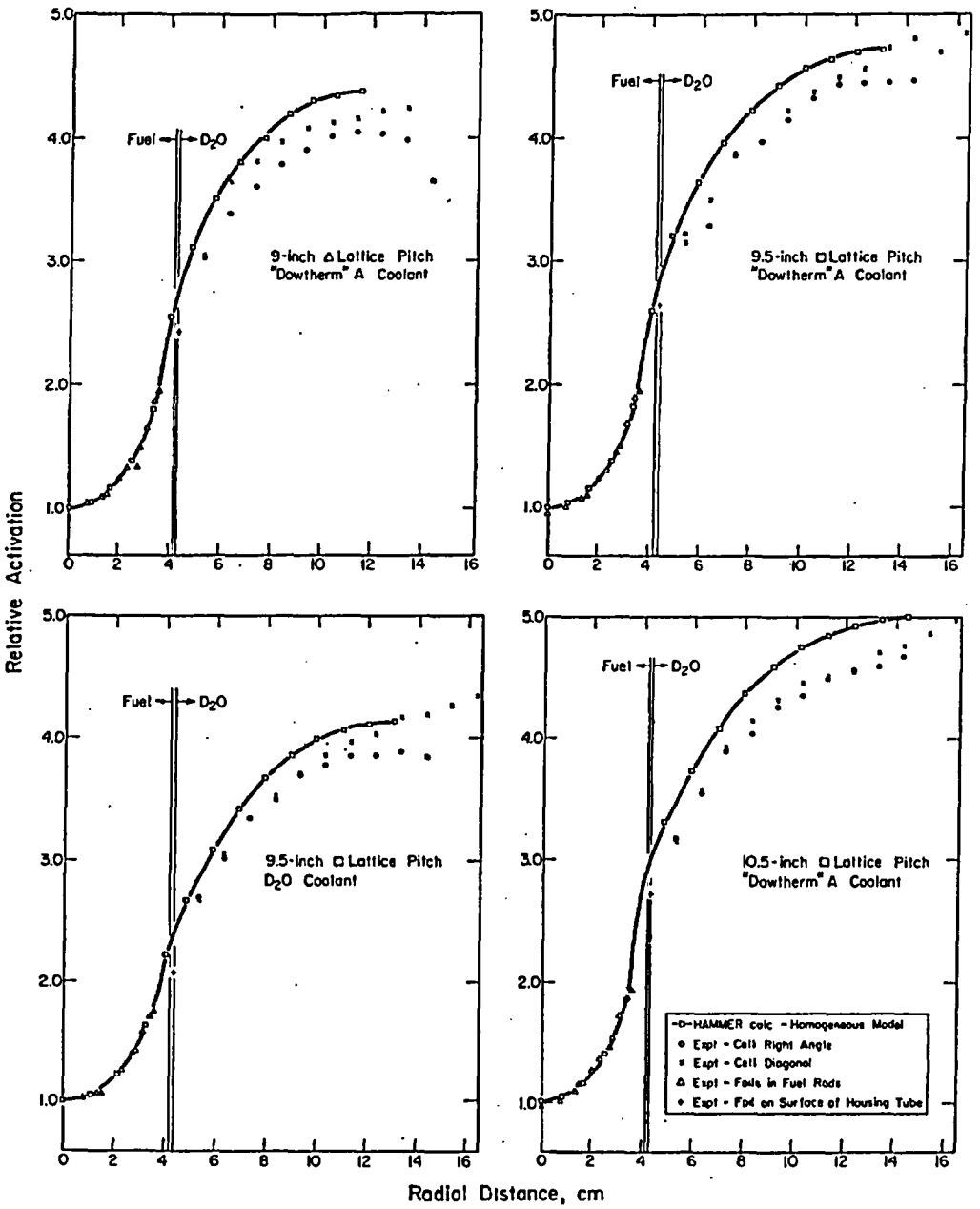

FIG. 17 SUBCADMIUM COPPER ACTIVATION PROFILES - THUD I

THUD II

A summary of the scope of the activation measurements for the THUD II lattices is given in Table XIII.

TABLE XIII

THUD II Lattice Parameter Measurements

Lattice Pitch	Coolant	Fast Fission δ Meas	Resonance Escape ρ Meas	Thermal Neutron Distr Meas	Spectral Index Meas
9.33" Δ	"Dowtherm" A	-	x	x	x
9.33" Δ	D_2O	x	x	-	-
9.33" Δ	Air	x	x	-	-
11.5" □	"Dowtherm" A	-	x	x	x
11.5" □	D_2O	-	x	x	x
11.5" □	Air	-	x	x	x
∞	Air	x	x	-	-

The SE lattices used for the THUD II activation measurements are shown in Figure 18. The irradiation assembly containing the foils was placed in the central site. The 6 or 8 fuel assemblies immediately surrounding the irradiation assembly were identical to it and provided a uniform environment for the measurement. The remaining fuel positions in the outer region of the SE contained NUOR fuel (Figure 6). The "infinite-pitch" measurement was made with the test assembly at the center of the lattice and only the outermost ring of 18 host assemblies in place.

The THUD II irradiation assembly was identical to the THUD II assemblies used in the buckling measurements (Figures 1 and 2), except that it was constructed in two separate "halves", with the split located along the line AA shown in Figure 19. The individual rods in each "half" had been assembled, spaced to the 0.351-inch THUD II internal pitch in a form, and then rigidly glued together using epoxy resin at the top and bottom and at selected locations along the length. With this arrangement, a 5-1/4-inch-long rod segment from a fuel rod representative of each radius, as designated by the numerals in Figure 19, was accessible for removal after the two halves were separated. The removable rod sections were centered at 21-5/8 inches from the bottom of the assembly.

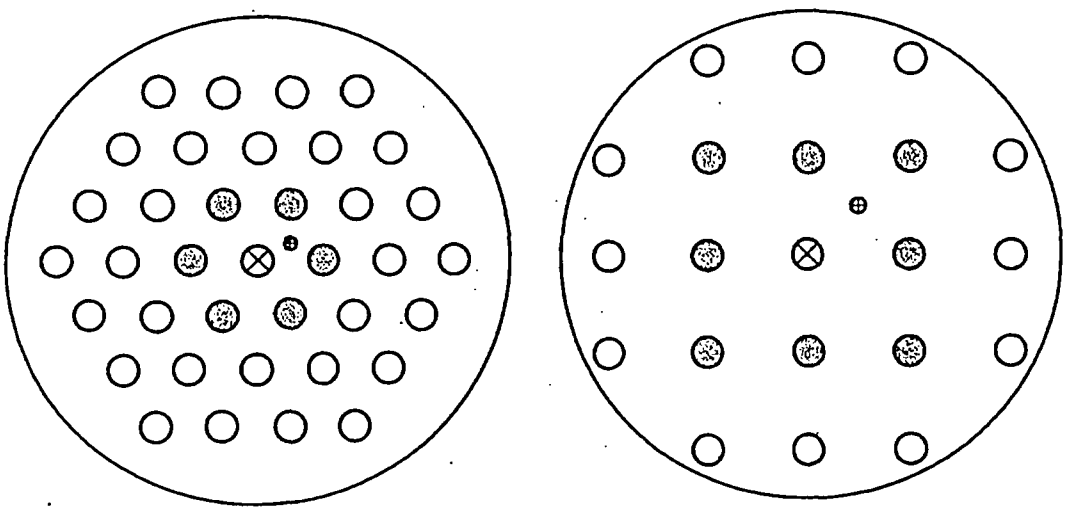

9.33-inch △ Lattice Pitch

11.5-inch □ Lattice Pitch

⊗ THUD II Irradiation Assembly

◎ THUD II Test Lattice

○ Natural UO_2 Host Lattice

⊕ Interstitial Foil Holder

FIG. 18 THUD II IRRADIATION LATTICES

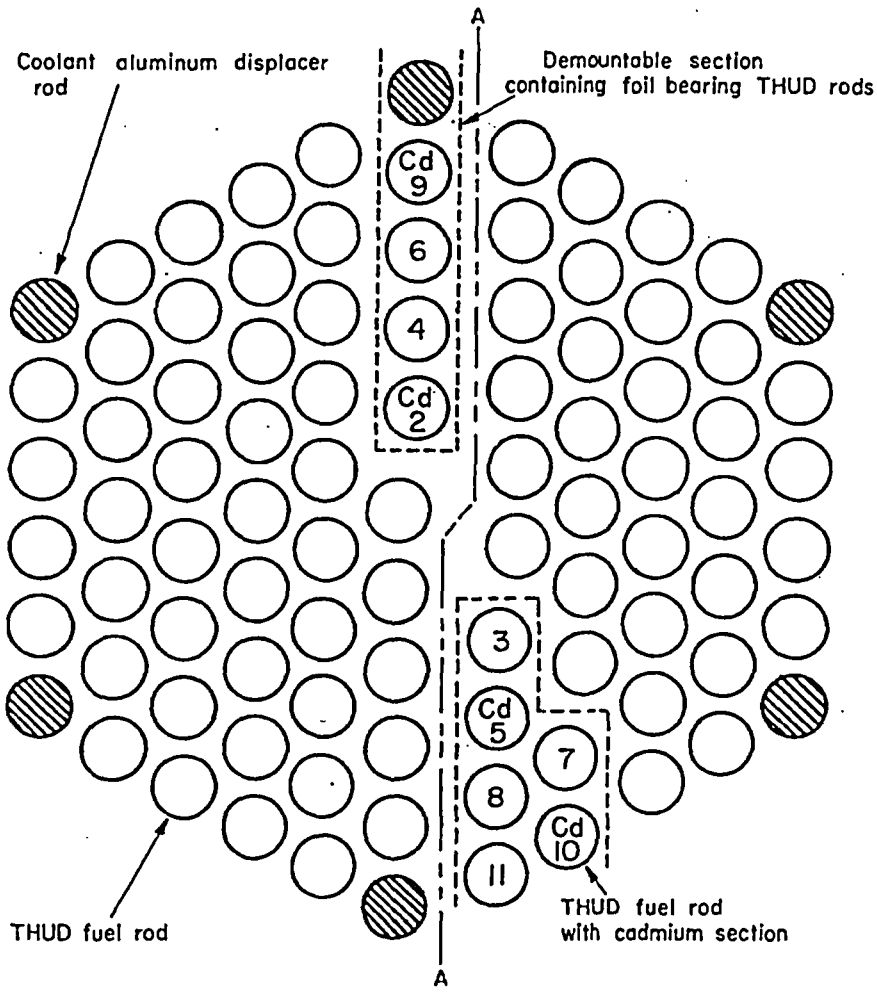

FIG. 19 THUD II IRRADIATION ASSEMBLY MADE UP OF PREASSEMBLED HALVES

They were identical to the rod segments used in the THUD I experiments (Figure 16) with the cadmium section removed. To minimize the thermal flux perturbation caused by cadmium only four of the rods, marked Cd on Figure 19, contained cadmium. The cadmium "pillbox" was constructed by wrapping a 1/4-inch wide strip of cadmium around the exterior of the rod. Details are shown in the foil loading diagram (Figure 20). Although this "pillbox" was not completely tight, calculations indicated that thermal neutron leaking through the gaps would contribute negligible errors for any of the parameters measured. The 1/4-inch long cadmium-wrapped section in each of the four test rods was about 1.8 inches away from the nearest thermal neutron foil detector.

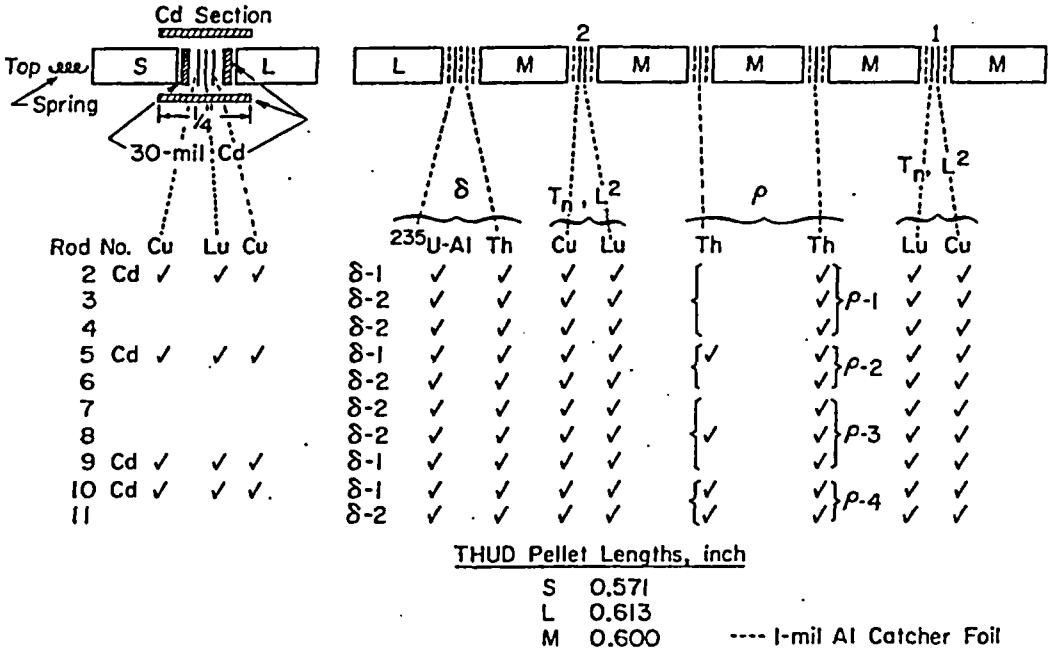

FIG. 20 THUD II FOIL LOADING

The results of the resonance capture measurements are summarized in Table XIV and are compared with HAMMER calculations based both on the homogeneous model and the ring model. The experimental results for $\overline{\rho}$ are consistently higher than the calculated values indicating a larger resonance capture in the thorium than the HAMMER code predicts.

TABLE XIV

THUD II Resonance Capture Measurements

Run No.	Lattice Pitch	Coolant	D_2O Purity, mol %	Th Cd Ratio[a] Rods 2,3,4	Rods 5,6	Rods 7,8,9	Rods 10,11	$\bar{\rho}$ Expt	HAMMER Homog	HAMMER Ring
132	11.5" □	Air	99.44	6.65	6.93	6.60	7.59	.166	.148	.141
133	11.5" □	D_2O	99.43	5.31	5.84	6.47	7.98	.182	-	.161
134	11.5" □	"Dowtherm" A	99.43	4.65	5.53	6.66	8.40	.184	-	.164
128	9.33" Δ	D_2O	99.57	4.11	4.34[b]	4.83[c]	5.16	.274	-	.242
129	9.33" Δ	Air	99.57	4.53	4.72	4.76	4.93	.266	.239	.225
131	9.33" Δ	Air	99.46	4.61	4.80[b]	5.15[c]	5.07	.255	.238	.224
135	9.33" Δ	"Dowtherm" A	99.43	3.92	4.48	5.11	6.20	.248	-	.230
130	∞	Air	99.49	8.54	7.77	8.02	9.83	.132	.098	-

(a) See Figure 19 for rod number identification.
(b) Cd ratio for rods 5, 6, and 7.
(c) Cd ratio for rods 8 and 9.

The results of the fast fission measurements are summarized in Table XV and compared with HAMMER calculations based on the 6-ring model.

TABLE XV

THUD II Fast Fission Measurements[a]

Lattice Pitch	Coolant	D_2O Purity, mol %	$\left[\frac{Th_1}{U_1}\right]^{eso}_{FP}$	$\left[\frac{Th_2}{U_2}\right]^{eso}_{FP}$	$\bar{\gamma}$ (t = 60 min)	$\epsilon - 1$	P(t)	ϵ Expt	ϵ HAMMER
∞	Air	99.49	$.176 \times 10^{-3}$	$.176 \times 10^{-3}$	$.176 \times 10^{-3}$	.0062	.96	1.0065	1.0051
9.33" Δ	"Dowtherm" A	99.43	$.178 \times 10^{-3}$	$.175 \times 10^{-3}$	$.177 \times 10^{-3}$	.0062	.96	1.0065	1.0049

(a) See Appendix D for identification of symbols.

The subcadmium copper activation profiles in the fuel and moderator are shown and compared with HAMMER (homogeneous model) calculations in Figure 21. Similar profiles in the fuel only are shown in Figure 22. The experimental data have been normalized to agree with the HAMMER normalization (unity at r = 0) by requiring the volume-weighted activation value in the experimental fuel to equal that computed by HAMMER.

The subcadmium activity ratio, $g_L/g_R = \dfrac{\left[^{177}Lu/^{64}Cu\right]_{\text{Lattice}}}{\left[^{177}Lu/^{64}Cu\right]_{\text{Reference}}}$,

used as a spectral index is plotted and compared with HAMMER (homogeneous model) calculations in Figure 23. An intuitively surprising result is the fact that although "Dowtherm" A is the

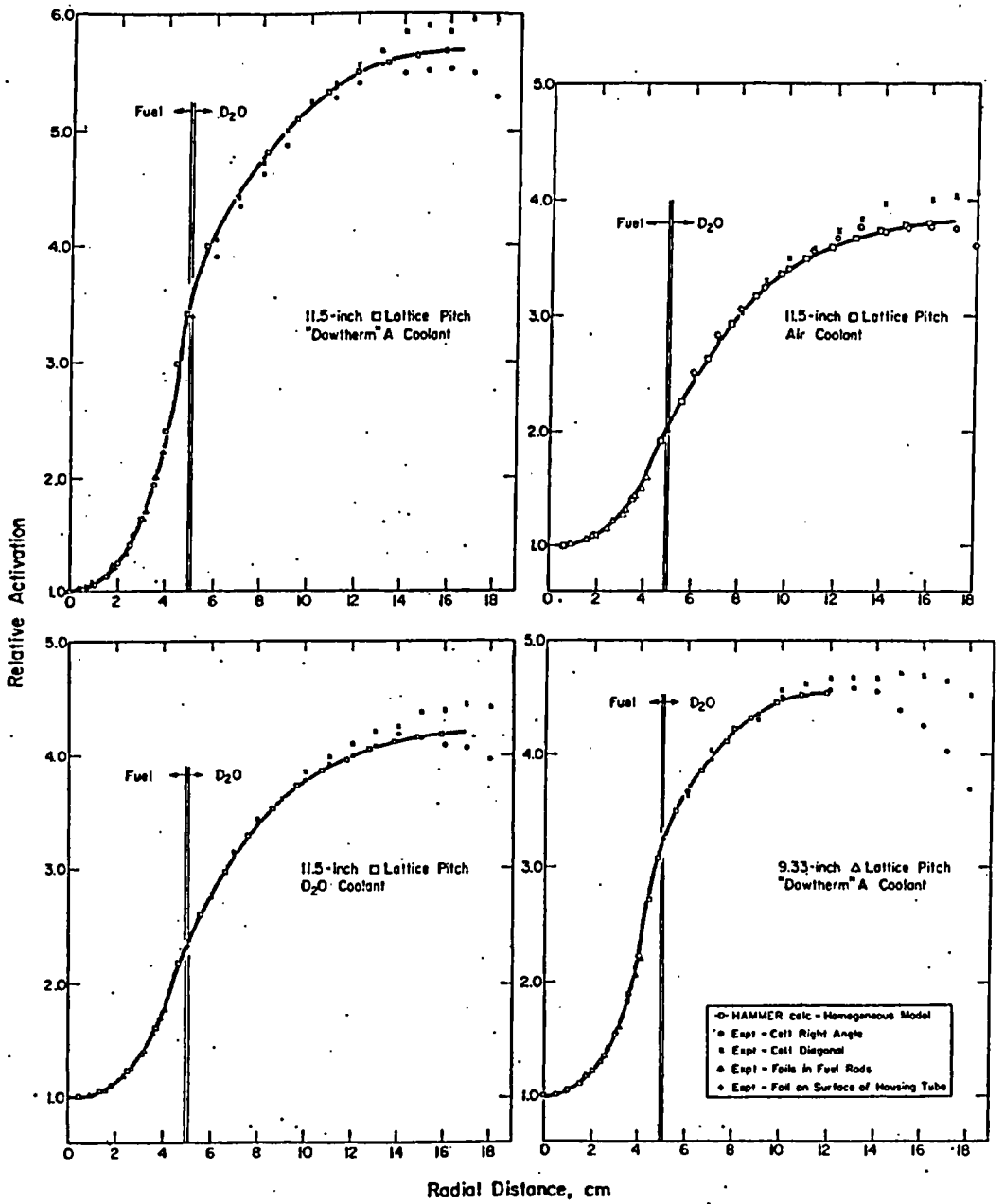

FIG. 21 SUBCADMIUM COPPER ACTIVATION PROFILES - THUD II

- 46 -

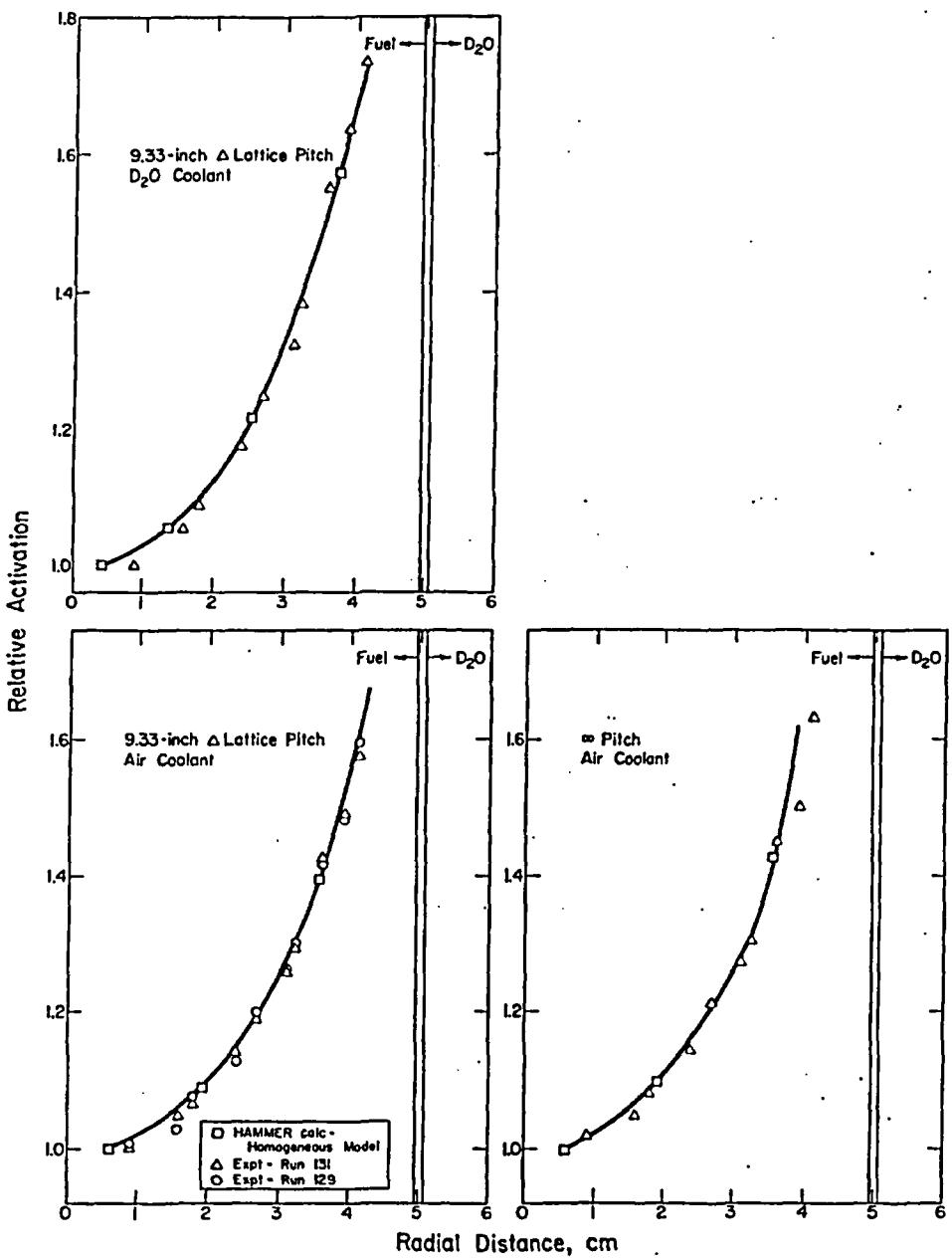

FIG. 22 SUBCADMIUM COPPER ACTIVATION PROFILES IN THE FUEL ONLY - THUD II

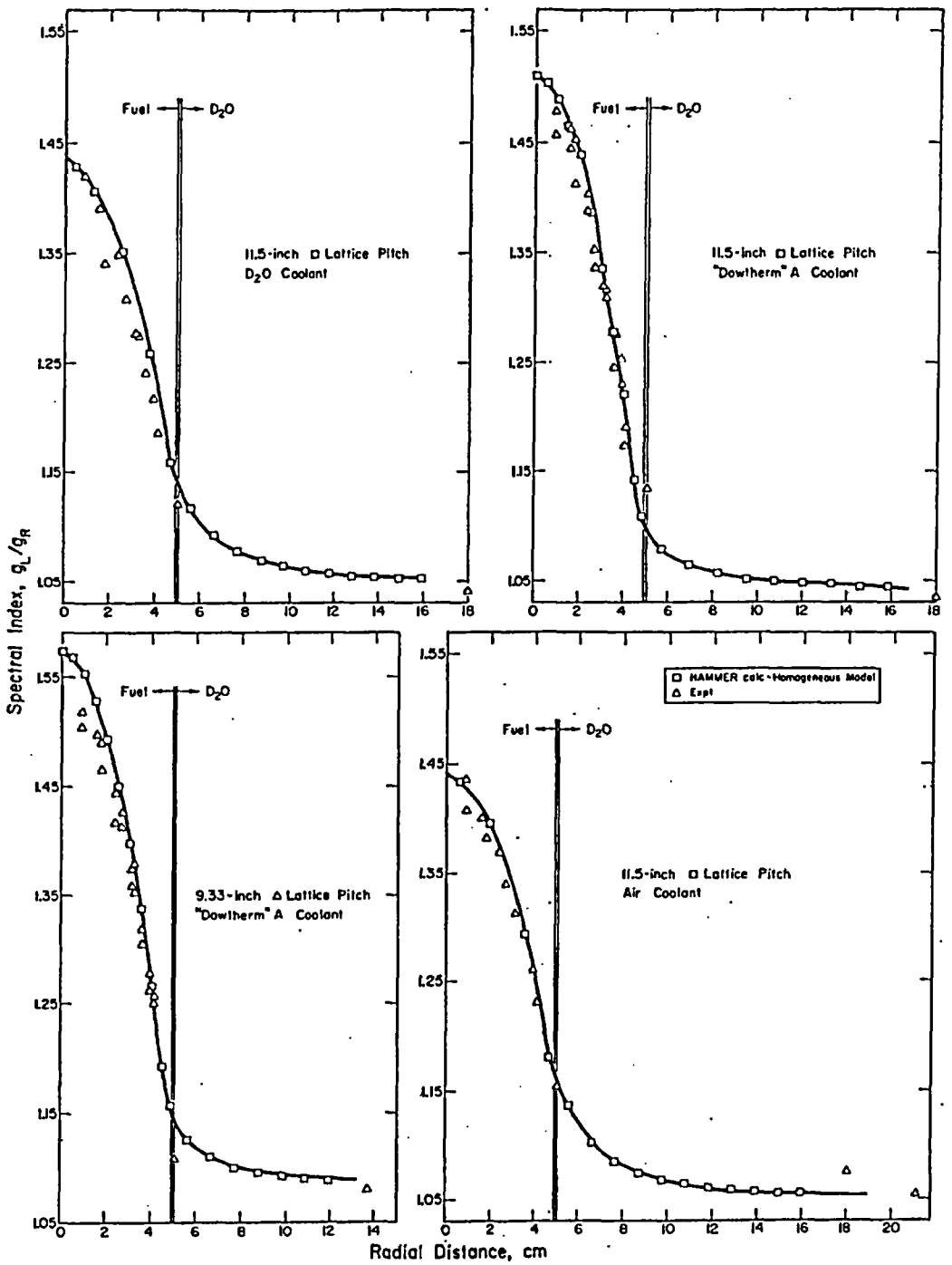

FIG. 23 SPECTRAL INDEX PROFILES - THUD II

best moderator of the coolants studied, the spectral index (g_L/g_R) in the center of the organic-filled THUD II assembly is higher than in the D_2O- or gas-cooled (air) cases at the same lattice pitch. The HAMMER code predicts the same result. A simple qualitative explanation can be made. The scattering cross section for hydrogen in organic increases strongly at low neutron energies. This serves to selectively reflect the lower energy neutrons incident on the outer surface of the fuel assembly, allowing only the higher energy neutrons to reach the center of the assembly. Energy exchanges between hydrogen and neutrons within the assembly do tend to restore the low energy end of the spectrum, and do decrease the average neutron temperature over the entire lattice. However, within the fuel assembly this effect is less important than the diffusion hardening effect.

TMT

A summary of the scope of the activation measurements for the TMT lattices is given in Table XVI.

TABLE XVI

TMT Lattice Parameter Measurements

Lattice Pitch	Coolant	TMT Assembly Type	Fast Fission δ Meas	Resonance Escape ρ Meas	Thermal Neutron Distr Meas	Spectral Index Meas	^{235}U Cd Ratio Meas
9.5" □	"Dowtherm" A	I	x	x	x	x	x
9.5" □	D_2O	I	x	x	x	x	x
9.5" □	Air	I	x	x	x	x	x
10.5" □	"Dowtherm" A	I	x	x	x	x	x
9.5" □	"Dowtherm" A	II	x	x	x	x	x
10.5" □	"Dowtherm" A	II	x	x	x	x	x

The SE lattices used for the TMT parameter measurements are shown in Figure 24. The irradiation assembly containing the detector foils was placed in the central site. The eight fuel assemblies immediately surrounding the test assembly were identical to it and provided a uniform environment for the measurement. The remaining fuel positions in the outer region of the SE contained NUOR fuel assemblies (Figure 6).

The Type I and Type II TMT irradiation assemblies were identical to the TMT assemblies used in the SE buckling measurements (Figures 3 and 4), except that the center fuel piece in each column contained two machined window sections as shown in Figures 25 and 26. The removable window sections permitted foil loading and unloading operations with a minimum of radiation exposure. The foil loading details are summarized in Figure 27. The speci-

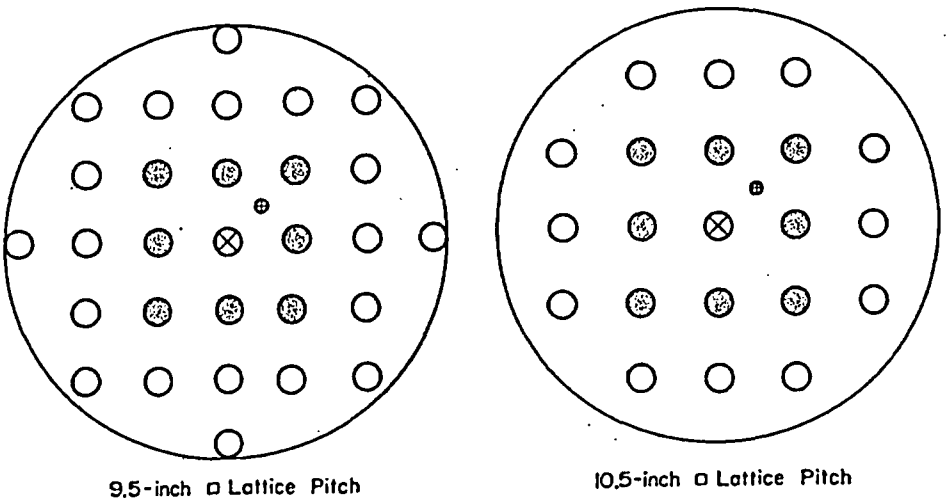

FIG. 24 TMT IRRADIATION LATTICES

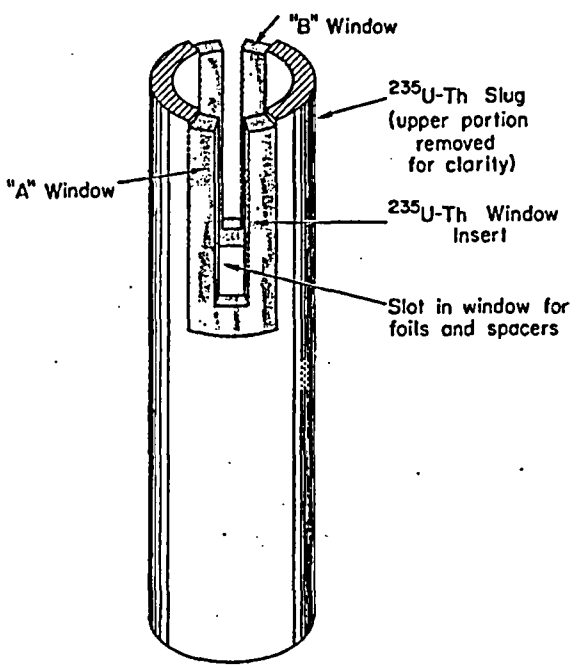

FIG. 25 TMT IRRADIATION SLUG

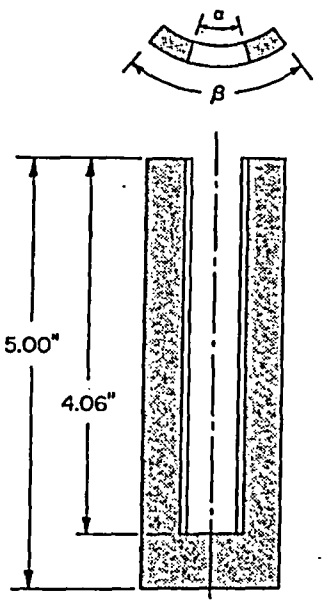

		TMT Slug OD	TMT Slug ID	Angle Covered by Insert, degrees α	Angle Covered by Insert, degrees β
A Section	Outer	3.620"	3.260"	16.3	47.7
	Intermediate	2.505"	2.035"	27.4	68.6
	Inner	1.210"	0.710"	43.9	139.1
B Section	Outer	3.620"	3.260"	18.5	47.7
	Intermediate	2.505"	2.035"	30.5	68.6
	Inner	1.210"	0.710"	50.5	139.1

FIG. 26 TMT WINDOW SECTIONS

A = Small Window Section, Figs. 25 and 26

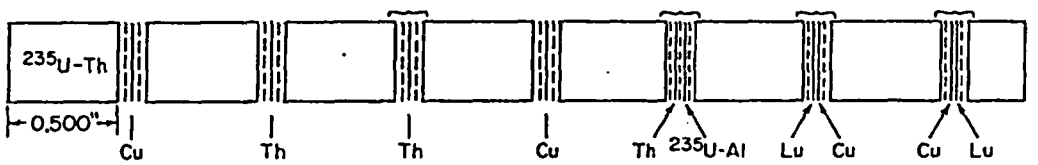

Bottom

B = Large Window Section, Figs. 25 and 26

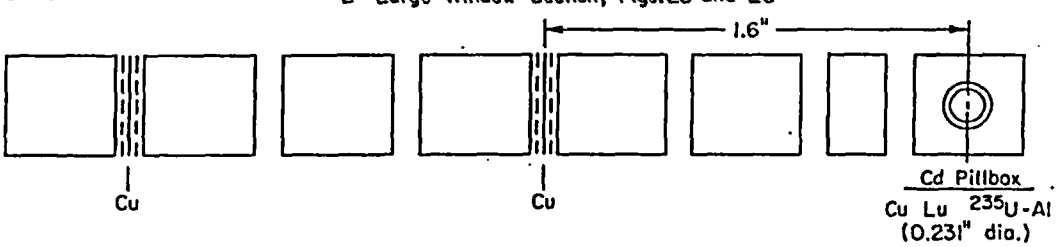

--- = 1-Mil Al Catcher Foil

FIG. 27 FOIL LOADING FOR TMT FUEL

fications for the foils and the counting procedures used in the measurements are given in Table X. The epicadmium activations of Cu, Lu, and ^{235}U were obtained by including small, 0.231-inch diameter foils of the same materials used for the other measurements in a small (0.375-inch diameter x 0.125-inch thick) cadmium pillbox located in a recess in the top filler piece of the "B" window section for each of the three concentric fuel cylinders. The window sections in each of the fuel cylinders were azimuthally aligned at 120° intervals during loading to minimize the effect of the cadmium on the foil measurements in the adjacent tube(s).

The results of the resonance capture measurements are summarized in Table XVII and compared with HAMMER (ring model) calculations. The measurements of the cadmium ratios for the ^{235}U fission product activities are listed in Table XVIII. Individual fuel tubes as well as assembly average values are listed. The latter are compared to HAMMER computed values. The results of the fast fission measurements and of the corresponding HAMMER (ring model) calculations are summarized in Table XIX.

TABLE XVII

Thorium Resonance Capture in TMT Lattices

Lattice Pitch	Coolant	TMT Assembly Type	D_2O Purity, mol %	Th Cd Ratio			δ	
				Inner	Interm	Outer	Expt	HAMMER
9.5" □	Air	I	99.42	3.18	4.00	4.07	0.343	0.298
9.5" □	D_2O	I	99.42	2.86	3.53	4.17	0.363	0.318
9.5" □	"Dowtherm" A	I	99.41	2.74	3.44	4.53	0.351	0.307
9.5" □	"Dowtherm" A	I	99.40	2.76	3.44	4.59	0.345	0.307
10.5" □	"Dowtherm" A	I	99.40	2.81	3.92	5.18	0.295	0.272
9.5" □	"Dowtherm" A	II	99.41	-	3.74	4.93	0.292	0.272
10.5" □	"Dowhterm" A	II	99.41	-	4.16	5.49	0.254	0.240

TABLE XVIII

^{235}U Cd Ratio Measurements in TMT Lattices

Lattice Pitch	Coolant	TMT Assembly Type	D_2O Purity, mol %	^{235}U Cd Ratio			^{235}U Fission Cd Ratio Fuel Avg	
				Inner	Interm	Outer	Experiment	HAMMER
9.5" □	Air	I	99.42	7.10	10.4	14.4	11.64	11.59
9.5" □	D_2O	I	99.42	7.24	9.69	14.7	11.53	11.92
9.5" □	"Dowtherm" A	I	99.41	7.09	9.42	15.9	11.95	13.09
9.5" □	"Dowtherm" A	I	99.40	6.42	9.04	15.2	11.37	13.09
10.5" □	"Dowtherm" A	I	99.40	7.86	9.67	16.9	12.62	14.93
9.5" □	"Dowtherm" A	II	99.41	-	10.3	14.8	12.76	14.88
10.5" □	"Dowtherm" A	II	99.41	-	12.0	18.3	15.44	17.06

TABLE XIX

Fast Fission Effect in TMT Lattices

Lattice Pitch	Coolant	TMT Assembly Type	D_2O Purity, mol %	$\left[\frac{Th}{235_U}\right]_{FP}^{>850\ kev} \times 10^3$				$\epsilon - 1$	ϵ	
				Inner	Interm	Outer	Avg		HAMMER	Expt Norm to Calc
9.5" □	Air	I	99.42	.513	.307	.209	.270	.0097	1.0087	1.0084
9.5" □	D_2O	I	99.42	.410	.320	.190	.248	.0090	1.0078	1.0078
9.5" □	"Dowtherm" A	I	99.41	.417	.306	.170	.228	.0083	1.0080	1.0072
9.5" □	"Dowtherm" A	I	99.40	.433	.338	.167	.234	.0086	1.0080	1.0075
10.5" □	"Dowtherm" A	I	99.40	.459	.349	.160	.231	.0085	1.0080	1.0074
9.5" □	"Dowtherm" A	II	99.41	-	.301	.187	.219	.0080	1.0069	1.0069
10.5" □	"Dowtherm" A	II	99.41	-	.294	.183	.213	.0078	1.0068	1.0067

The fission product activity ratio curve P(t) was not established for these experiments. Instead the results are standardized to a counting time of 60 minutes after shutdown, and the experiments are normalized [by adjustment of P(t)] to the HAMMER calculation for the Type I assemblies with D_2O coolant in a 9.5-inch square lattice. The results thus normalized are shown in the last column of the table.

The subcadmium copper activation profiles in the fuel and moderator are compared with HAMMER (homogeneous model) calculations in Figures 28 and 29. The results of the HAMMER calculations are shown as the solid lines. The experimental data are normalized as for the lattices discussed previously.

The measured spectral indices, g_L/g_R, defined as for the previous lattices, are compared with HAMMER calculations in Figures 30 and 31.

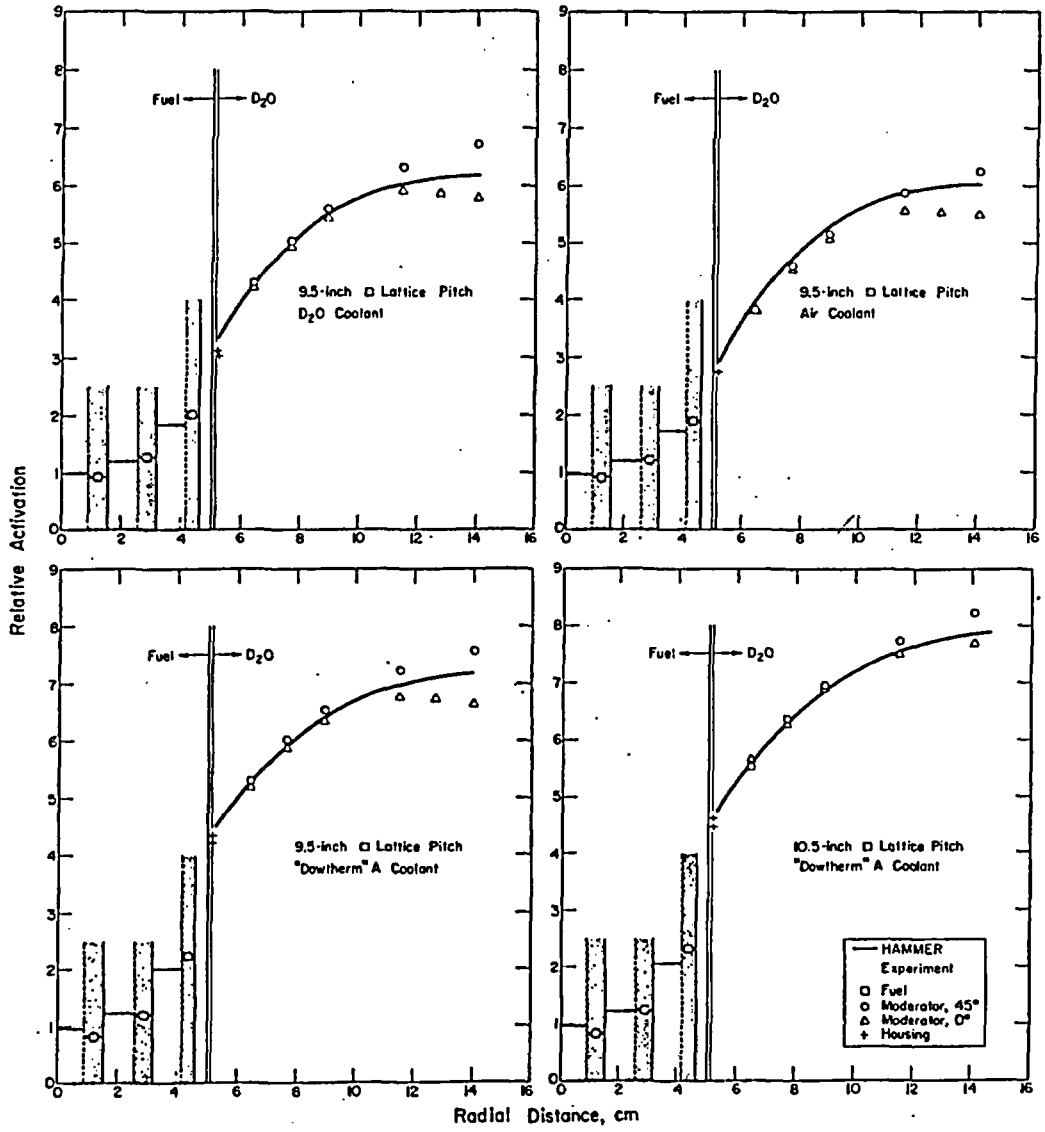

FIG. 28 SUBCADMIUM COPPER ACTIVATION PROFILES - TMT TYPE I

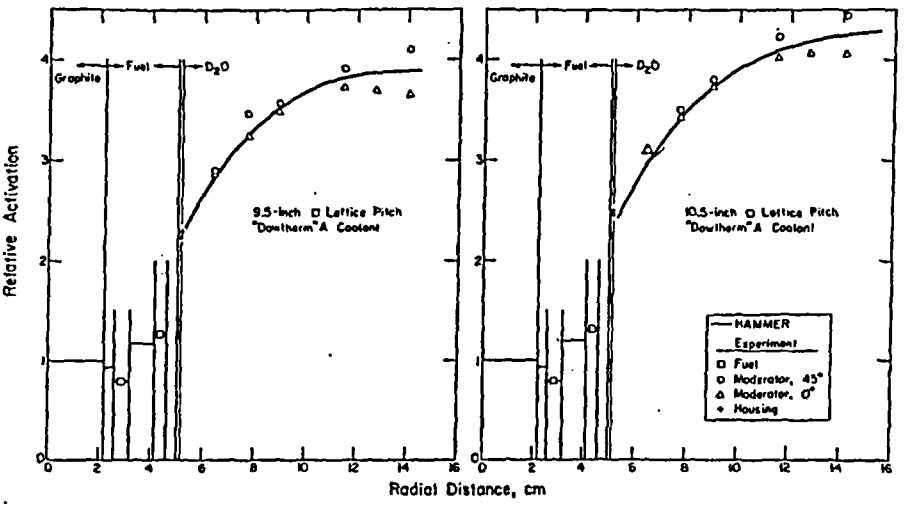

FIG. 29 SUBCADMIUM COPPER ACTIVATION PROFILES - TMT TYPE II

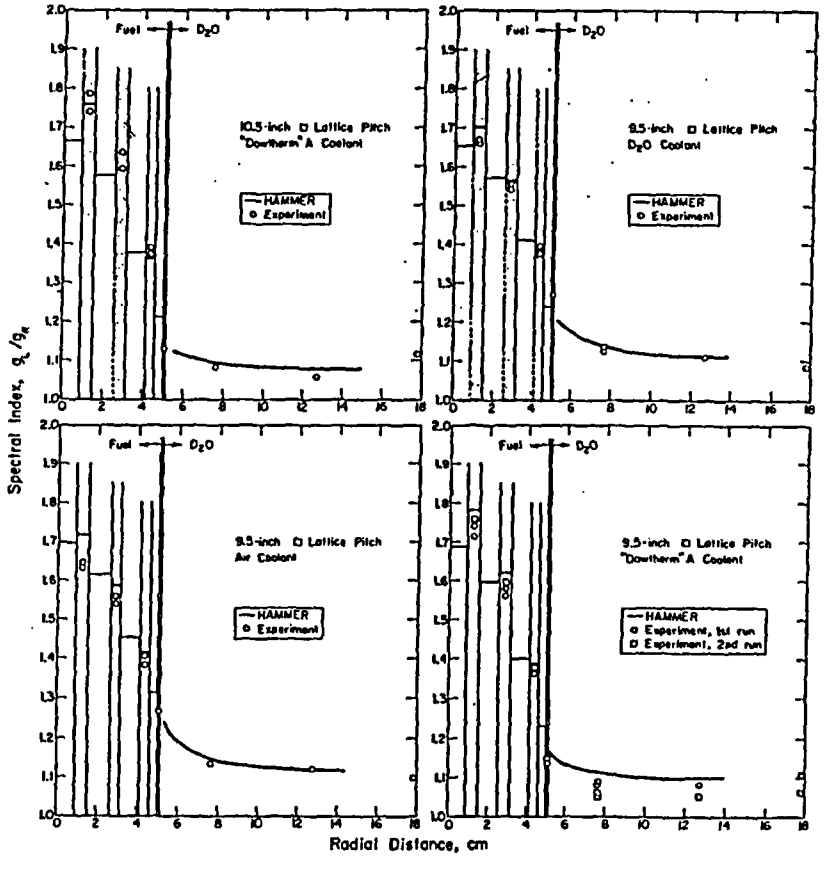

FIG. 30 SPECTRAL INDEX PROFILES - TMT TYPE I

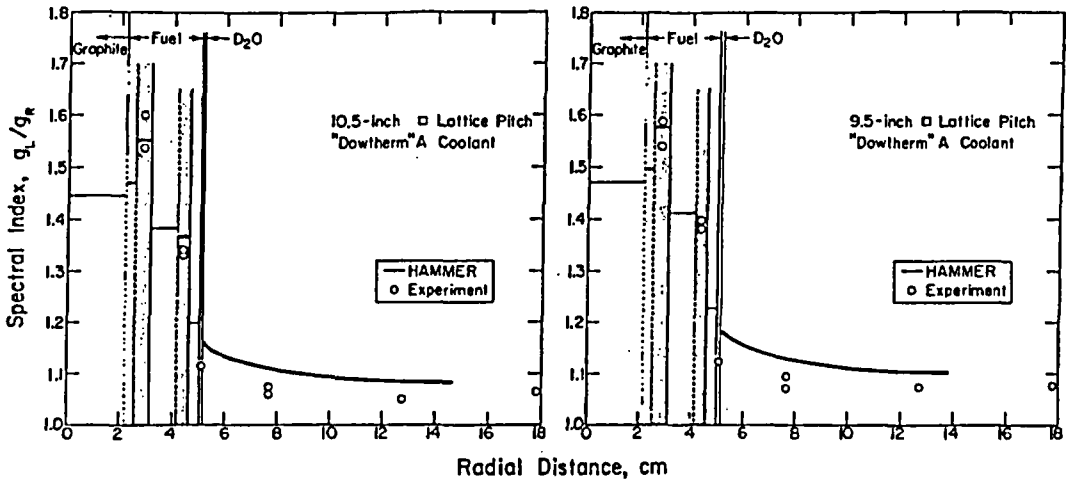

FIG. 31 SPECTRAL INDEX PROFILES - TMT TYPE II

Hot Organic Loop

The room temperature activation measurements described in the preceding sections were supplemented by some limited experiments in a hot organic loop, which circulated "Dowtherm" A at temperatures up to 195°C through a single, insulated irradiation test assembly placed at the center of an appropriate host lattice in the SE. The loop arrangement is shown in Figure 32. The experiments consisted of thermal neutron spectral index determinations for 55-rod clusters of THUD fuel, for UO_2 tubes, and for "Dowtherm" A alone.

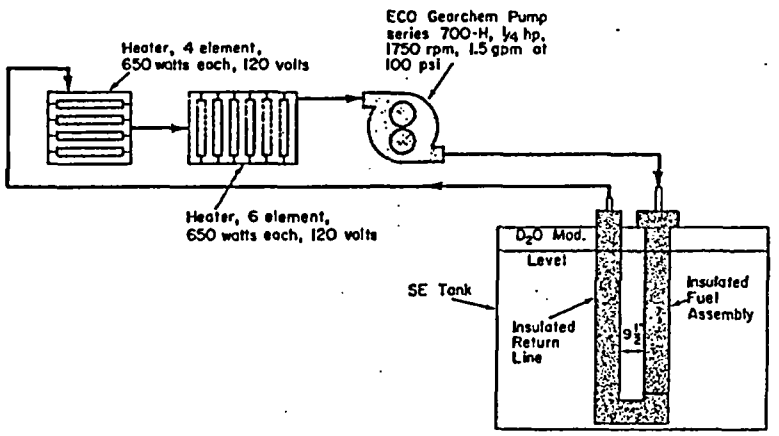

FIG. 32 HOT ORGANIC LOOP

THUD A and THUD B

Two 55-rod THUD clusters, designated as THUD A and THUD B, were used for the hot organic loop irradiations. The THUD A assembly is shown in Figure 33. It was a 55-rod cluster of THUD rods (Figure 1) at 0.0351-inch center-to-center rod spacing. The "Dowtherm" A coolant filled the area (ID = 3.110 inches) inside the inner can. The triple wall construction provided two air spaces for thermal insulation. The THUD B irradiation assembly is illustrated in Figure 34. The same foil holders and loading arrangements were used in the THUD A and THUD B irradiation assemblies as were used in the THUD I measurements. The positions of the rods containing foils are shown in Figure 34. The details of the foil loadings are given in Figure 35. The foils and counting conditions were identical to those listed in Table X. A detailed description of the counting techniques and the data analysis for the spectral index measurement is given in Appendix D.

The experiments were performed with the THUD A or THUD B irradiation assembly at the center position of 9.5-inch square lattice of "Dowtherm" A cooled THUD I fuel assemblies in the SE. Spectral index profiles were measured with the test assemblies at 25 and at 195°C. The results are compared with HAMMER calculations in Figure 36.

"Dowtherm" A

The THUD A and THUD B hot organic loop measurements were supplemented by additional measurements of subcadmium Lu-Mn activation ratios in an assembly containing only "Dowtherm" A. The purpose of the experiment was to investigate the effect of different epithermal neutron distributions in the HAMMER calculations and to test, in a simple system free of absorption hardening effects, the energy exchange kernel used for "Dowtherm" A. The comparison between theory and experiment is shown in Figure 36. The calculated curve was almost unchanged by introducing large changes in the assumed feed of epithermal neutrons into the hot organic or by arbitrarily changing the density of the surrounding D_2O in the calculations.

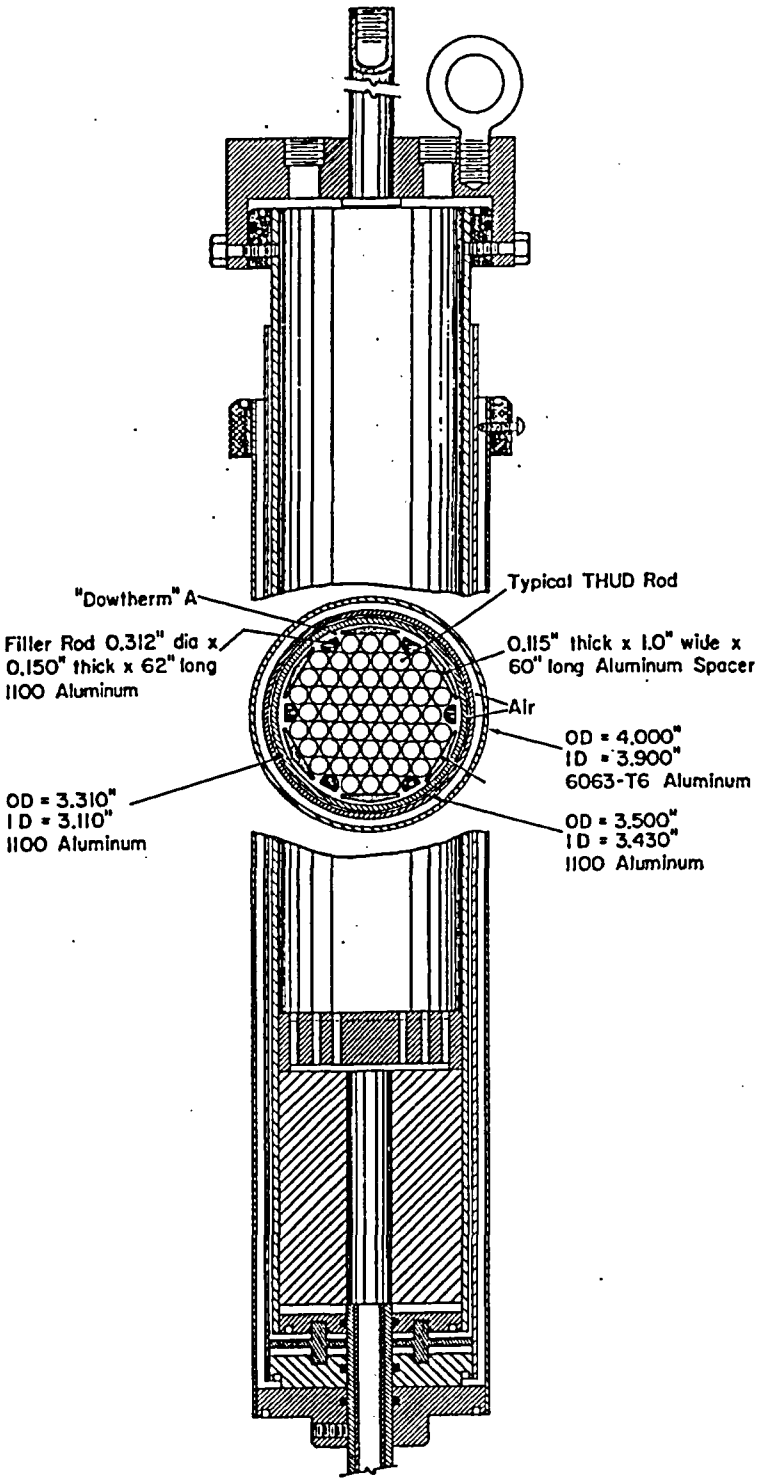

FIG. 33 THUD A FUEL ASSEMBLY

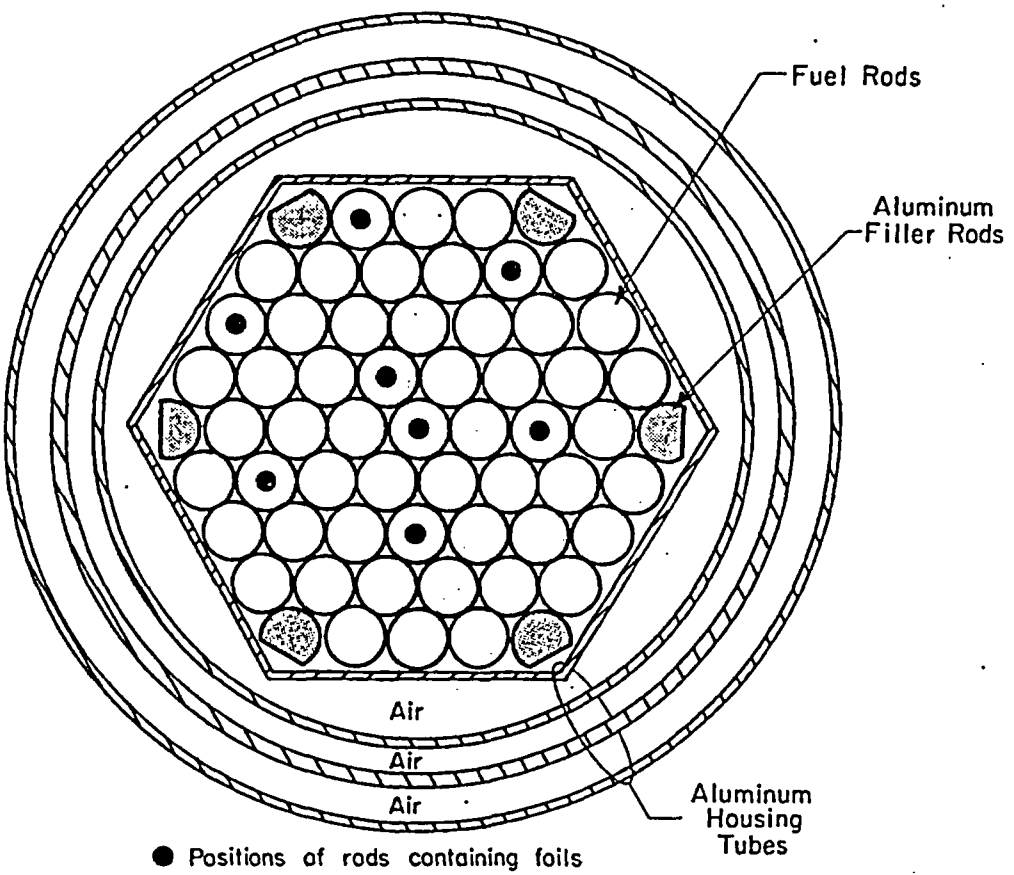

FIG. 34 THUD B FUEL ASSEMBLY

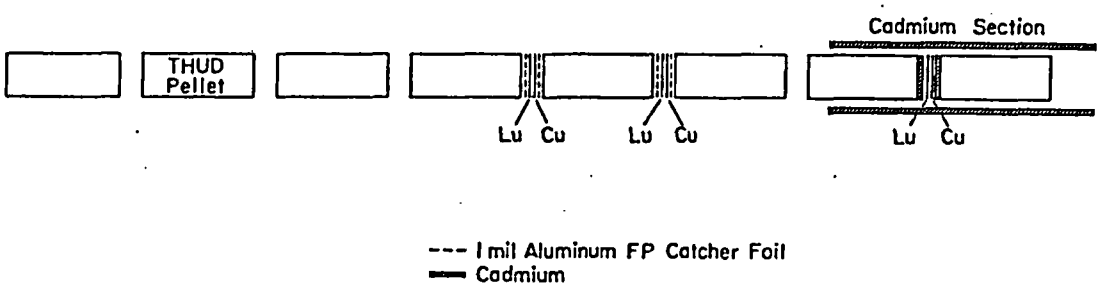

FIG. 35 FOIL LOADINGS FOR THUD A AND THUD B

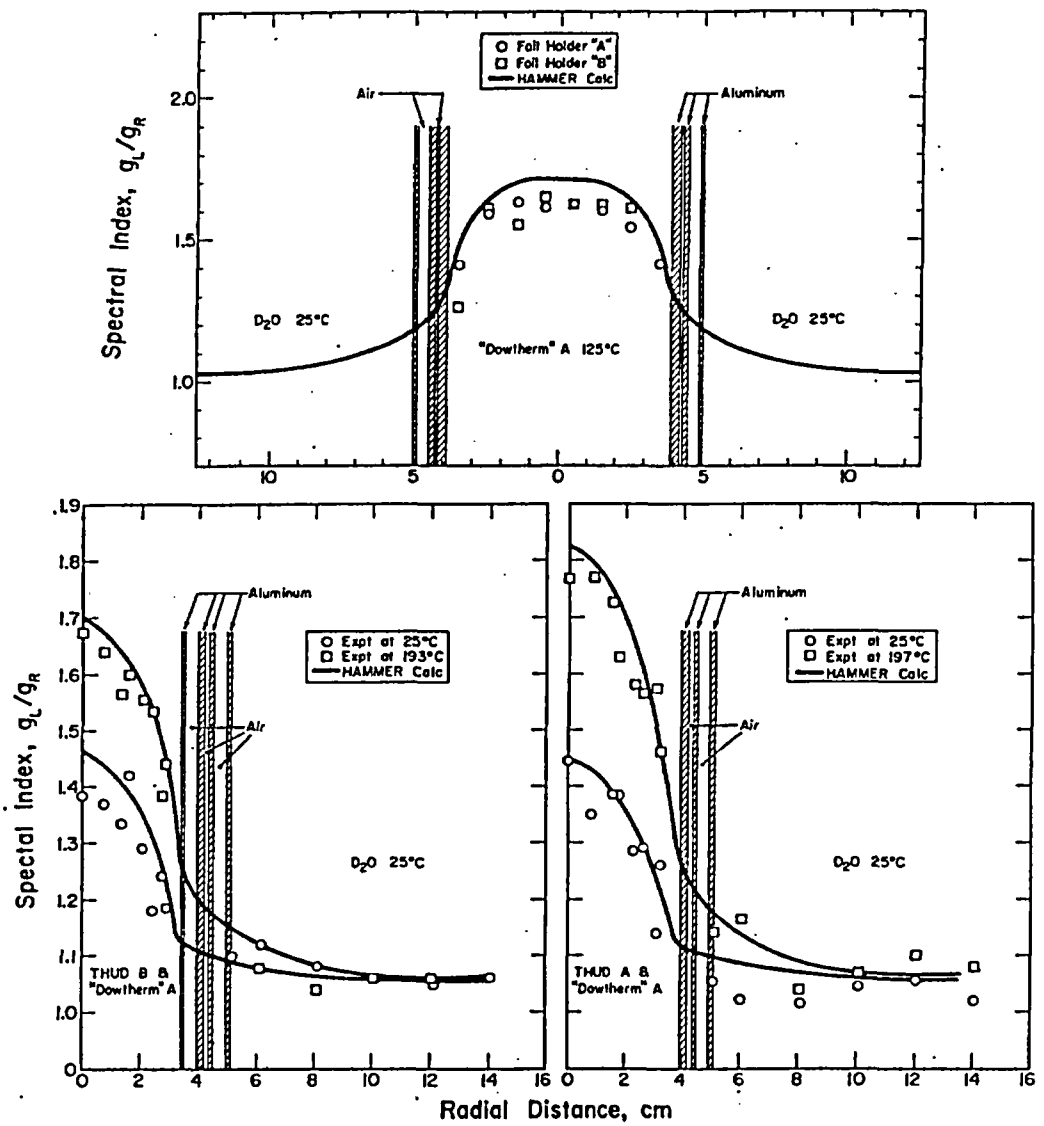

FIG. 36 SPECTRAL INDEX PROFILES FROM ORGANIC LOOP MEASUREMENTS

UO_2 Tubular Assembly

In order to determine to what extent the HAMMER calculations of neutron spectral indices for the THUD clusters depended on the one-dimensional cluster mockup, a series of measurements were made with an assembly of natural uranium oxide tubes for which the exact geometry could be entered into the calculations.

A cross section of the two-tube UO_2 irradiation assembly inside the hot organic loop facility is shown in Figure 37. The fuel tubes were fabricated by vibratorily compacting UO_2 into aluminum tubes to a nominal density of 8.83 g/cm^3. Each tube was composed of three vertical sections screwed together. The center section of each tube contained four small holes defined by thin-walled aluminum tubes, welded to the inner and outer tubes of the fuel piece. The positions and the spacings of the holes are indicated in Figure 37. Into each hole a long, narrow foil sandwich of manganese and lutetium was inserted. Similar foil packets were placed in the thermal reference flux. A small plug of "Silastic"* was used to seal the hole after the foil was inserted to prevent organic from entering. The cadmium-covered lutetium and manganese foils on the surface of the fuel assembly in Figure 37 provided data to correct for epithermal activations. (Previous experiments had indicated a flat epithermal flux activation in this lattice.)

The measured spectral indices, g_L/g_R, are compared with calculation in Figure 38. Here the HAMMER calculations are given in spatial detail whereas the experimental data, closely the average index per tube, are shown as single points. The results indicate poorer agreement between experiment and calculation than was observed in THUD rod clusters (Figure 36). This suggests that the cylindrization process may introduce compensating errors.

---

* Trademark of Dow Corning Silicone Rubber, Dow Corning Corp., Midland, Mich.

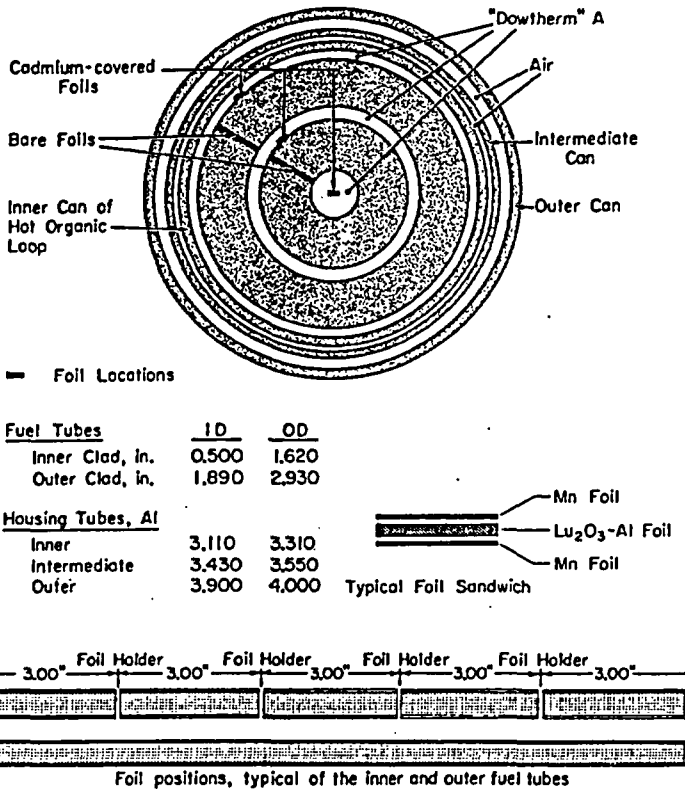

FIG. 37 UO_2 FUEL ASSEMBLY FOR NEUTRON TEMPERATURE MEASUREMENTS

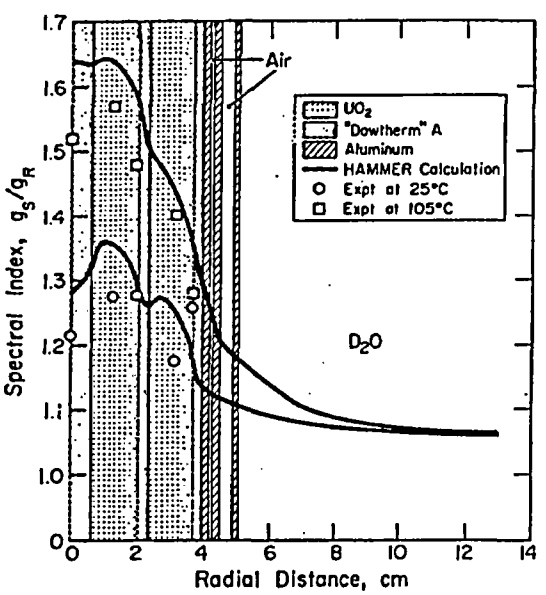

FIG. 38 RADIAL DISTRIBUTIONS OF THE SPECTRAL INDEX FOR TUBULAR UO_2

CALCULATIONS

The HAMMER Code

As discussed in the earlier sections, all of the experimental data were compared with calculations performed by the HAMMER[6] code on an IBM System/360-65 or 704 computer. This code, which was written by H. C. Honeck at Brookhaven National Laboratory and by J. E. Suich at Savannah River, provides multigroup calculations of lattice parameters, neutron distributions, and neutron reaction rates in individual, one-dimensional lattice cells plus few-group calculations of the overall reactor parameters. An extensive printout allows direct comparisons of calculated and experimental quantities.

The overall HAMMER system will sequentially perform any or all of the following operations:

(1) Program CAPN interprets input data, performs extensive error checking, and establishes path of control among the following programs.

(2) Program THERMOS performs an integral transport calculation in 30 energy groups to determine the thermal neutron distribution ($E < 0.625$ ev) in a cell of an infinite lattice and follows this calculation by using a multigroup Fourier transform to determine the leakage spectrum corrections based on homogenized-cell parameters (multigroup flux-volume weighting). Energy-averaged cross sections and diffusion parameters are provided in the output, as well as neutron fluxes and reaction rates. The THERMOS program is also available as an independent code[13] which was used in some of the calculations.

(3) Program HAMLET is the same as (2) except that the energy range extends from 0.625 ev to 10 Mev in 54 energy groups according to the MUFT[14] group structure. Collision probabilities are computed under the assumption of cosine currents crossing region boundaries, and the energy spectrum during moderation is computed as in MUFT. This approach automatically produces a heterogeneous calculation of ϵ and p; for the latter, the ZUT/TUZ[7] codes are employed as a subroutine to determine the self-shielded resonance cross sections. In addition to the output described in (2), a set of four-group cross sections (10 Mev - 1.05 Mev - 9.12 kev - 0.625 ev - 0) is produced, from which the asymptotic spectrum and the buckling of the infinite lattice are determined.

(4) Program FLOG utilizes the four-group constants produced in (2) and (3), to perform a one-dimensional, many-region reactor calculation. This program is a modification of FOG[15]. In addition to the standard criticality searches, FLOG will perform least-squares fitting of reactor fluxes to obtain experimental values of the buckling.

(5) Program DIED combines (2) through (4) to obtain the fluxes and cross sections and to produce neutron balance sheets in this final edit program. For an infinite lattice cell edit [results of (2) and (3) only], the output is either (a) absorptions versus fissions by isotope and group, split into "smooth" and "resonance" event contributions, or (b) total absorptions versus total fissions by isotope and group. For a composite reactor edit [results from (4)], neutron balance sheets are produced for total absorptions versus total fission neutron production by isotope and region. These latter tables can be produced for all regions, for all fissioning regions, or for selected regions. The flux weighting employed in the tables can be that appropriate to the region average, the asymptotic core, the interfaces, or all of these.

Input to the code consists of a geometrical description of the reactor system and of cross section libraries for the various reactor materials. Some special problems arose in specifying fuel cluster geometries and the "Dowtherm" A energy transfer cross sections.

Models of the Experimental Fuel Assemblies

The current one-dimensional HAMMER system restricts the lattice cell representation to a maximum of 20 regions in slab or cylindrical array. No difficulties are experienced in applying this representation to cylindrical fuel assemblies such as the Thorium Metal Tubes. Table XX gives a listing of the cell regions used in the calculations for the various type TMT assemblies; Tables XXI and XXII give similar listings for the tubular UO_2 assemblies.

Problems do arise, however, in providing a one-dimensional representation for rod cluster lattices. Two different models were developed to mock up the THUD I and THUD II fuel assemblies. The first model homogenized all the fuel assembly materials (i.e., fuel, coolant, and cladding) into a single region with cross sections given by volume-weighted averages. D_2O and clad exterior to the fuel were then placed in concentric rings around the homogenized region as described in Tables XXIII and XXIV. This model was also used for the THUD A and THUD B irradiation assemblies as described in Tables XXV and XXVI.

TABLE XX

TMT Regions for HAMMER Calculations[a]

Region	Materials	OD, inches
Type I Fuel Assemblies		
1	Al, coolant	0.710
2	^{232}Th, ^{235}U, ^{238}U	1.224
3	Al, coolant	2.034
4	^{232}Th, ^{235}U, ^{238}U	2.510
5	Al, coolant	3.263
6	^{232}Th, ^{235}U, ^{238}U	3.640
7	Al, coolant	4.060
8	D_2O	(b)
Type II Fuel Assemblies		
1	C	1.210
2	Al, coolant	2.034
3	^{232}Th, ^{235}U, ^{238}U	2.510
4	Al, coolant	3.263
5	^{232}Th, ^{235}U, ^{238}U	3.640
6	Al, coolant	4.060
7	D_2O	(b)
Type III Fuel Assemblies		
1	Al, coolant	0.710
2	^{232}Th, ^{235}U, ^{238}U	1.224
3	Al, coolant	2.034
4	^{232}Th, ^{235}U, ^{238}U	2.510
5	Al, coolant	3.085
6	D_2O	(b)

(a) See Table III for actual configuration.
(b) Cylindricized OD of lattice cell.

TABLE XXI

Tubular UO_2 Regions for HAMMER Calculations - Hot Organic Loop

Region	Materials	OD, inches
1	"Dowtherm" A, Al	0.560
2	UO_2	1.560
3	"Dowtherm" A, Al	1.950
4	UO_2	2.870
5	"Dowtherm" A, Al	3.1317
6	Al	4.000
7	D_2O	5.3598

TABLE XXII

Tubular UO_2 Regions for HAMMER Calculations - PDP Measurements

Region	Materials	OD, inches
1	Al, coolant	0.560
2	UO_2	1.560
3	Al, coolant	1.950
4	UO_2	2.870
5	Al, coolant	3.1317
6	Al	3.550
7	D_2O	(a).

(a) Cylindricized OD of lattice cell.

TABLE XXIII

THUD I Regions for HAMMER Calculations

Region	Materials	OD, inches
Homogeneous Model		
1	^{232}Th, ^{234}U, ^{235}U, ^{236}U, ^{238}U, Al, oxygen, coolant	3.0012
2	Al, coolant	3.4200
3	D_2O	(a)
Concentric Ring Model		
1	^{232}Th, ^{235}U, ^{236}U, ^{238}U, ^{234}U, ^{16}O	0.231
2	Al, coolant	0.4595
3	^{232}Th, ^{235}U, ^{236}U, ^{238}U, ^{234}U, ^{16}O	0.7289
4	Al, coolant	1.0024
5	^{232}Th, ^{235}U, ^{236}U, ^{238}U, ^{234}U, ^{16}O	1.2826
6	Al, coolant	1.5602
7	^{232}Th, ^{235}U, ^{236}U, ^{238}U, ^{234}U, ^{16}O	1.8425
8	Al, coolant	2.1212
9	^{232}Th, ^{235}U, ^{236}U, ^{238}U, ^{234}U, ^{16}O	2.4042
10	Al, coolant	2.6239
11	^{232}Th, ^{235}U, ^{236}U, ^{238}U, ^{234}U, ^{16}O	2.8575
12	Al, coolant	3.420
13	D_2O	(a)

(a) Cylindricized OD of lattice cell.

TABLE XXIV

THUD II Regions for HAMMER Calculations

Region	Materials	OD, inches
Homogeneous Model		
1	^{232}Th, ^{234}U, ^{235}U, ^{236}U, ^{238}U, Al, oxygen, coolant	3.398
2	Al, coolant	4.000
3	D_2O	(a)
Concentric Ring Model		
1	^{232}Th, ^{235}U, ^{236}U, ^{238}U, ^{234}U, ^{16}O	0.231
2	Al, coolant	0.5485
3	^{232}Th, ^{235}U, ^{236}U, ^{238}U, ^{234}U, ^{16}O	0.7880
4	Al, coolant	1.1676
5	^{232}Th, ^{235}U, ^{236}U, ^{238}U, ^{234}U, ^{16}O	1.4155
6	Al, coolant	1.8003
7	^{232}Th, ^{235}U, ^{236}U, ^{238}U, ^{234}U, ^{16}O	2.0498
8	Al, coolant	2.4359
9	^{232}Th, ^{235}U, ^{236}U, ^{238}U, ^{234}U, ^{16}O	2.686
10	Al, coolant	2.9911
11	^{232}Th, ^{235}U, ^{236}U, ^{238}U, ^{234}U, ^{16}O	3.1980
12	Al, coolant	4.000
13	D_2O	(a)

(a) Cylindricized OD of lattice cell.

TABLE XXV

THUD A Regions for Homogeneous Model HAMMER Calculations

Region	Materials	OD, inches
1	Al, ^{232}Th, ^{235}U, ^{238}U, ^{234}U, ^{16}O, "Dowtherm" A	2.7334
2	Al, "Dowtherm" A	3.110
3	Al, air	4.00
4	D_2O	5.3598

TABLE XXVI

THUD B Regions for Homogeneous Model HAMMER Calculations

Region	Materials	OD, inches
1	Al, ^{232}Th, ^{235}U, ^{238}U, ^{234}U, ^{16}O, "Dowtherm" A	2.4142
2	Al, "Dowtherm" A	2.7512
3	Al, air	4.00
4	D_2O	5.3598

The second model divided THUD I and THUD II 85-rod clusters into six concentric, cylindrical fuel rings each surrounded by a ring of homogenized cladding and coolant. Each circular fuel ring in the model corresponded to a hexagonal ring of THUD rods in the actual cluster, and the actual fuel volume was matched by adjusting the ring thickness in the model. The concentric rings of coolant and cladding adjoining the fuel rings in the model were homogenized by volume weighting and again matched the actual cluster volumes. The assignment of material to a particular ring was ascertained by dividing at lines connecting midpoints of fuel rods making up each ring. The dimensions of the ring models of the THUD I and THUD II clusters are given in Tables XXIII and XXIV.

The ring model permits approximate allowance for intracluster heterogeneous effects such as thermal flux peaking in coolant and also makes it possible to use the "Effective Surface" concept for resonance capture. As one test of the model, the effective surfaces, $\sum_i \gamma_i S_i$, were calculated for the rod clusters and for the cylindricized rings. The γ's are effectiveness factors that were computed on the basis of isotropic fluxes and the assumption of narrow resonances; i.e., that the average energy lost by a collision of a neutron with coolant atoms is large compared to the resonance energy width. For the close-packed THUD I fuel assemblies, the values were 41.3 cm^2/cm for the actual cluster and 41.2 cm^2/cm for the ring model; i.e., the effective surfaces were found to agree closely even though total surfaces and γ's were quite different.

Table XXVII shows the effect of the different cluster models on the calculated parameters for the THUD I lattices. The ring model and the homogeneous B model are those described in Tables XXIII and XXIV. The tabulated dimensions for the Homog B model were obtained by dividing the cluster into microcells and then cylindricizing. However this procedure gives a fuel assembly radius somewhat bigger than that of the ring model. The Homog A model was adjusted to the ring model dimensions in order to

TABLE XXVII

HAMMER Computed Parameters for THUD I Lattices
85 r/c, 20°C, "Dowtherm" A coolant

Lattice	D_2O Purity, mol %	Cluster Model	B^2, μB	p	τ, cm^2	L^2, cm^2	Σ_a, cm^{-1}	D, cm	ηf
9" Δ	99.62	Ring	578	.8845	121.16	127.54	.006484	.8290	1.2101
		Homog A	572	.8878	121.77	129.85	.006364	.8283	1.2074
		Homog B	617	.8897	121.69	125.59	.006585	.8290	1.2159
9.5" □	99.65	Ring	519	.9037	120.77	171.22	.004817	.8263	1.206
		Homog A	509	.9061	121.09	174.84	.004714	.8258	1.203
		Homog B	549	.9078	121.01	169.33	.004870	.8263	1.212
10.5" □	99.61	Ring	452	.9154	119.85	214.90	.003822	.8224	1.198
		Homog A	439	.9169	120.19	220.37	.003725	.8220	1.194
		Homog B	475	.9185	120.11	213.68	.003843	.8225	1.204

investigate separately the effects of homogenization and cluster size. For these rather homogeneous clusters, the effect of the model is seen to be comparatively small. Based on qualitative arguments, the ring model is expected to give the most accurate results for resonance capture calculations and the Homog B model the best thermal neutron flux profiles. The two models have been separately used for these purposes in the experimental comparisons.

HAMMER Cross Sections

The capture cross sections of primary importance were those for ^{235}U, ^{238}U, and ^{232}Th. These cross sections were obtained from BNL compilations. Resonance parameters for ^{238}U and ^{232}Th were compiled by B. R. Sehgal of BNL. Reference 2200 m/s cross sections and infinite dilution resonance integrals, in barns, are listed below.

	^{235}U	^{238}U	^{232}Th
σ_a (2200)	682.00	2.710	7.560
σ_f (2200)	582.20	-	-
RI_a^∞ (>0.625 ev)	408.66	271.54	90.13
RI_f^∞ (>0.625 ev)	276.96	-	-

The thorium epithermal cross sections given by Sehgal deviate strongly from 1/v law behavior in the near thermal region, giving a value of 1.5 barns for the resonance integral from 0.5 to 15 ev vs. 3.0 barns obtained by assuming 1/v law behavior. The present HAMMER thermal cross section does assume 1/v law behavior below 0.625 ev. This inconsistency between the two sets of cross sections may be largely responsible for the discrepancy between measured and computed cadmium ratios for thorium capture indicated in Tables XIV and XVII.

The scattering kernel used for thermal neutrons in D_2O was the Honeck-Nelkin kernel[13]. For "Dowtherm" A, a Nelkin type kernel was constructed by using Ardente's data for benzene[16] in the GAKER code[13]. Both kernels have been demonstrated to give good agreement with measured diffusion coefficients for both systems[17].

CALCULATIONS AND EXPERIMENTS

Comparison of Bucklings

HAMMER computed buckling values for the thorium metal tubes (TMT) lattices are in good agreement with those measured in both the PDP and the SE. The only exception is the Persson value for the gas-cooled lattice in the SE for which the measured buckling greatly exceeds that calculated. This discrepancy is explained by the fact the analysis took no account of the known diffusion coefficient mismatch.

For the THUD rod clusters, consideration must be given to geometric model used. The homogeneous model is expected to predict too large a buckling because of the dominant effect of underestimating thermal neutron absorption in the cladding and coolant. The concentric ring model is expected to predict too low a buckling because of an overestimate of thermal neutron leakage (L^2). Of the two models, the concentric-ring model is expected to be the most accurate and provides the basis for comparison. The computed values again show generally good agreement with both THUD I and THUD II bucklings except for the air-filled THUD II lattice, for which the measured values obtained by the modified Persson analysis are significantly higher than those calculated. Inasmuch as none of the measured quantities such as resonance capture or thermal neutron flux profiles and temperatures support the higher values for the gas-cooled lattices of either the TMT or THUD fuel, the measured values may be in error due to the method of analysis. This analysis does not take into account the difference in diffusion coefficients between test and reference lattices. To include the effect of the different diffusion coefficients, analysis of this SE lattice was also made by means of two-region, four-energy group diffusion theory[15]. The results are included in Tables V and VI. Inclusion of diffusion coefficients is seen to significantly reduce the measured buckling values and improve the agreement with the computations.

Foil Activation

The HAMMER or THERMOS calculations generally show excellent agreement with the experiments in the calculation of the subcadmium copper foil activations to determine the thermal neutron flux distributions. A small exception is provided by the THUD I measurements where, when the calculated and measured activations are normalized at the center of the fuel assembly, the calculated activations rise about 4% above the measured activations at the cell boundary. Based on other experiments, there is some possibility that this discrepancy represents a poisoning effect by the flux measuring equipment in the experiments. However, no direct evidence was obtained for this conclusion.

The calculated and measured ratios of the subcadmium ^{177}Lu and ^{64}Cu activities used to determine the thermal spectral indices were also in quite good agreement. However, there was a consistent tendency for the calculations to overemphasize the spectrum hardening which occurred in the fuel assemblies. This effect, which amounted to only a few percent, was particularly noticeable in the simple geometry lattices such as those involving the tubular UO_2 fuel assemblies or simple "Dowtherm" A tubes. The excellent agreement obtained with the fuel clusters may thus in part represent a small compensating error in the cluster homogenization calculations.

The cadmium ratio measurements of the epithermal-to-thermal ratios were also in quite good agreement with the experiments although there was some tendency for the calculations to overestimate the cadmium ratios in the "Dowtherm" A cooled fuel assemblies.

In the detailed measurements of the ^{232}Th neutron interactions, the HAMMER calculations tended to underestimate the thorium resonance capture by 5 to 20%. There was some evidence of systematic structure in these discrepancies, but it was near the noise level of the measurements. As expected, the ring model for the THUD clusters in the HAMMER code gave better agreement with the measured ^{232}Th captures than the homogenized model. The HAMMER calculations of fast fission in ^{232}Th were in good agreement with the experiments for the thorium metal tubes but underestimated the fast fissions by about 20% in the rod cluster lattices. It is thought that this discrepancy is primarily due to the deficiencies of the cluster homogenization procedure.

APPENDIX A

PHYSICAL PROPERTIES OF "DOWTHERM" A

"Dowtherm" A[18] is a eutectic mixture containing 73.5 wt % diphenyl oxide ($C_{12}H_{10}O$) and 26.5 wt % diphenyl ($C_{12}H_{10}$). It is a clear, straw-colored liquid that freezes at 53.6°F and boils at 495.8°F. It has a density of 66.7 lb/ft^3 at 60°F. The atom density values for "Dowtherm" A used in HAMMER calculations are summarized in Table XXVIII.

TABLE XXVIII

Atom Densities for "Dowtherm" A

Element	Atomic Density, atoms/cm^3 21.1°C	200°C
^1H	3.868×10^{22}	3.286×10^{22}
^{12}C	4.641×10^{22}	3.943×10^{22}
^{16}O	2.766×10^{21}	2.350×10^{21}

APPENDIX B

DETAILS FOR SE BUCKLING MEASUREMENTS

The detailed loading arrangements of the SE for the substitution buckling measurements on the THUD I, THUD II, and TMT lattice are summarized in Tables XXIX, XXX, and XXXI. The alphabetical designations for each fuel assembly refer to the lattice positions which these assemblies occupied within the SE (Figure 39).

The measured values of the vertical buckling (κ^2), the moderator purity, and the moderator temperature for each experiment are given in the tables.

The Persson plots used in obtaining the infinite lattice buckling from the substitution measurements are given in Figures 40-42.

TABLE XXIX

SE Fuel Loading Patterns - THUD I Buckling Measurements

Run No.	Lattice Pitch	Fuel Assembly Position (see Figure 39) EUMT D_2O Coolant	NUOR D_2O Coolant	THUD I D_2O Coolant	THUD I Air Coolant	THUD I H_2O Coolant	THUD I "Dowtherm" A Coolant	κ_z^2, μB	D_2O Purity, mol %	D_2O Temp, °C
3	9" Δ	ABCDEF						-136	99.28	23.5
4	9" Δ	BCDEF	A					- 93	99.27	24
5	9" Δ	$B_{3-6}CDEF$	$AB_{1,2}$					- 46	99.27	24
6	9" Δ	CDEF	AB					+ 82	99.27	24.5
7	9" Δ	ACDEF	B					+ 27	99.26	24
8	9" Δ	DEF	ABC					+193	99.25	24.5
9	9" Δ	ADEF	BC					+145	99.25	24.5
10	9" Δ	$B_{1,3,5}DEF$	$AB_{2,4,6}C$					+ 83	99.25	24.5
11	9" Δ	EF	ABCD					+263	99.25	25
12	9" Δ	F	ABCDE					+329	99.25	25
13	9" Δ	-	ABCDEF					+349	99.24	25
16	9" Δ	A	BCDEF					+297	99.23	24
17	9" Δ	$AB_{1,2}$	$B_{3-6}CDEF$					+226	99.23	24
18	9" Δ	AB	CDEF					+101	99.23	24
19	9" Δ	B	ACDEF					+139	99.22	22.5
20	9" Δ	ABC	DEF					- 5	99.22	22.5
21	9" Δ	BC	ADEF					+ 35	99.21	24
22	9" Δ	$AB_{1,3,5}C$	$B_{2,4,6}DEF$					+ 87	99.21	23.5
23	9" Δ	ABCD	EF					- 87	99.20	24
24	9" Δ	ABCDE	E					-134	99.16	23
25[a]	9" Δ	ABCDE	F					-135	99.16	23
26	9" Δ	ABCDEF	-					-142	99.15	23
29[b]	9" Δ	ABCDEF	-					-148	99.83	24
30[c]	9" Δ	ABCDEF	-					-153	99.83	24
31	9" Δ	BCDEF	-				A	-121	99.83	24
32	9" Δ	$B_{2-6}CDEF$	-				$AB_{1,2}$	- 80	99.83	24
33	9" Δ	CDEF	-				AB	+ 48	99.83	24
34	9" Δ	DEF	-				ABC	+137	99.82	24
35	9" Δ	ADEF	-				BC	+123	99.82	24
36	9" Δ	$B_{2,4,6}CEF$	-				$AB_{1,3,5}$	+ 69	99.82	25
39	9" Δ	ABCDEF	-					-153	99.73	24
40	9" Δ	BDE	ACF				-	- 8	99.72	24
41	9" Δ	BDE	-				ACF	- 20	99.72	24
63	9" Δ	-	DEF				ABC	+318	99.65	24
64	9" Δ	-	ADEF				BC	+326	99.65	24
65	9" Δ	-	$B_{1,3,5}DEF$				$AB_{2,4,6}C$	+324	99.65	24
66	9" Δ	-	BDE				ACF	+334	99.62	24
69	9" Δ	-	ABCDEF				-	+330	99.61	24

(Continued on next page)

TABLE XXIX (Continued)

Run No.	Lattice Pitch	Fuel Assembly Position (see Figure 39) EUMT D_2O Coolant	NUOR D_2O Coolant	THUD I D_2O Coolant	THUD I Air Coolant	THUD I H_2O Coolant	THUD I "Dowtherm" A Coolant	κ_z^2, μB	D_2O Purity, mol %	D_2O Temp, °C
42	9.5"□	BEF	-				ACDG	+133	99.72	24
43	9.5"□	BEFG	-				ACD	+120	99.72	24
44	9.5"□	EFG	-				ABCD	+294	99.72	24
45	9.5"□	AEFG	-				BCD	+227	99.72	24
46	9.5"□	ADEFG	-				BC	+177	99.72	24
47	9.5"□	DEFG	-				ABC	+229	99.72	24
48	9.5"□	CDEFG	-				AB	+115	99.71	24
49	9.5"□	ABCDEFG	-				-	- 94	99.71	24
50	9.5"□	ACEF	-				BDG	+132	99.70	24
53	9.5"□	ABCDEFG	-				-	- 90	99.69	24
56	9.5"□	-	ABCDEFG				-	+394	99.68	24
57	9.5"□	-	CDEFG				AB	+400	99.68	24
58	9.5"□	-	ACEF				BDG	+407	99.68	24
59	9.5"□	-	BEF				ACDG	+399	99.68	24
60	9.5"□	-	EFG				ABCD	+399	99.68	24
84	9.5"□	-	EFG	ABCD				+358	99.56	23
85	9.5"□	-	DEFG	ABC				+350	99.56	23
86	9.5"□	-	BEF	ACDG				+382	99.56	23
87	9.5"□	-	ACEF	BDG				+379	99.55	23
89	9.5"□	-	EFG		ABCD			+342	99.52	23
90	9.5"□	-	BEF		ACDG			+378	99.52	23
91	9.5"□	-	BDFG		ACE			+368	99.52	23
92	9.5"□	-	DEFG		ABC			+340	99.52	23
93	9.5"□	-	ABCDEFG	-	-	-	-	+399	99.52	23
94	9.5"□	-	EFG			ABCD		+444	99.52	23
95	9.5"□	-	BEF			ACDG		+434	99.52	23
96	9.5"□	-	BDFG			ACE		+438	99.51	23
97	9.5"□	-	DEFG			ABC		+431	99.51	23
75	10.5"□	-	ABCDEG				-	+479	99.61	23
76	10.5"□		DEG				ABC	+483	99.61	23
77	10.5"□		BE				ACDG	+477	99.61	23
78	10.5"□		ACE				BDG	+480	99.61	23
79	10.5"□	-	EG				ABED	+485	99.61	24

(a) Cadmium was placed atop SE to determine effect of room return of thermal neutrons.
(b) Higher purity water was charged just prior to Run 29.
(c) Run 30 was a repeat of Run 29 with the D_2O at a higher level.

TABLE XXX

SE Fuel Loading Patterns - THUD II Buckling Measurements

Run No.	Lattice Pitch		Fuel Assembly Position (See Figure 39) NUOR	THUD II D_2O Coolant	THUD II Air Coolant	THUD II H_2O Coolant	THUD II "Dowtherm" A Coolant	κ_z^2, μB	D_2O Purity, mol %	D_2O Temp, °C
107	9"	Δ	ABCDEF					+360	99.20	21
108	9"	Δ	CDEF				AB	+450	99.20	21
109	9"	Δ	DEF				ABC	+489	99.19	23
110	9"	Δ	BDE				ACF	+421	99.19	23
111	9"	Δ	ADEF				BC	+478	99.19	23
102	10.5"	□	BE				ACDG	+567	99.46	23
103	10.5"	□	BDG				ACE	+549	99.46	23
104	10.5"	□	EG				ABCD	+608	99.46	23
105	10.5"	□	DEG				ABC	+596	99.46	23
106	10.5"	□	ABCDEG				-	+484	99.46	23
98	9.5"	□	DEFG				ABC	+521	99.49	23
99	9.5"	□	EFG				ABCD	+538	99.49	23
100	9.5"	□	BDFG				ACE	+490	99.49	23
101	9.5"	□	BEF				ACDG	+481	99.47	23
112	9.5"	□	EFG	ABCD				+436	99.17	21
113	9.5"	□	DEFG	ABC				+428	99.17	21
114	9.5"	□	BDFG	ACE				+442	99.17	23
115	9.5"	□	BEF	ACDG				+447	99.17	23
116	9.5"	□	ABCDEFG	-				+448	99.17	23
117	9.5"	□	DEFG		ABC			+390	99.16	23
118	9.5"	□	EFG		ABCD			+395	99.16	23
119	9.5"	□	BEF		ACDG			+428	99.16	23
120	9.5"	□	BDEG		ACE			+434	99.15	23
121	9.5"	□	BDFG			ACE		+571	99.15	23
123	9.5"	□	EFG			ABCD		+652	99.14	23
124	9.5"	□	BEF			ACDG		+564	99.14	23
125	9.5"	□	DEFG			ABC		+624	99.14	23

TABLE XXXI

SE Fuel Loading Patterns - TMT Buckling Measurements

Run No.	Lattice Pitch	TMT Assembly Type	Fuel Assembly Position				κ_z^2, μB	D_2O	
			NUOR	TMT D_2O Coolant	TMT Air Coolant	TMT "Dowtherm" A Coolant		Purity, mol %	Temp, °C
M-17	9.5" □	I	DEFG	ABC	-	-	+268	99.40	23
M-18	9.5" □	I	BEFG	ACD	-	-	+301	99.40	23
M-19	9.5" □	-	ABCDEFG	-	-	-	+410	99.40	23
M-20	9.5" □	I	BEFG	-	ACD	-	+284	99.39	23
M-21	9.5" □	I	DEFG	-	ABC	-	+246	99.39	23
M-23	9.5" □	I	DEFG	-	-	ABC	+320	99.37	23
M-24	9.5" □	I	BEFG	-	-	ACD	+345	99.37	23
M-26	9.5" □	II	DEFG	-	-	ABC	+329	99.36	23
M-27	9.5" □	II	BEFG	-	-	ACD	+341	99.36	23
M-28	10.5" □	II	BEG	-	-	ACD	+406	99.36	23
M-29	10.5" □	II	DEG	-	-	ABC	+369	99.36	23
M-32	10.5" □	I	DEG	-	-	ABC	+369	99.33	23
M-33	10.5" □	I	BEG	-	-	ACD	+419	99.33	23
M-34	10.5" □	-	ABCDEG	-	-	-	+510	99.32	23
M-35	12.12" △	-	ABCD	-	-	-	+562	99.32	23
M-36	12.12" △	I	CD	-	-	AB	+451	99.32	23
M-37	12.12" △	I	BD	-	-	AC	+509	99.32	23

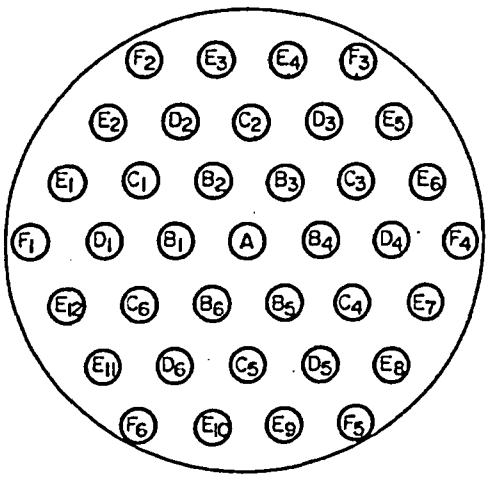

9-inch △ Lattice Pitch

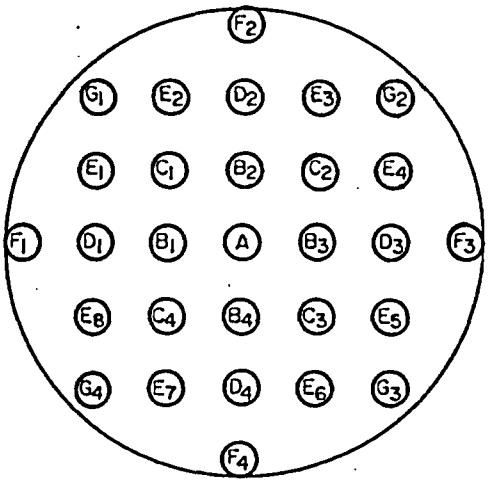

9.5-inch □ Lattice Pitch

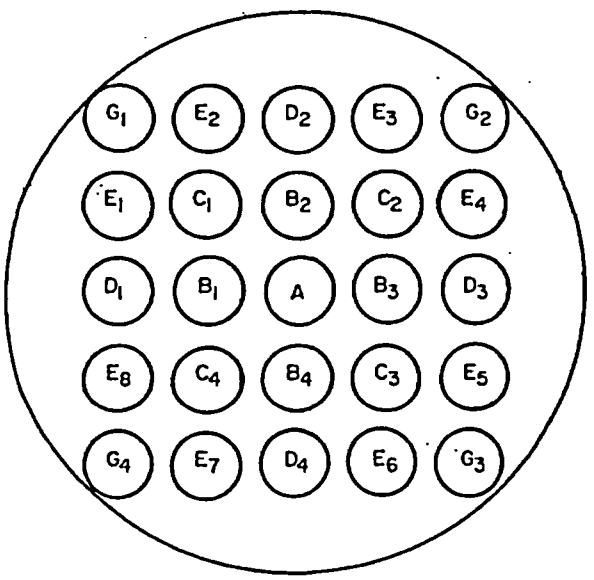

10.5-inch □ Lattice Pitch

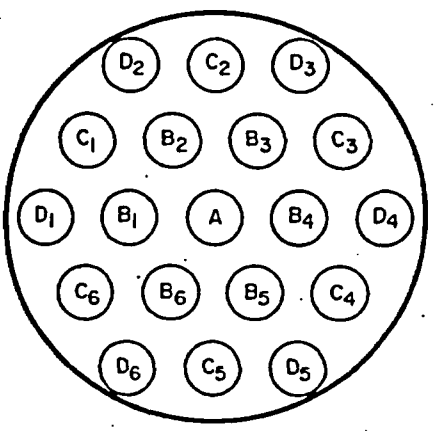

12.12-inch △ Lattice Pitch

FIG. 39 SE LOADINGS

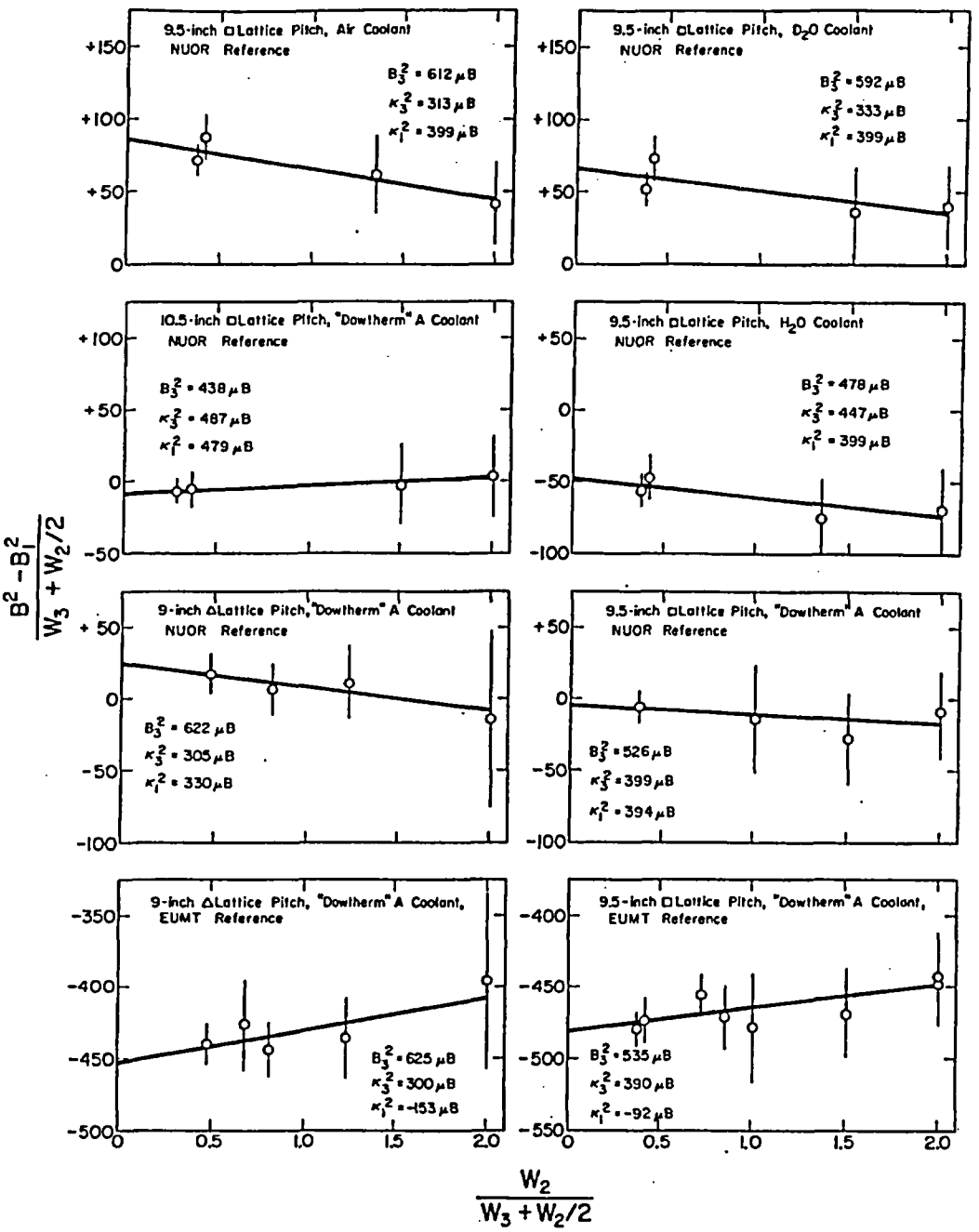

FIG. 40 PERSSON SUBSTITUTION ANALYSES - THUD I - SE

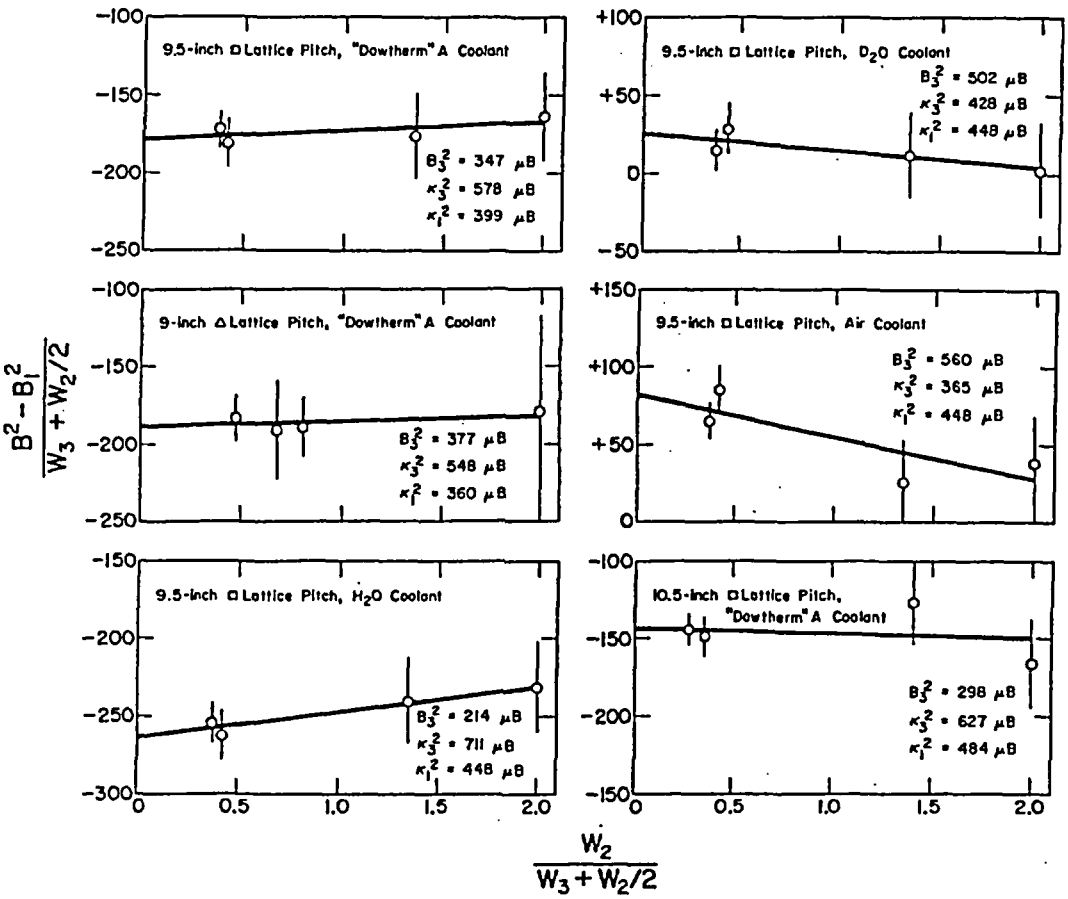

FIG. 41 PERSSON SUBSTITUTION ANALYSES - THUD II - SE

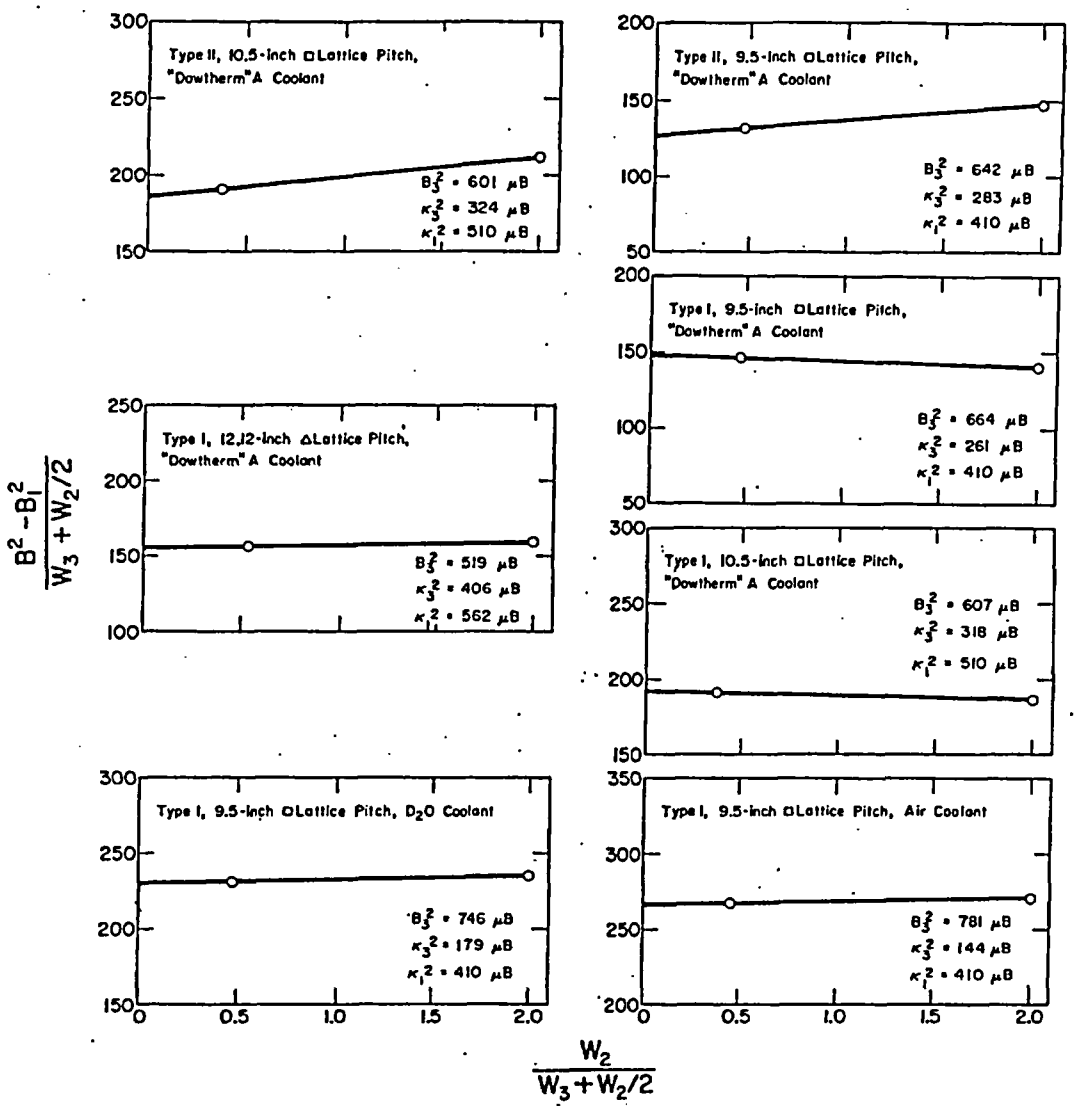

FIG. 42 PERSSON SUBSTITUTION ANALYSES - TMT - SE

APPENDIX C

DETAILS FOR PDP BUCKLING MEASUREMENTS

The detailed loading arrangements in the PDP for the substitution buckling measurements in the thorium metal tubes at a 12.12-inch triangular lattice pitch are summarized in Table XXXII. The numerical designations for each measurement refer to the seven fuel positions in the center of the PDP as shown in Figure 13. The measured values of the vertical buckling (B_z^2), moderator purity, and moderator temperature for each experiment also are given in the table.

Figure 43 gives the Persson plots used in obtaining the infinite lattice bucklings from the substitution measurements.

TABLE XXXII

PDP Fuel Loading Patterns - TMT - 12.12-inch Δ Pitch

Run No.	TMT Assembly Type	Fuel Assembly Position: Mark IX	TMT: D_2O Coolant	TMT: Air Coolant	TMT: "Dowtherm" A Coolant	B_z^2, μB	D_2O: Purity, mol %	D_2O: Temp, °C
22	I	2-7	1	-	-	196.417	99.50	22.00
22	I	2-7	-	1	-	195.111	99.50	22.00
23	I	1,2,4,6	3,5,7	-	-	199.838	99.50	22.12
23	I	1,2,4,6	-	3,5,7	-	202.490	99.50	22.12
24	I	1	2-7	-	-	206.264	99.50	22.10
24	I	1	-	2-7	-	211.258	99.50	22.10
26	-	1-7	-	-	-	191.872	99.50	21.76
27	II	2-7	1	-	-	194.477	99.50	21.79
27	II	2-7	-	1	-	194.996	99.50	21.79
28	II	1,2,4,6	3,5,7	-	-	199.341	99.50	21.78
28	II	1,2,4,6	-	3,5,7	-	200.056	99.50	21.78
29	II	1	2-7	-	-	205.025	99.50	21.79
29	II	1	-	2-7	-	207.107	99.50	21.79
30	-	1-7	-	-	-	191.623	99.50	21.76
31	III	2-7	1	-	-	187.632	99.50	21.55
31	III	2-7	-	1	-	188.669	99.50	21.55
32	III	2-7	1	-	-	187.632	99.50	21.60
33	-	1-7	-	-	-	191.499	99.50	21.55
34	III	1,2,4,6	3,5,7	-	-	183.172	99.50	21.52
34	III	1,2,4,6	-	3,5,7	-	185.494	99.50	21.52
35	III	2,4,6	1,3,5,7	-	-	179.014	99.50	21.50
35	III	2,4,6	-	1,3,5,7	-	182.604	99.50	21.50
36	III	4,7	1,2,3,5,6	-	-	175.743	99.50	21.51
36	III	4,7	-	1,2,3,5,6	-	180.370	99.50	21.51

(Continued on next page)

TABLE XXXII (Continued)

PDP Fuel Loading Patterns - TMT - 12.12-inch A Pitch

Run No.	TMT Assembly Type	Fuel Assembly Position				B_z^2, μB	D_2O	
		Mark IX	TMT D_2O Coolant	TMT Air Coolant	TMT "Dowtherm" A Coolant		D_2O Purity, mol %	D_2O Temp, °C
37	III	1	2-7	-	-	172.576	99.50	21.55
37	III	1	-	2-7	-	177.857	99.50	21.55
38	-	1-7	-	-	-	191.103	99.50	21.51
40	II	2-7	1	-	-	193.789	99.50	21.45
40	II	2-7	-	1	-	194.315	99.50	21.45
41	II	2,4,6	1,3,5,7	-	-	201.033	99.49	21.48
41	II	2,4,6	-	1,3,5,7	-	202.681	99.49	21.48
42	II	4,7	1,2,3,5,6	-	-	202.359	99.49	21.56
42	II	4,7	-	1,2,3,5,6	-	204.370	99.49	21.56
43	-	1-7	-	-	-	190.663	99.49	21.64
44	I	2-7	1	-	-	193.438	99.49	21.61
44	I	2-7	-	1	-	194.625	99.49	21.61
45	I	2,4,6	1,3,5,7	-	-	201.407	99.49	21.62
45	I	2,4,6	-	1,3,5,7	-	205.160	99.49	21.62
46	I	4,7	1,2,3,5,6	-	-	203.296	99.49	21.69
46	I	4,7	-	1,2,3,5,6	-	207.795	99.49	21.69
47	-	1-7	-	-	-	190.818	99.49	21.69
48	I	2-7	-	-	1	188.013	99.49	21.60
49	I	1,2,4,6	-	-	3,5,7	184.234	99.49	21.62
50	I	2,4,6	-	-	1,3,5,7	181.756	99.49	21.69
51	I	4,7	-	-	1,2,3,5,6	179.142	99.49	21.71
52	I	1	-	-	2-7	177.958	99.49	21.78
53	-	1-7	-	-	-	190.305	99.49	21.75
54	II	2-7	-	-	1	187.318	99.49	21.78
55	II	1,2,4,6	-	-	3,5,7	184.050	99.49	21.43
56	II	2,4,6	-	-	1,3,5,7	180.811	99.49	21.40
57	II	4,7	-	-	1,2,3,5,7	178.239	99.49	21.41
59	II	1	-	-	2-7	176.999	99.49	21.40
60	-	1-7	-	-	-	190.338	99.49	21.31
61	III	2-7	-	-	1	178.519	99.49	21.28
62	III	1,2,4,6	-	-	3,5,7	162.667	99.49	21.06
63	-	1-7	-	-	-	190.046	99.49	21.08
64	III	2,4,6	-	-	1,3,5,7	150.026	99.49	21.06

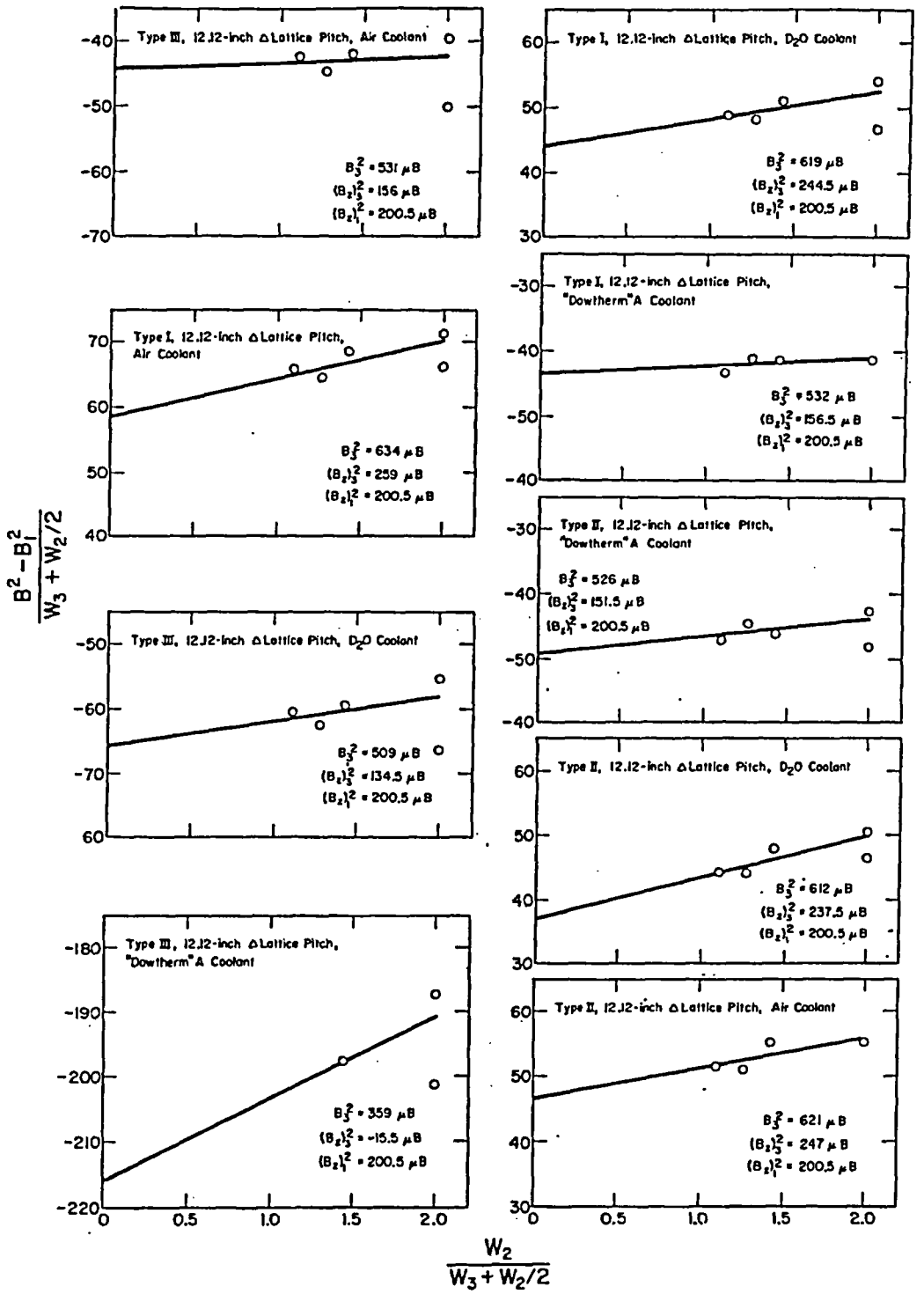

FIG. 43 PERSSON SUBSTITUTION ANALYSES - TMT - PDP

APPENDIX D

DETAILS OF ACTIVATION MEASUREMENTS

Resonance Capture in Thorium (ρ Measurement)

The cadmium ratios for neutron captures in thorium ($\frac{1+\rho}{\rho}$) were determined by an indirect technique that eliminated the flux perturbation introduced by the use of cadmium-covered thorium foils in the fuel assembly. The technique is based on the fact that both copper and thorium have a 1/v variation of their neutron capture cross sections with energy in the subcadmium region. This fact permits the subcadmium activations of the copper foils placed within the fuel to be used to represent the subcadmium activation for thorium. The measurement is thus made in two steps: a measurement of the cadmium ratio of the copper in the fuel (which requires only a very small epithermal correction) and a normalization between the thorium/copper neutron capture ratio and the thorium/copper activity ratio of identical foils exposed to a thermal neutron flux.

A location about 8 inches inside the thermal column of the SP was used as the thermal reference for the normalization measurements. A 1/v cadmium ratio $>10^4$ was measured at this position. The copper and thorium foils were mounted on an aluminum disc that was rotated during the irradiation to eliminate the effect of any flux nonuniformity. The reference irradiation was performed simultaneously with the test lattice irradiation in the SE.

The copper foils used in the ρ measurements were counted at an integral bias of 400 kev with thick (2 x 2 inches) opposed sodium iodide crystals. Copper foils representative of all the various shapes, in the case of the TMT measurements, were included on the thermal reference spinner in each TMT experiment to establish the γ-counter geometry correction factors for the different shapes.

The 22.1-minute β decay of ^{233}Th (E_β = 1.23 Mev) was counted in the energy window from 100-400 kev using a thin (1/16-inch thick) plastic phosphor (NE-102*)during the time interval from 20 to 90 minutes after irradiation. Aluminum absorbers served to establish the energy window. The fission product gamma ray contribution to the counting rate was negligibly small because it was minimized by the counting conditions and because it very nearly cancelled in the difference technique used in analyzing the counts.

*Nuclear Enterprise No.102

Three separate, time-coupled, but otherwise independent β-scintillation counters were used in the arrangement shown in Figure 44. The foil to be counted was placed on the rotating spinner, and one-minute counts were obtained in the counter systems, A and B, with small acceptance angles. The 0.016-inch-thick aluminum β attenuator was first interposed between the foil and the "A" photomultiplier; then the procedure was repeated with the absorber in the "B" position. The difference between the counting rates in the two balanced systems was the desired counting rate in the 100 to 400 kev (β energy) energy window. The foil was then moved to the "C" counter position and counted for one minute with large-angle counter geometry and with a 0.080-inch-thick aluminum β attenuator interposed. The resulting counts were due primarily to thorium fission product β activity in excess of 1.3 Mev (the maximum β energy for ^{233}Th is 1.23 Mev). The counting intervals for the three counters were synchronized, and the intervals between counts were maintained at a constant 15 or 30 seconds.

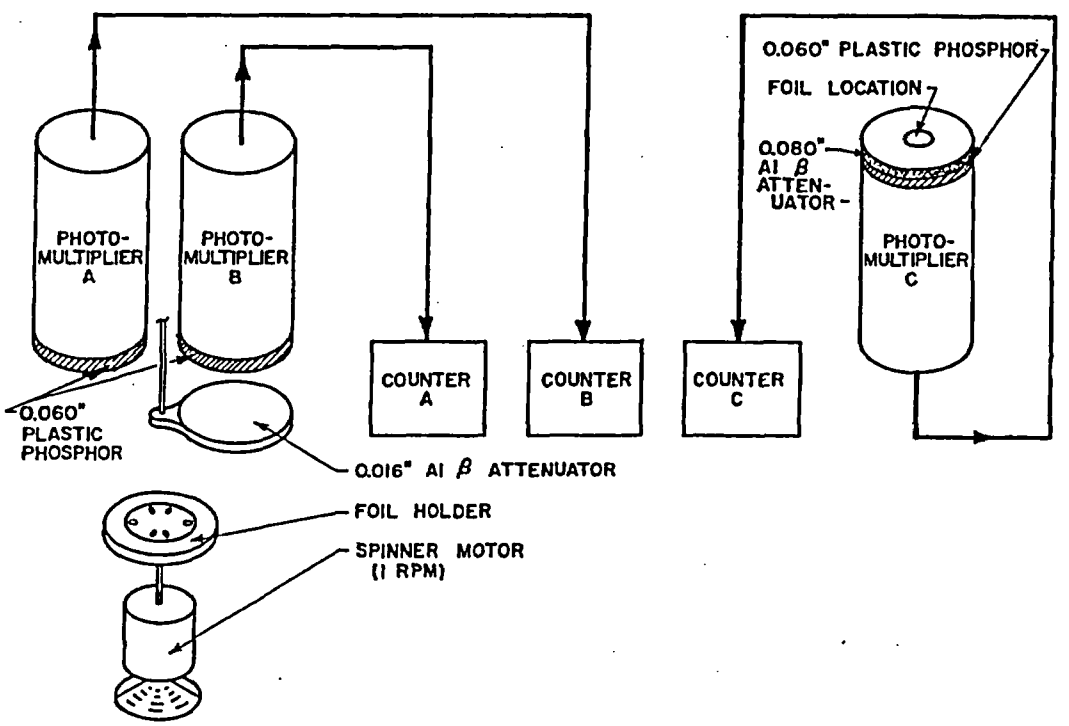

FIG. 44 SPECIALIZED β-COUNTING APPARATUS FOR ^{233}Th

The desired ^{232}Th capture counting rate was obtained from the total measured activity by

$$\left[100 - 400\right]^{\text{Th Capt}} = \frac{\left[100 - 400\right]^{\text{Meas}}}{1 + C(t)}$$

The quantities in brackets are the window count rates. The time-dependent correction term, C, is given in terms of measured activity ratios by

$$C(t) \equiv \frac{A - R(t)^{\text{Capt}}}{R(t)^{\text{FP}} - A}$$

where

$$A \equiv \frac{\left[1300\right]^{\text{Th Meas}}}{\left[100 - 400\right]^{\text{Th Meas}}} = \text{measured activity ratio}$$

$$R(t)^{\text{Capt}} \equiv \frac{\left[100 - 400\right]^{\text{Th Capt}}}{\left[1300\right]^{\text{Th Capt}}} = \text{activity ratio for pure } ^{232}Th \text{ capture}$$

$$R(t)^{\text{FP}} \equiv \frac{\left[100 - 400\right]^{\text{Th FP}}}{\left[1300\right]^{\text{Th FP}}} = \text{activity ratio for pure } ^{232}Th \text{ fission products}$$

$R(t)^{FP}$ for pure thorium fission was obtained by irradiating thorium foils (identical to those used in the ρ measurements) in the 14-Mev neutron flux of a (D,T) neutron generator for 40 minutes. (The same exposure time used in the ρ measurements.) Several independent tests showed that the activity from 14-Mev neutrons was almost completely due to fission products with a negligible contribution from capture radiation. $R(t)^{Capt}$ for pure thorium capture was redetermined in each experiment by counting thorium foils (identical to those used in the ρ measurements) that had been irradiated in the pure thermal flux of the SP thermal column at the same time the experimental irradiation was made in the SE. $R(t)^{FP}$ was found to be very nearly constant over the time interval of 20-90 minutes in which the thorium counting rate data were obtained, and a single value was used. The magnitude of the correction for the fission product contribution in the 100-400 kev energy window ranged from about 1% to 3%. Data reduction was accomplished by use of the THODAT code, described in Appendix E.

The individual thorium foils used in the THUD ρ measurements were "weight" calibrated by determining relative activations after a uniform neutron irradiation in a thermal flux. The foils were β-counted using the same counting arrangement employed for the ρ measurements. The individual foils differed in weight by

less than 2%, and the composite foils used to represent the various radii in the THUD cluster were uniform to within 1%.

For the shaped foils used in the TMT ρ measurements, the foil weight and counter geometry corrections were determined simultaneously. The foil set was irradiated uniformly in a thermal flux, and the relative activations were determined using the identical β-counting conditions employed for the ρ measurements.

In the THUD measurements, no correction was made for the use of thorium metal rather than oxide foils. Previous experiments have shown that a 2- to 3-mil metal foil with its aluminum catcher foils closely approximates the average thorium atom density in the rod and thus should cause a negligible perturbation in the thermal and epithermal flux. The thorium atom density in the THUD fuel was 1.9×10^{23} atoms/cc; the effective thorium atom density for foil and spacer was 2.0×10^{23} atoms/cc. For the TMT measurements, the 0.008-inch-thick thorium metal foils were deliberately made thicker than the corresponding THUD II foils in order to minimize the perturbation by the addition of the catcher foils. Here, no dilution of the thorium in the foil packet is desired since the TMT fuel is approximately 97.7 wt % thorium.

An averaged value of the resonance capture, $\bar{\rho}$, for the fuel assembly was obtained from

$$\bar{\rho} = \frac{\sum_i V_i f_i \rho_i}{\sum_i V_i f_i}$$

where

f_i = specific subcadmium activity of the thorium foil used in the ρ measurement

V_i = volume of region represented by the ρ_i measurement

$\rho_i = \frac{1}{CdR - 1}$ = ratio of epicadmium to subcadmium specific activation for thorium

Fast Fission Effect (δ Measurement)

The technique used to measure fast fissions in the thorium assemblies was similar to that used for natural uranium lattices, i.e., gamma counting of the fission product activities of paired foils. The fission product activities were then related to fission rates.

The fast fission factor, ϵ, is expressed as

$$\epsilon = 1 + \left[\frac{\nu(^{232}\text{Th}) - 1}{\nu(^{235}\text{U})}\right] \delta$$

where ν^{232}Th and ν^{235}U are the numbers of neutrons emitted per fission in ^{232}Th and ^{235}U, respectively. ν^{232}Th = 2.72 and ν^{235}U = 2.43; and δ is the ratio of the number of fissions in ^{232}Th to the number of fissions in ^{235}U. The quantity δ may be written as

$$\delta = \left(\frac{235}{232}\,\bar{\gamma}(t)N\right)P(t)$$

where N is the ratio of the thorium to ^{235}U atom densities in the fuel, $\bar{\gamma}(t)$ is the cluster averaged ratio of the fission product activities due to thorium and ^{235}U in the measurement foils, and P(t) is the ratio of the fission product activity per ^{235}U fission to the fission product activity per thorium fission.

The irradiation and counting conditions for the measurements were standardized. Foils were counted from 20 to 120 minutes after irradiation using two independent, opposed scintillators with thick (2" x 2") sodium iodide crystals. Data were obtained simultaneously in each system at an integral bias of 850 kev and in the energy window from 60 to 110 kev.

The counting rate data obtained above 850 kev for the ^{235}U-Al foils is due to fission products. However, for the thorium foils a small contribution to this activity arises from radiative neutron capture. The desired ^{232}Th fission product counting rate was obtained from the total measured activity by

$$\left[850\text{ kev}\right]^{\text{Th FP}} = \frac{\left[850\text{ kev}\right]^{\text{Meas}}}{1 + C'(t)}$$

The quantities in brackets are the integral bias counting rates. The time-dependent correction term, $C'(t)$, is given in terms of measured activity ratios by

$$C'(t) = \frac{1 - A'R'(t)^{\text{Capt}}}{A'R'(t)^{\text{FP}} - 1}$$

where

$$A' \equiv \frac{\left[850\text{ kev}\right]^{\text{Meas}}}{\left[60\text{-}110\text{ kev}\right]^{\text{Meas}}} = \text{measured activity ratio}$$

$$\dot{R}(t)^{Capt} \equiv \frac{\left[60\text{-}110\ kev\right]^{Th\ Capt}}{\left[850\ kev\right]^{Th\ Capt}} = \text{activity ratio for pure } {}^{232}Th \text{ capture}$$

$$\dot{R}(t)^{FP} \equiv \frac{\left[60\text{-}110\ kev\right]^{Th\ FP}}{\left[850\ kev\right]^{Th\ FP}} = \text{activity ratio for pure } {}^{232}Th \text{ fission products}$$

The $\dot{R}$ values were evaluated in special experiments. $\dot{R}(t)^{FP}$ for pure thorium fission was obtained by irradiating thorium foils, identical to those used in the fast fission measurement, in the 14-Mev neutron flux of a (D,T) neutron generator for the same exposure time used in the fast fission measurement. Several independent tests showed that the activity from 14-Mev neutrons was almost completely due to fission products with a negligible contribution from capture radiation. $\dot{R}(t)^{Capt}$ for pure thorium capture was redetermined in each experiment by counting thorium foils (of the same type used in the ϵ measurement) that had been irradiated on the reference spinner in the pure thermal flux of the SP thermal column at the same time the experimental irradiation was made in the SE.

The thorium foils used in the THUD measurements were combined into two composite foils (Figure 20) to improve the counting statistics. The foils from each "6 of a kind" rod type were combined into a second large foil. The counter efficiency for each small foil was kept constant by arranging the foils in a ring and centering the midpoint of the ring along the axis of the scintillator crystals. No foil was included on the center rod of the THUD clusters since its contribution to the measurement is small and its effect could be estimated with negligible loss of accuracy.

Standard weight, background, and dead time corrections were applied to the thorium and ^{235}U-Al foil gamma activity data. The ^{235}U content of the ^{235}U-Al foils were determined in a separate activation assay with natural uranium as the standard.

A fuel assembly average value of $\bar{\gamma}(t)$ was obtained from

$$\bar{\gamma}(t) = \frac{\sum_i V_i f_i \gamma(t)_i}{\sum_i V_i f_i}$$

where

f_i = specific activity of the ^{235}U-Al foil that was paired with the thorium foil

$\gamma(t)_i$ = ratio of specific activity of ^{232}Th fission product gammas to ^{235}U fission product gammas (This ratio is noted as $\left[\frac{Th}{U}\right]_{FP}^{850}$ in Tables XII, XV, and XIX.)

V_i = volume of region represented by the $\gamma(t)_i$ measurement

which the value of ^{238}U to ^{235}U fissions, δ, for a natural uranium foil was known. This reference was a 1-inch-diameter natural uranium bar embedded in a very large block of graphite. The value of δ for a 1-inch-diameter natural uranium foil at the center of the bar was 0.053. The fission ratio expected for the paired thorium and ^{235}U-Al foils in the same position was computed from the known atom density and the ratio of the effective fission cross section of thorium relative to ^{238}U. (This ratio, 0.24, was obtained by numerically integrating the fission cross sections in BNL-325[18] over the ^{235}U fission neutron spectrum.) The "known" fission ratio was then compared to the measured fission product activity (identical exposure times and counting conditions). The value of P(t) for the THUD experiments was approximately 0.96 and nearly independent of time over the time interval used. P(t) was not separately determined for the foils and counting conditions used in the TMT experiments.

Thermal Neutron Density Distribution

Subcadmium neutron density profiles in the fuel and moderator were obtained from bare and cadmium-covered activations of copper foils placed in the fuel (Figures 15, 19, 25, 34, and 37), on the surface of the housing tube, and supported on aluminum wire frames that were affixed to the irradiation assembly and projected into the moderator (Figures 45 and 46).

A correction for the overall radial flux shape in the SE was applied by dividing the measured activity at each radius r by the Bessel function $J_o(\frac{2.405r}{R})$ where R, the extrapolated radius of the SE, was assumed constant at 79.1 cm.

Elevation corrections were applied in the form $\epsilon^{-\kappa z}$ where the inverse axial relaxation length κ was determined for each experiment either from previous κ_z^2 measurements for the same lattice or from activation data of copper foils positioned at 2-inch intervals on an aluminum foil holder rod placed in the moderator at the cell boundary (Figures 14, 18, and 24).

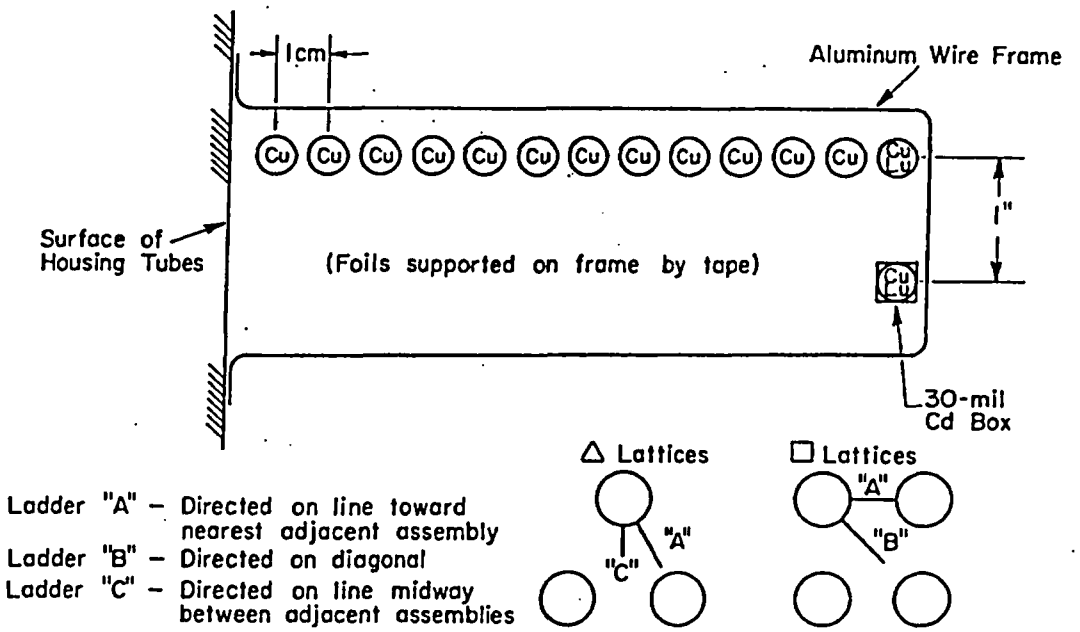

FIG. 45 TYPICAL FOIL LADDER IN THE MODERATOR FOR THUD MEASUREMENTS

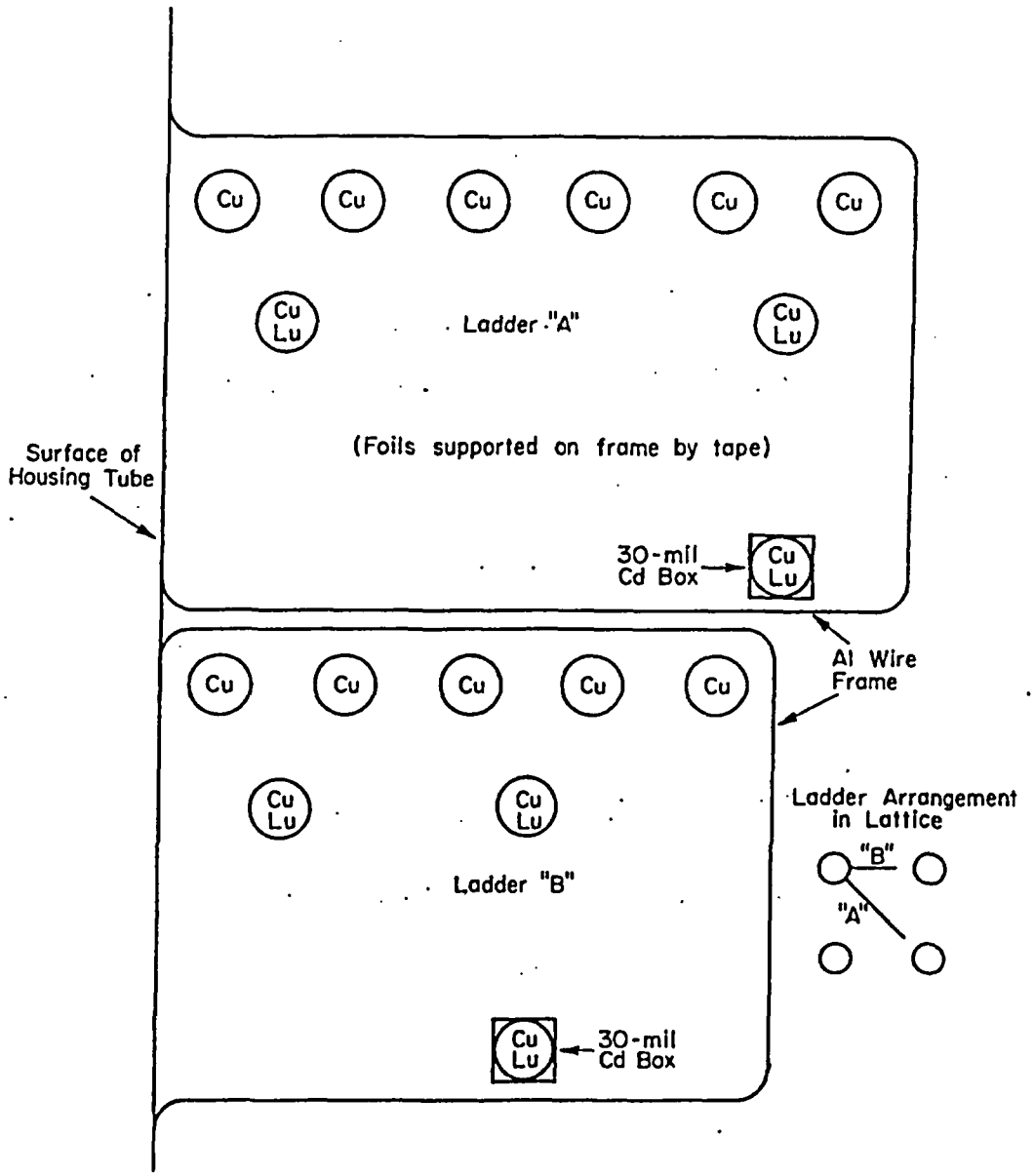

FIG. 46 FOIL LADDERS IN MODERATOR FOR TMT MEASUREMENTS

Spectral Index Measurements

Neutron spectral index measurements were made by the ^{177}Lu-^{64}Cu foil activation technique[12]. Paired bare and cadmium-covered lutetium and copper foils were located in the fuel (Figures 15, 19, 25, 34, and 37), on the surface of the housing tube, on aluminum wire frame ladders affixed to the irradiation assembly and projecting into the moderator (Figures 45-46), and on aluminum rods located at the cell boundary in the moderator (Figures 14, 18, and 24). Paired ^{177}Lu-^{64}Cu reference foils representative of the various shapes and thicknesses used in the lattice measurements were irradiated simultaneously on the reference spinner in the SP thermal column.

The subcadmium activity ratio

$$g_L/g_R \equiv \frac{\left[^{177}Lu/^{64}Cu\right]_{\text{Lattice}}}{\left[^{177}Lu/^{64}Cu\right]_{\text{Th Col Ref}}}$$

is used as a spectral index.

^{235}U Cadmium Ratio

The ^{235}U cadmium ratio was determined by counting the fission product gamma activity of bare and cadmium-covered 4.4 wt % ^{235}U - Al foils with an integral bias of 850 kev during the time interval from 30 to 120 minutes after irradiation. Corrections for the elevation differences between the bare and cadmium-covered foils were obtained as described in the preceding section.

APPENDIX E

THORIUM DATA REDUCTION CODE (THODAT)

THODAT corrects the raw data obtained in the beta counting of the irradiated thorium foils (see Appendix D) for background counts for weight variations between the foils, for fission product counts, and for shutter-in and shutter-out times.

The input is shown in Section A. The manipulations performed by the code are described in Section B. The FORTRAN source deck is listed in Section C.

A. Input

Card	Data	Format	Column
1	Identification		2-72
2	Cycle	I1	1
	Foil	I2	2-3
	$T_{\frac{1}{2}}$	F6.2	4-9
	Fission product factor	9(F7.4)	10-16
	(one for each cycle)		17-23
	etc.		
3	A room background	F6.0	1-6
	B room background	F6.0	7-12
	C room background	F6.0	13-18
4	Two cards for each background (shutter in and out)		
	Foil No.	I2	1-2
	Kind (1 = rod, 2 = reference)	I1	3
	Shutter (1 = on A, 2 = on B)	I1	4
	Weight factor	F6.4	5-10
	A background	F6.0	11-16
	B background	F6.0	17-21
	C background	F6.0	22-28
	Repeat cards 4 for each foil.		
5	Two cards for each foil		
	Cycle	I1	1
	Foil	I2	2-3
	Kind (1 = rod, 2 = reference)	I1	4
	Shutter (1 = on A, 2 = on B)	I1	5
	Clock time	F6.2	6-11
	A counts	F6.0	12-17
	B counts	F6.0	18-23
	C counts	F6.0	24-29
	Repeat cards 5 for each foil.		
	Repeat card 5 for each cycle.		
	Insert 2 blank cards at the end of the data.		

B. Logic

1. For each data card, subtract off room background for A, B, and C separately.

2. Divide all difference A, B, C values by the proper WFACT.

3. For each znny value, there will be two m values m = 1, 2

   znny1
   znny2

   Obtain averages for data cards.

   a. TAVG (z,nn,y) ≡ [CLOCKTIME (z,nn,y,1) X CLOCKTIME (z,nn,y,2)]$^{\frac{1}{2}}$

   b. BAREB (z,nn,y)≡ ["A" (m=2) X "B" (m=1)]$^{\frac{1}{2}}$

   c. ABSB (z,nn,y) ≡ ["A" (m=1) X "B" (m=2)]$^{\frac{1}{2}}$

   d. VMONB (z,nn,y)≡ ["C" (m=1) X "C" (m=2)]$^{\frac{1}{2}}$

   e. DIFFB (z,nn,y)≡ BAREB - ABSB

   Obtain averages for background cards.

   Repeat b,c,d,e above BAREBG, ABSBG, VMONBG, DIFFBG.

4. Subtract backgrounds.

   a. VMON (z,nn,y) ≡ VMONB - VMONBG

   b. DIFF (z,nn,y) ≡ DIFFB - DIFFBG

5. From all pairs of <u>y = 2</u> data cards obtain

   KAVG ≡ [Sum of All MON] / [Sum of All DIFF]

6. Delta Monitor

   DMON (z,nn,y) ≡ KAVG X DIFF (z,nn,y)

7. Corrected Monitor

   CMON (z,nn,y) ≡ MON - DMON

8. Delta difference

   DDIFF (z,nn,y) ≡ CMON X FPFACT (z)

9. Fission corrected difference

   FCDIFF (z,nn,y) ≡ DIFF - DDIFF

10. Time corrected

    TCDIFF (z,nn,y) ≡ FCDIFF X $e^{0.693\left(\frac{TAVG}{T_{\frac{1}{2}}}\right)}$

C. FORTRAN Source Deck

```
LEVEL 2 NOV 66  3/1/67 SRL                    OS/360  FORTRAN  H                              DATE  67.102/08.42.19

          COMPILER OPTIONS - NAME=  MAIN,OPT=00,LINECNT=50,SOURCE,EBCDIC,NOLIST,NODECK,LOAD,MAP,NOEDIT,ID**************

                C     THODAT  M.STROUD
 ISN 0002               COMMON    WFACT(99,2,2),ABGD(99,2,2)                                  THO40010
 ISN 0003               COMMON    BBGD(99,2,2),CBGD(99,2,2)                                   THO40020
 ISN 0004               COMMON    CLOCK(99,2,2),ADA(99,2,2)                                   THO40030
 ISN 0005               COMMON    BDA(99,2,2),CDA(99,2,2)                                     THO40040
 ISN 0006                COMMON   TAVG(9,99,2),BAREB(9,99,2)                                  THO40050
 ISN 0007               COMMON    ABSB(9,99,2),DIFFB(9,99,2)
 ISN 0008               COMMON    BAREBG(9,99,2),ABSBG(9,99,2)
 ISN 0009               COMMON    VMONBG(9,99,2),DIFFBG(9,99,2)
 ISN 0010               COMMON    VMON(9,99,2),DIFFX(9,99,2)
 ISN 0011               COMMON    DMON(9,99,2),DDIFFX(9,99,2)
 ISN 0012               COMMON    IDEN(17),FPFACT(9)
 ISN 0013               COMMON    NFO(99),KIND(99)
 ISN 0014                COMMON   MSHUT(99),W(99)
 ISN 0015               COMMON    A(99),B(99)
 ISN 0016               COMMON    C(99),NCYCLE(99)
 ISN 0017               COMMON    CL(99),KK(99)
 ISN 0018               COMMON    SUMTC(99),FCDIFX(9,99,2)
 ISN 0019               COMMON    TCDIFX(9,99,2)
                C      THODAT                                                                 THO70010
                C      THORIUM DATA REDUCTION                                                 THO70020
 ISN 0020               NTOUT=6                                                               THO70030
 ISN 0021               NTIN=5                                                                THO70040
                C                                                                            THO70050
                C      J=CYCLE NO.   I=NO. OF FOILS                                          THO70060
                C      READ  IDENTIFICATION  AND  INSTRUCTION CARDS                          THO70070
                C                                                                            THO70080
 ISN 0022         100 CONTINUE                                                               THO70090
 ISN 0023               DO 200 I=1,9
 ISN 0024               DO 200 J=1,99
 ISN 0025               DO 200 K=1,2
 ISN 0026               VMON(I,J,K)=0.0
 ISN 0027               TCDIFX(I,J,K)=0.0
 ISN 0028         200 DIFFX(I,J,K)=0.0
 ISN 0029               READ (NTIN,1)(IDEN(K),K=1,17)                                         THO70100
 ISN 0030               READ (NTIN,2)JT,IT,TIO2,(FPFACT(J),J=1,JT)                            THO70110
 ISN 0031               IF (JT)102,102,120                                                    THO70120
 ISN 0032         120 READ (NTIN,110) AR, BR, CR
 ISN 0033         110 FORMAT (3F6.0)                                                          THO70140
 ISN 0034           1 FORMAT (1X,17A4)                                                        THO70180
 ISN 0035           2 FORMAT (11,I2,F6.2,9(F7.4))                                             THO70190
                C      READ BACKGROUND CARDS                                                THO70200
 ISN 0036               DO 10 I=1,IT                                                          THO70210
 ISN 0037               ISIG=0                                                                THO70220
 ISN 0038           4 READ (NTIN,3)NFO(I),KIND(I),MSHUT(I),W(I),A(I),B(I),C(I)               THO70230
 ISN 0039               IF (NFO(I))102,102,101                                                THO70240
 ISN 0040         101 CONTINUE                                                              THO70250
 ISN 0041               K=KIND(I)                                                             THO70260
 ISN 0042               M=MSHUT(I)                                                            THO70270
 ISN 0043               WFACT(I,K,M)=W(I)                                                     THO70280
 ISN 0044               ABGD(I,K,M)=A(I)                                                      THO70290
 ISN 0045               BBGD(I,K,M)=B(I)                                                      THO70300
 ISN 0046               CBGD(I,K,M)=C(I)                                                      THO70310
 ISN 0047               IF (ISIG)40,40,10                                                     THO70320
 ISN 0048           40 ISIG=1                                                                 THO70330
 ISN 0049               GO TO 4                                                               THO70340
 ISN 0050           10 CONTINUE                                                               THO70350
 ISN 0051            3 FORMAT (I2,2I1,F6.4,3(F6.0))                                           THO70360
                C      READ DATA CARDS                                                      THO70370
 ISN 0052           24 FORMAT (I1,I2,2I1,F6.2,3(F6.0))                                       THO70380
 ISN 0053               DO 20 J=1,JT                                                          THO70390
 ISN 0054               DO 21 I=1,IT                                                          THO70400
 ISN 0055               ISIG=0                                                                THO70410
 ISN 0056           22 READ (NTIN,24)NCYCLE(I),NFO(I),KIND(I),MSHUT(I),CL(I),A(I),B(I),C(  THO70420
                     1I)                                                                     THO70430
 ISN 0057               K=KIND(I)                                                             THO70440
 ISN 0058               M=MSHUT(I)                                                            THO70450
 ISN 0059               KK(I)=K                                                               THO70460
 ISN 0060               CLOCK(I,K,M)=CL(I)                                                    THO70470
```

C. FORTRAN Source Deck (Cont.)

```
ISN 0061          ADA(I,K,M)=(A(I)-AR)/WFACT(I,K,M)                                THO70480
ISN 0062          BDA(I,K,M)=(B(I)-BR)/WFACT(I,K,M)                                THO70490
ISN 0063          CDA(I,K,M)=(C(I)-CR)/WFACT(I,K,M)                                THO70500
ISN 0064          IF (ISIG)41,41,21                                                THO70510
ISN 0065       41 ISIG=1                                                           THO70520
ISN 0066          GO TO 22                                                         THO70530
ISN 0067       21 CONTINUE                                                         THO70540
               C     THE ABOVE DATA HAS BEEN BACKGROUND AND WEIGHT CORRECTED       THO70550
               C                                                                   THO70560
ISN 0068          DO 25 I=1,IT                                                     THO70570
ISN 0069          K=KK(I)                                                          THO70580
ISN 0070          TAVG(J,I,K)=SQRT(CLOCK(I,K,1)*CLOCK(I,K,2))                      THO70590
ISN 0071          BAREB(J,I,K)=SQRT(ADA(I,K,2)*BDA(I,K,1))                         THO70600
ISN 0072          ABSB(J,I,K)=SQRT(ADA(I,K,1)*BDA(I,K,2))                          THO70610
               C     VMON IS VMONB HERE                                            THO70620
ISN 0073          VMON(J,I,K)=SQRT(CDA(I,K,1)*CDA(I,K,2))                          THO70630
ISN 0074          DIFFB(J,I,K)=BAREB(J,I,K)-ABSB(J,I,K)                            THO70640
ISN 0075          BAREBG(J,I,K)=SQRT(ABGD(I,K,2)*BBGD(I,K,1))                      THO70650
ISN 0076          ABSBG(J,I,K)=SQRT(ABGD(I,K,1)*BBGD(I,K,2))                       THO70660
ISN 0077          VMONBG(J,I,K)=SQRT(CBGD(I,K,1)*CBGD(I,K,2))                      THO70670
ISN 0078          DIFFBG(J,I,K)=BAREBG(J,I,K)-ABSBG(J,I,K)                         THO70680
ISN 0079          VMON(J,I,K)=VMON(J,I,K)-VMONBG(J,I,K)                            THO70690
ISN 0080       25 DIFFX(J,I,K)=DIFFB(J,I,K)-DIFFBG(J,I,K)                          THO70700
ISN 0081          SUMMON=0.0                                                       THO70710
ISN 0082          SUMDI=0.0                                                        THO70720
ISN 0083          DO 26 I=1,IT                                                     THO70730
ISN 0084          K=KK(I)                                                          THO70780
ISN 0085          SUMMON=SUMMON+VMON(J,I,2)                                        THO70740
ISN 0086       26 SUMDI=SUMDI+DIFFX(J,I,2)                                         THO70750
ISN 0087          AVGK=SUMMON/SUMDI                                                THO70760
ISN 0088          DO 27 I=1,IT                                                     THO70770
ISN 0089          K=KK(I)                                                          THO70780
ISN 0090          DMON(J,I,K)=AVGK*DIFFX(J,I,K)                                    THO70790
               C     LET CMON BE DMON                                              THO70800
ISN 0091          DMONI(J,I,K)=VMON(J,I,K)-DMON(J,I,K)                             THO70810
ISN 0092          DDIFFX(J,I,K)=DMON(J,I,K)*FPFACT(J)                              THO70820
ISN 0093          FCDIFX(J,I,K)=DIFFX(J,I,K)-DDIFFX(J,I,K)                         THO70830
ISN 0094          EXPON=          (TAVG(J,I,K)/TLOG)*.6931472
ISN 0095          TCDIFX(J,I,K)=FCDIFX(J,I,K)*EXP(EXPON)                           THO70850
ISN 0096       27 CONTINUE                                                         THO70860
ISN 0097       20 CONTINUE                                                         THO70870
               C                                                                   THO70880
               C     NOW WE HAVE BEEN OVER ALL CYCLES, JT                          THO70890
               C                                                                   THO70900
ISN 0098          DO 28 I=1,IT                                                     THO70910
ISN 0099       28 SUMTC(I)=0.                                                      THO70920
ISN 0100          DO 30 I=1,IT                                                     THO70930
ISN 0101          K=KK(I)                                                          THO70940
ISN 0102          DO 29 J=1,JT                                                     THO70950
ISN 0103          SUMTC(I)=SUMTC(I)+TCDIFX(J,I,K)                                  THO70960
ISN 0104       29 CONTINUE                                                         THO70970
ISN 0105       30 CONTINUE                                                         THO70980
ISN 0106          VJT=JT                                                           THO70990
ISN 0107          DO 33 I=1,IT                                                     THO71000
ISN 0108       33 SUMTC(I)=SUMTC(I)/VJT                                            THO71010
               C                                                                   THO71020
               C     NOW EDIT THE RESULTS                                          THO71030
ISN 0109          WRITE (NTOUT,32)(IDEN(ID),ID=1,17)                               THO71040
ISN 0110          WRITE (NTOUT,31)                                                 THO71050
ISN 0111          DO 34 I=1,IT                                                     THO71060
ISN 0112          K=KK(I)                                                          THO71070
ISN 0113          N=NFO(I)                                                         THO71080
ISN 0114       34 WRITE (NTOUT,35) N,K,(TCDIFX(J,I,K),J=1,JT),SUMTC(I)
ISN 0115          GO TO 100                                                        THO71100
ISN 0116       32 FORMAT (1H1,30X,31HTHORIUM DATA REDUCTION - THODAT///,1X,17A4////// THO71110
                 1)                                                                THO71120
ISN 0117       31 FORMAT (1X,52HFOIL  ROD OR    TIME CORRECTED COUNTS FOR EACH CYCLE THO71130
                 1/2X,48HNO.   REF.        THE LAST COLUMN IS THE AVERAGE//)      THO71140
ISN 0118       35 FORMAT (2X,I2,5X,I1,6X,10(F10.2))                               THO71150
ISN 0119      102 CONTINUE                                                         THO71160
ISN 0120          CALL EXIT                                                        THO71170
ISN 0121          STOP
ISN 0122          END                                                              THO71180
```

BIBLIOGRAPHY

1. Heavy Water Organic Cooled Reactor, 1000 Mwe Nuclear Power Plant, Preliminary Conceptual Design. USAEC Report AI-CE-Memo 6 Vol. I, II and III, Combustion Engineering and Atomics International (1965). Also Heavy Water Organic Cooled Reactor Quarterly Technical Progress Reports.

2. Thorium Fuel Cycle for Heavy Water Moderated Power Reactors Quarterly Technical Reports. The Babcock and Wilcox Company Atomic Energy Division (1965-1967).

3. W. C. Redman, et al. Critical Experiments with Thoria-Urania Fuel in Heavy Water. USAEC Report ANL-6378, Argonne National Lab., Argonne, Ill. (1961).

4. A. E. Dunklee. The Heavy Water System of the Process Development Pile. USAEC Report DP-567, E. I. du Pont de Nemours and Co., Savannah River Laboratory, Aiken, S. C. (1961);
J. L. Crandall. Status of the United States Effort in D_2O Reactor Physics. DP-787 (1962);
J. L. Crandall. Efficacy of Experimental Physics Studies on Heavy Water Lattices. DP-833 (1963).

5. R. C. Axtmann and O. A. Towler, Jr. The Savannah River Exponential Facility. USAEC Report DP-49, E. I. du Pont de Nemours and Co., Savannah River Laboratory, Aiken, S. C. (1954).

6. J. E. Suich and H. C. Honeck. The HAMMER System. USAEC Report DP-1064, E. I. du Pont de Nemours and Co., Savannah River Laboratory, Aiken, S. C. (1967).

7. G. F. Kuncir. A Program for the Calculation of Resonance Integrals. USAEC Report GA-2525, General Dynamics Corp., General Atomic Div., San Diego, Calif. (1961).

8. R. C. Axtmann, et al. Initial Operation of the Standard Pile. USAEC Report DP-32, E. I. du Pont de Nemours and Co., Savannah River Laboratory, Aiken, S. C. (1953) (Declassified 8/29/57).

9. R. Persson. One-Group Perturbation Theory Applied to Substitution Measurements with Void. A. B. Atomenergie, Studsvik, Sweden, Report RFX-74 (1961);
W. B. Rogers, V. D. Vandervelde and N. P. Baumann. "Buckling Measurements by Successive Substitution in a Subcritical Assembly." Trans. Amer. Nucl. Soc. 8, 449-50 (1965).

10. W. E. Graves. Analysis of the Substitution Technique for the Determination of D_2O Lattice Bucklings. USAEC Report DP-832, E. I. du Pont de Nemours and Co., Savannah River Laboratory (1963).

11. D. R. Finch. User's Manual for SRL-HERESY I. USAEC Report DP-1027, E. I. du Pont de Nemours and Co., Savannah River Laboratory (1966);
C. N. Klahr, L. B. Mendelsohn, and J. Heitner. Heterogeneous Reactor Calculation Methods. USAEC Report NYO-2678, TRG, Inc., Syosset, N. Y. (1960) (TRG-129-QTR-6);
C. N. Klahr, J. Heitner, and N. Stein. Test and Verification of Heterogeneous Reactor Calculation Methods - Annual Report - April 1963 - January 1964. USAEC Report NYO-3194-1, Fundamental Methods Associates, Inc., New York;
C. N. Klahr and L. B. Mendelsohn. Heterogeneous Reactor Calculation Methods. USAEC Report NYO-2674, TRG, Inc., Syosset, N. Y. (1959) (TRG-129-QTR-2).

12. C. H. Westcott. Effective Cross Section Values for Well-Moderated Thermal Reactor Spectra. Chalk River, Ontario, Canada, Report CRRP-960 (1960); CRRP-662 (1956); CRRP-680 (1957); CRRP-787 (1958); CRRP-862 (1959); and CRRP-960 (1960);
L. C. Schmid and W. P. Stinson. "Calibration of Lutetium for Measurements of Effective Neutron Temperatures." Nucl. Sci. and Eng. 7, 477-478 (1960). See also HW-70716 p. 35 (1961); HW-66319 (1960), HW-69475 (1965).

13. H. C. Honeck. THERMOS, A Thermalization Transport Theory Code for Reactor Lattice Calculations. USAEC Report BNL-5826, Brookhaven National Lab., Upton, N. Y. (1961).

14. R. A. Dannels and D. J. Bredin. Compilation of a MUFT Library (Library 567). USAEC Report WCAP-3709, Westinghouse Electric Corporation, Atomic Power Division, Pittsburgh, Pa. (1962).

15. H. P. Flatt. The FOG One-Dimensional Diffusion Equation Codes. USAEC Report NAA-SR-6104, North American Aviation, Inc., Atomics International, Canoga Park, Calif. (1961).

16. V. Ardente. "Remarks on the Slow Neutron Scattering by Organic Molecules." J. Phys. 641 (1964). See also "Some Theoretical Results Concerning Neutron Thermalization by H Bound in Polyphenyls," by V. Ardente. Paper presented at the Meeting of the Joint Euratom Nuclear Data and Reactor Physics Committee, in Ispra (Feb. 25-26, 1965).

17. N. P. Baumann, P. B. Parks, and D. J. Pellarin. "Spectral Index and Relaxation Length Determinations in Borated D_2O and H_2O", to be published in the Proceedings of the IAEA Symposium on Neutron Thermalization and Reactor Spectra, University of Michigan, Ann Arbor, July 17-21, 1967;
P. B. Parks, D. J. Pellarin, N. H. Prochnow, and N. P. Baumann. Thermal Neutron Diffusion in Light and Heavy Water. USAEC Report DP-1090, E. I. du Pont de Nemours and Co., Savannah River Laboratory, Aiken, S. C. (1968);
N. H. Prochnow and P. B. Parks. Unpublished Measurements of Diffusion Coefficients for "Dowtherm" A (1967).

18. "Dowtherm" A and "Dowtherm" E Handbook, Dow Chemical Company, Midland, Michigan.

19. M. D. Goldberg, et al. Neutron Cross Sections. USAEC Report BNL-325 (2nd Ed., Suppl. 2), Brookhaven National Laboratory, Upton, N. Y. (1966).